Project Report
NOAA-36

Impacts of WSR-88D SAILS and MRLE VCP Options on Severe Weather Warning Performance

J.Y.N. Cho
J.M. Kurdzo
B.J. Bennett
A.K. Anderson-Frey

31 July 2024

Lincoln Laboratory
MASSACHUSETTS INSTITUTE OF TECHNOLOGY
LEXINGTON, MASSACHUSETTS

This material is based upon work supported by the National Oceanic and Atmospheric Administration under Air Force Contract No. FA8702-15-D-0001.

This report is the result of studies performed at Lincoln Laboratory, a federally funded research and development center operated by Massachusetts Institute of Technology. This material is based upon work supported by the National Oceanic and Atmospheric Administration under Air Force Contract No. FA8702-15-D-0001. Any opinions, findings, conclusions or recommendations expressed in this material are those of the author(s) and do not necessarily reflect the views of the National Oceanic and Atmospheric Administration.

Massachusetts Institute of Technology
Lincoln Laboratory

Impacts of WSR-88D SAILS and MRLE VCP Options on Severe Weather Warning Performance

J.Y.N. Cho
J.M. Kurdzo
B.J. Bennett
Group 43

A.K. Anderson-Frey
Department of Atmospheric Sciences, University of Washington

Project Report NOAA-36

31 July 2024

This material is based upon work supported by the National Oceanic and Atmospheric Administration under Air Force Contract No. FA8702-15-D-0001.

Lexington Massachusetts

This page intentionally left blank.

EXECUTIVE SUMMARY

The impacts of supplemental adaptive intra-volume low-level scan (SAILS) and mid-volume rescan of low-level elevations (MRLE) usage on the Weather Surveillance Radar 1988-Doppler (WSR-88D) with respect to severe weather warning performance were evaluated. This is an update and expansion of an earlier study by Cho et al. (2022). Statistical methods applied to historical data from 2014–2022 yielded the following major results.

Severe thunderstorm (SVR) warning performance metrics are shown in the figure below, where the vertical bars represent 95% confidence intervals and the numbers at the bottom correspond to the sample sizes. The results are divided according to the scanning option that is estimated to have been used at the time the decision to issue (or not issue) a warning was made. The first point to note is that probability of detection (POD), false alarm ratio (FAR), and mean lead time (MLT) improvements were associated with the usage of supplemental adaptive intra-volume low-level scan (SAILS or MRLE) in a statistically meaningful manner. As for the different sub-modes of SAILS, the multiple elevation scan option (MESO), i.e., SAILSx2 and SAILSx3, appeared to give more benefit than SAILSx1. However, the fact that the fastest base-scan update rates provided by SAILSx3 hardly yielded more benefit than SAILSx2 may indicate that the slowdown in volume scan update rates counteracted the more frequent base scans when going from SAILSx2 to SAILSx3. For POD and FAR, MRLE+4 significantly outperformed MESO-SAILS, which may also indicate that more frequent updates of elevations angle scans higher than the lowest tilt are needed by forecasters to make accurate SVR warning decisions.

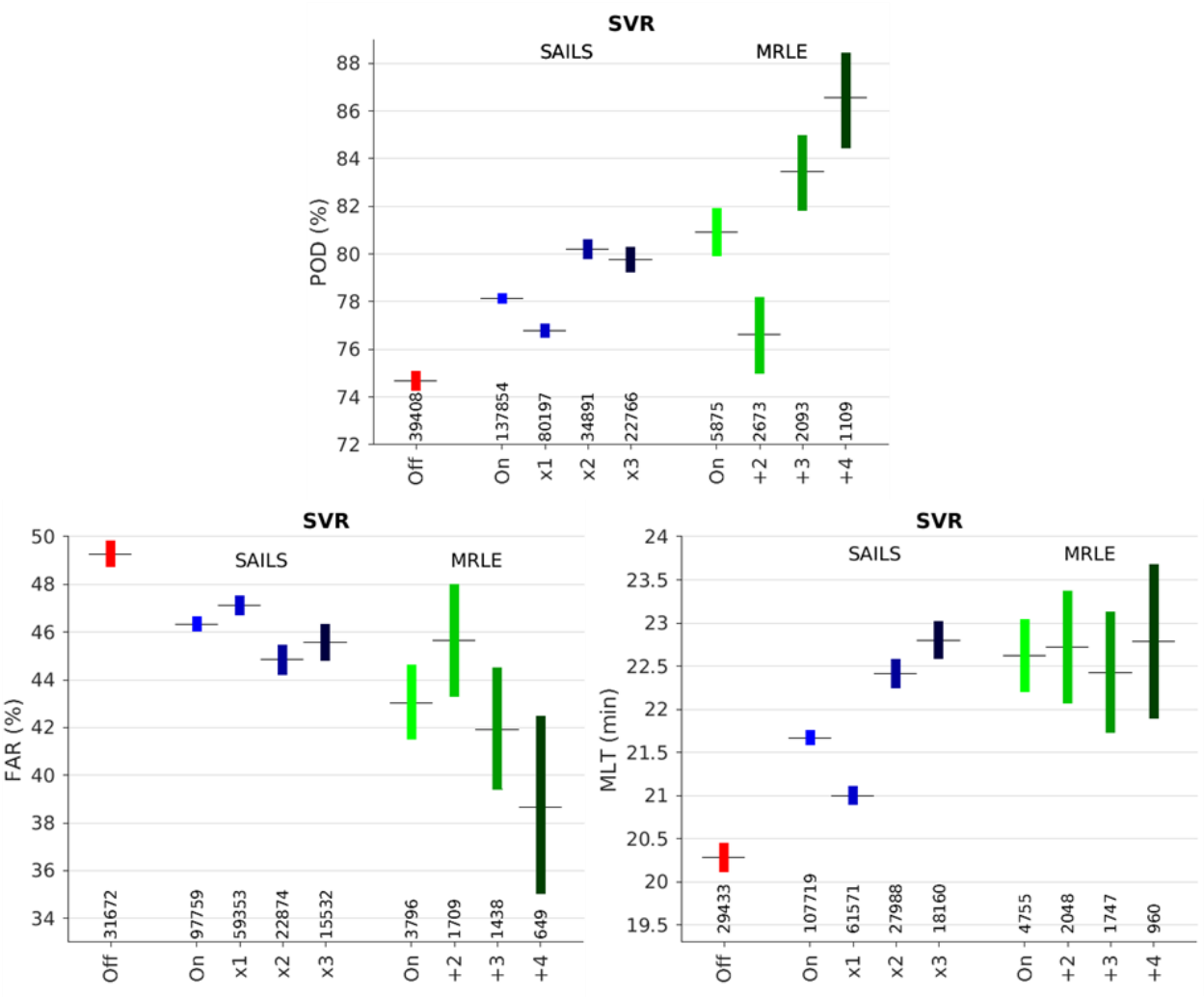

The SVR warning POD and MLT results were further parsed by event type—hail and thunderstorm wind—as shown in the figure below. The benefits of using SAILS were clearly greater for thunderstorm wind events. For hail events, there seems to be some benefit when choosing MRLE+3 or MRLE+4 over SAILS. A possible explanation is that more frequent higher-elevation scans are useful for tracking descending hail cores and for automated hail detection algorithms.

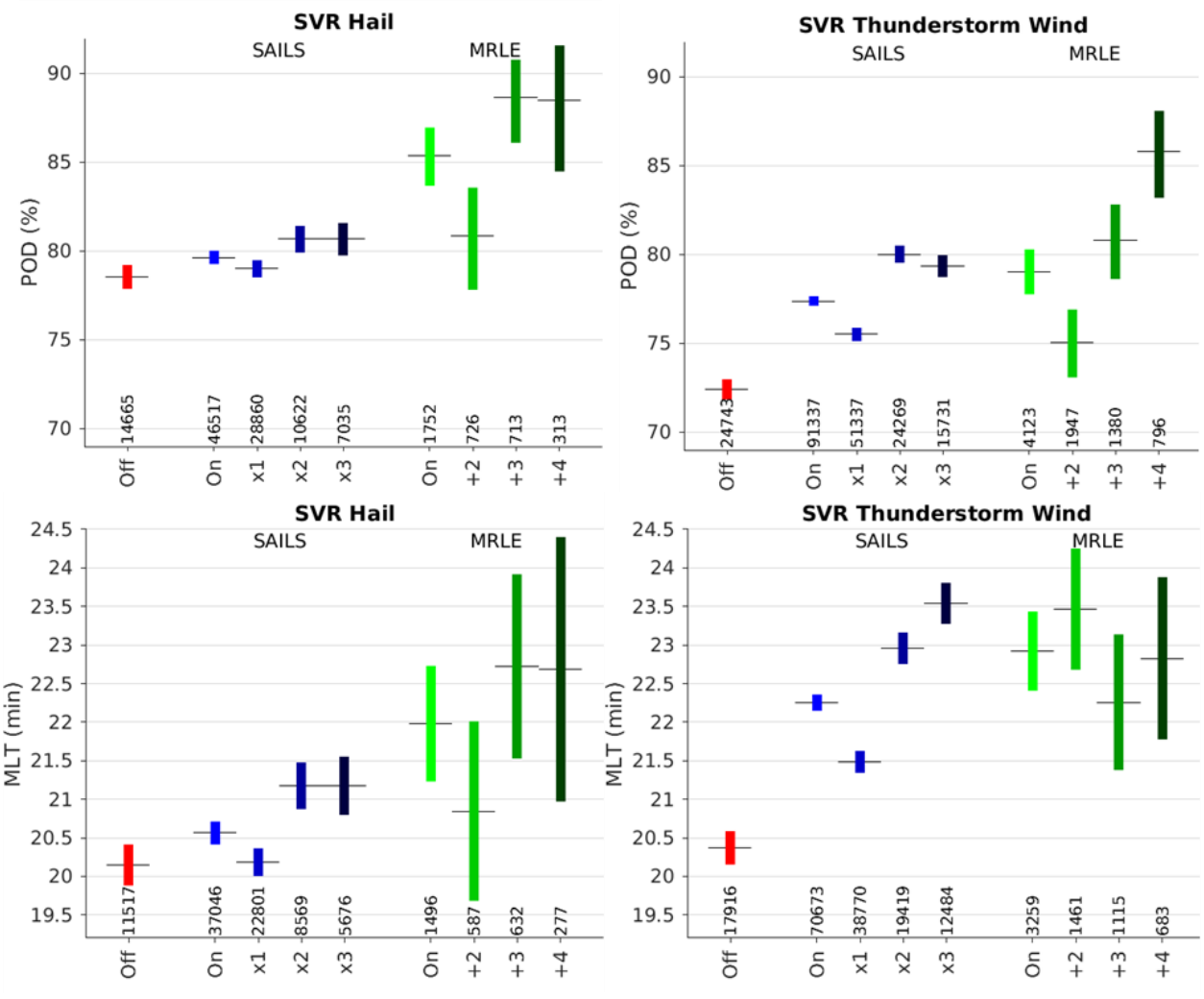

Flash flood (FF) warning performance metrics are shown in the figure below. As with SVR warnings, SAILS utilization corresponded with significant improvement in all three warning performance metrics, with SAILSx3 appearing to be the best SAILS sub-mode. There were not enough data for MRLE to form definitive conclusions, but it seems to yield similar levels of benefit as SAILS, with MRLE+4 doing best with FAR.

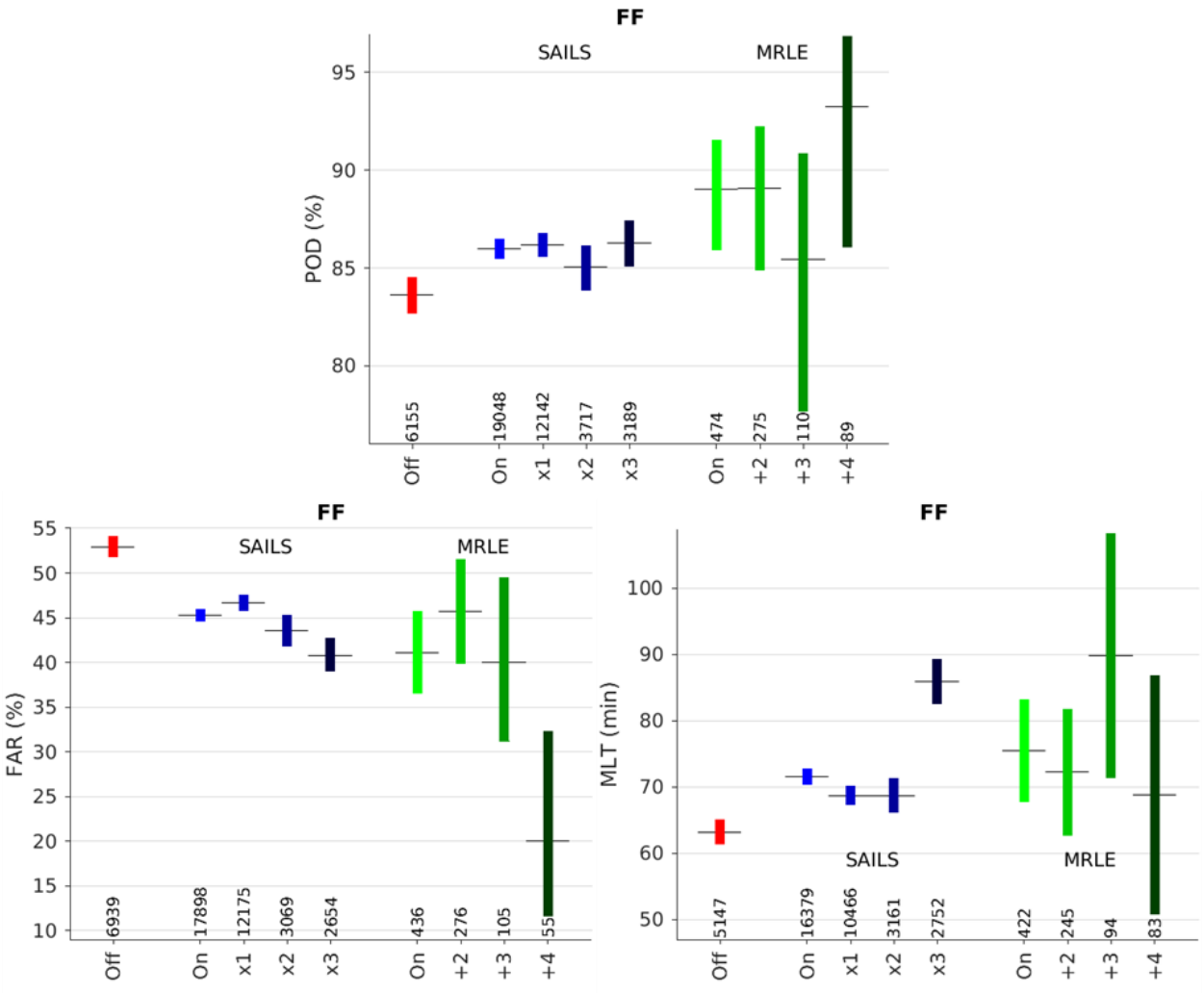

Tornado (TOR) warning performance metrics are shown in the figure below. SAILS usage had significant benefits for POD and FAR performance, with SAILSx3 showing a statistically meaningful improvement over the "SAILS and MRLE off" case in MLT. Thus, for TOR warnings, it appears that more frequent base scan updates are of paramount importance, even at the expense of slower volume update rates. MRLE does not seem to add value beyond SAILS for TOR warnings—in fact, it showed degraded lead time performance compared to SAILS. These observations raise the question of whether a new SAILSx4 option, with even more frequent base scan updates than SAILSx3, might be considered for targeted TOR warning use.

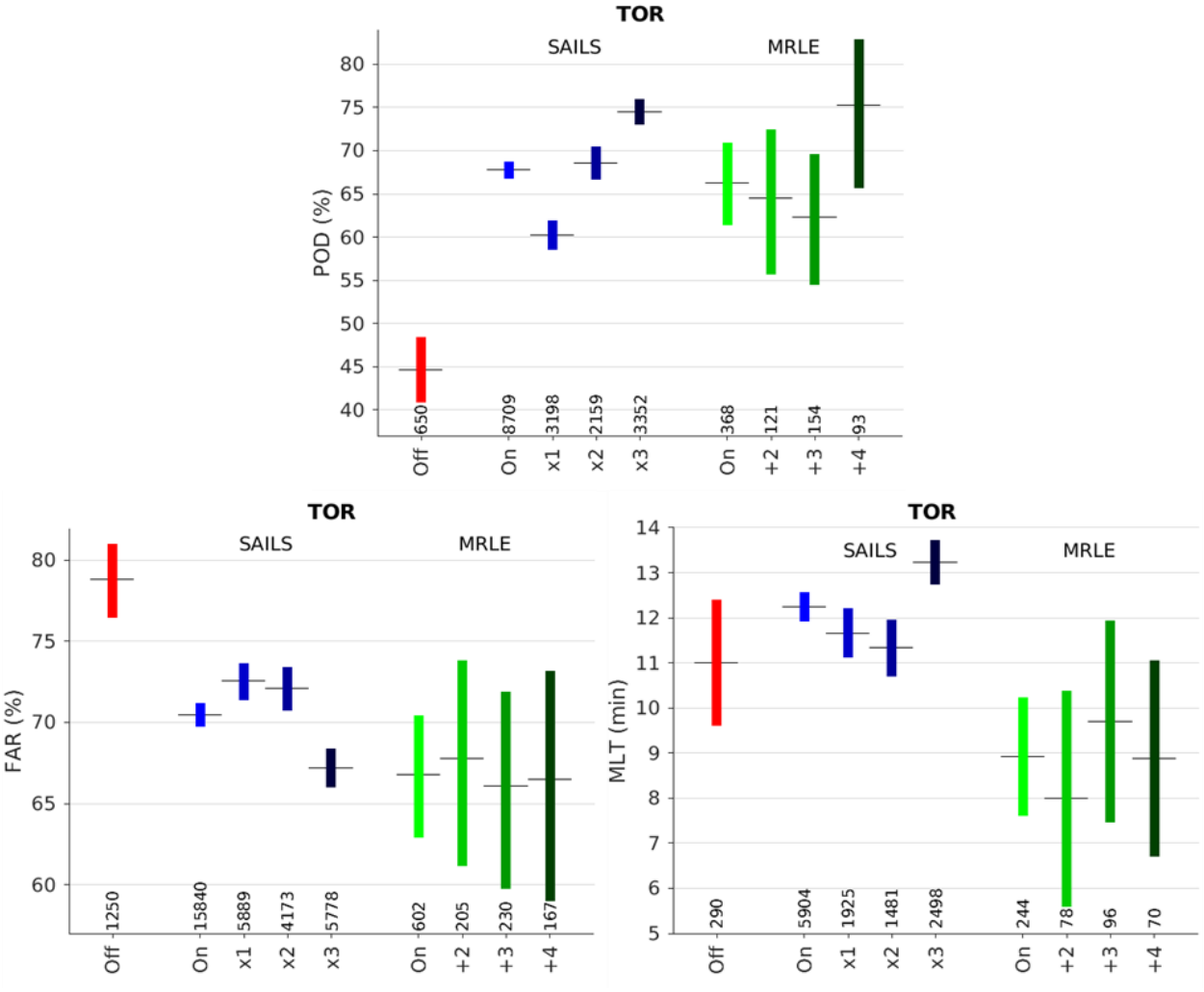

Since tornadoes form (or fail to form) under various convective conditions, different scanning options may be more effective for different situations. To investigate this issue, a further parsing of the TOR warning results by storm type was conducted for POD and MLT (FAR could not be parsed in this way because storm classification data for non-tornadic storms do not exist). The figure below shows the POD results for eight convective mode categories: right-moving (RM) supercell ("RMSup"), RM supercell/cell in line ("RMSupLine"), RM supercell/cell in cluster ("RMSupClust"), RM supercell/discrete cell ("RMSupDisc"), quasi-linear convective system ("QLCS"), disorganized ("Disorg"), supercell/cell in line + QLCS ("AnyLine"), and supercell/discrete + disorganized/discrete ("Discrete"). For all except the supercell/cell in line category (for which the sample size is smallest), SAILS usage was associated with significantly higher POD than with SAILS and MRLE turned off. Furthermore, SAILSx3 performed

significantly better than SAILSx1 and SAILSx2 for most of the storm types. Therefore, SAILS (especially SAILSx3) appears to be a good choice for TOR warning decisions in virtually any type of convective mode.

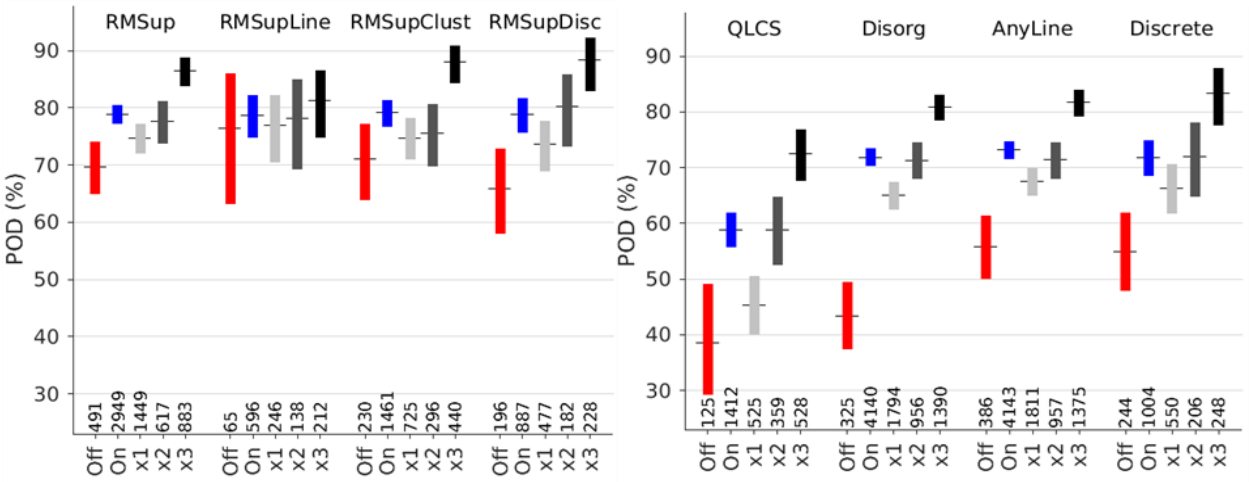

For the hardest-to-warn storm categories, the historical detection probabilities from the pre-SAILS era were: POD of 48.6 ± 6.2% for QLCS and 44.2 ± 4.7% for disorganized (Brotzge et al. 2013). Comparison with the figure above shows that these values are essentially equal to the current POD with SAILS and MRLE turned off. Thus, the significantly higher detection probabilities we see today with SAILS on for QLCS and disorganized storms make a strong case for claiming a tangible, likely life-saving, benefit of SAILS. Furthermore, SAILSx3 for QLCS was associated with a meaningfully longer MLT than SAILS off and the pre-SAILS value of 12.3 minutes (Brotzge et al. 2013). None of the other MLT usage and storm type categories showed statistically significant benefits for SAILS.

In an effort to provide objective input to the radar operational training program, the table below summarizes and compares the historically most used SAILS and MRLE options (including the "off" alternative) with the options that this study showed to be statistically associated with best warning performance. Because the optimal (or best compromise) radar scanning choice in any given situation will be dependent on many factors, this table is not meant to be used as a rigid basis for decision making. Since this strictly statistical study cannot explain why radar operators select certain scanning modes for certain situations, in order to most effectively exploit these study results, a nationwide survey of weather forecast offices is recommended to answer those questions. Results from the survey can then be synthesized with those from this study to provide enhanced guidance on WSR-88D usage in the future.

Category	SVR (hail)	SVR (wind)	FF	TOR
Historically most used	SAILSx1	SAILSx1	SAILSx1	SAILSx1
Option associated with top warning performance	MRLE+4	MRLE+4	MRLE+4	SAILSx3
Option(s) associated with second best warning performance	MRLE+3	SAILSx3	MRLE+3 SAILSx3	SAILSx2

Because forecasters sometimes need to monitor multiple threats simultaneously, there may not be one optimal scanning mode for any given instance. Furthermore, the different threats may be in different sectors, whereas the WSR-88D can only carry out one scanning pattern at a time. In principle, a phased-array radar (PAR) could be designed to execute different scan strategies adaptively tailored to different meteorological targets in different sectors, which comes closer to the ideal of optimizing surveillance parameters for each phenomenon. However, even a PAR would be limited by trade-offs between scan update rates, spatial coverage, and data quality, and the trade-off space would, in large part, be dictated by system cost. Therefore, it is of interest to understand better what the range of scan update parameters needs to be in future radar requirements. Experiments with the new generation of polarimetric PARs, such as the National Severe Storm Laboratory's Advanced Technology Demonstrator (ATD; Torres and Wasielewski 2022), where forecasters are tasked to make warning decisions based on a range of sub-sampled data from recorded high-update-rate-everywhere data (such as the Phased Array Radar Innovative Sensing Experiment [PARISE; Wilson et al. 2017]) could help refine such requirements.

This page intentionally left blank.

ACKNOWLEDGMENTS

We would like to thank Dave Smalley (MIT Lincoln Laboratory) for assistance in obtaining supplemental data, Bryan Smith (National Weather Service Storm Prediction Center) for assistance with the tornadic storm classification database, and Katie Wilson (University of Oklahoma School of Meteorology) for constructive comments and suggestions.

This page intentionally left blank.

TABLE OF CONTENTS

This page intentionally left blank.

LIST OF ILLUSTRATIONS

This page intentionally left blank.

LIST OF TABLES

1. INTRODUCTION

Weather forecasters consult different types of information when making severe weather warning decisions. For National Weather Service (NWS) forecasters, data from the Weather Surveillance Radar 1988-Doppler (WSR-88D; Crum and Alberty 1993) often play a leading role in the severe weather warning decision process (e.g., Burgess and Lemon 1990; Polger et al. 1994). The quality and timeliness of the radar data are, of course, important to the forecaster. For example, long-term statistical analyses have shown that higher operational performance for tornado (TOR; Cho and Kurdzo 2019a,b), flash flood (FF; Cho and Kurdzo 2020a), and non-tornadic severe thunderstorm (SVR; Cho and Kurdzo 2020b) warnings are associated with better radar coverage and spatial resolution. Studies conducted within testbed settings utilizing experimental, non-operational radar data have shown that faster radar data updates can also lead to improved TOR and SVR warning performance (Heinselman et al. 2015; Wilson et al. 2017).

Ideally, in terms of timeliness, weather radar observations from every point in space would be available continuously and instantaneously. This is impossible, because it takes the radar a finite amount of time to obtain high quality data from each resolution volume (e.g., Doviak and Zrnic 1993). In fact, there are interdependent trade-offs between spatial coverage, observation update frequency, and data quality. With the WSR-88D, the NWS forecaster manages these trade-offs in real time by selecting from a menu of available volume coverage patterns (VCPs), based on which VCP best suits the weather phenomenon of immediate interest (e.g., Brown et al. 2000).

The WSR-88D VCPs are defined as automated sets of 360° azimuthal antenna rotations, each at a constant elevation angle that make up an entire volume of scans. These have evolved over time in response to research outcomes and forecaster input. In the past decade, options to the basic VCPs were introduced that further expanded the WSR-88D's observational flexibility: 1) automated volume scan evaluation and termination (AVSET; Chrisman 2013), 2) supplemental adaptive intra-volume low-level scan (SAILS; Chrisman 2014), and 3) mid-volume rescan of low-level elevations (MRLE; Chrisman 2016). Briefly, AVSET shortens the volume update time whenever possible by adaptively skipping high-elevation-angle scans above 5° that contain no precipitation returns. SAILS inserts one to three extra lowest-elevation-angle (base) scan(s) dispersed evenly in time throughout the VCP cycle. MRLE is similar to SAILS, except other low-level elevations scans (e.g., 0.9°, 1.3°, and 1.8°) are updated more frequently as well. After an initial trial period, AVSET has been on by default at all sites since 2012, although it can be manually turned off when desired. SAILS and MRLE are options that are selected in real time by NWS weather forecast office (WFO) forecasters, and have been available since 2014–2015 and 2018–2019, respectively, depending on the date that each site was updated with the corresponding software build.

It is important to quantify the efficacy of these recent VCP enhancements to 1) provide better guidance and training for their usage, 2) aid in the development of future VCPs and options, 3) help inform scanning requirements for the eventual WSR-88D replacement, and 4) document benefits gained from optimizing scan strategies. Since the WSR-88D has a mechanically steered antenna that places physical

constraints on scanning methodologies, electronically scanned phased-array radars (PARs) are being considered as a potential future alternative (Weber et al. 2021). Points 3 and 4 inform the research-to-operations plan (NOAA 2020) for this alternative radar system.

In a recent study, we focused on the effects of SAILS on SVR, FF, and TOR warning performance (Cho et al. 2022). Here we expand on that study to increase the database span through the end of 2022 (Section 2.2), add an analysis of MRLE impacts (Section 2.3), explore TOR warning performance dependence on storm type (Section 2.4), investigate the relative importance of base vs. volume scan update rates (section 3), and parse the SAILS impact results by (anonymized) WFOs (section 4). The text in Sections 2.1 and 2.2 is almost entirely based on material from Cho et al. (2022), but the results have been completely updated based on 2014–2022 data instead of 2014–2020 data. All the other sections are composed of new and original material.

2. SAILS IMPACT ON WARNING PERFORMANCE

It is generally thought that faster radar scan updates would help forecasters make more accurate and timely severe weather warning decisions. The SAILS option provides more frequent base scan updates, but at the price of increasing the time between complete volume scan updates. Therefore, it is not a "slam dunk" proposition, a priori, that the usage of SAILS would improve warning performance. SAILS is further subdivided into SAILxN, where $N = 1$, 2, or 3 corresponds to the number of additional base scan(s) inserted into the VCP. (The $N > 1$ cases are referred to as MESO-SAILS, where MESO stands for "multiple elevation scan option.") This trade-off of base vs. volume scan update rates is illustrated in Figure 1. The relative impacts of the two update rate types on warning performance will be investigated in Section 3. (Note that, for transparency, the data points underlying plots are given as tables in Appendix A.)

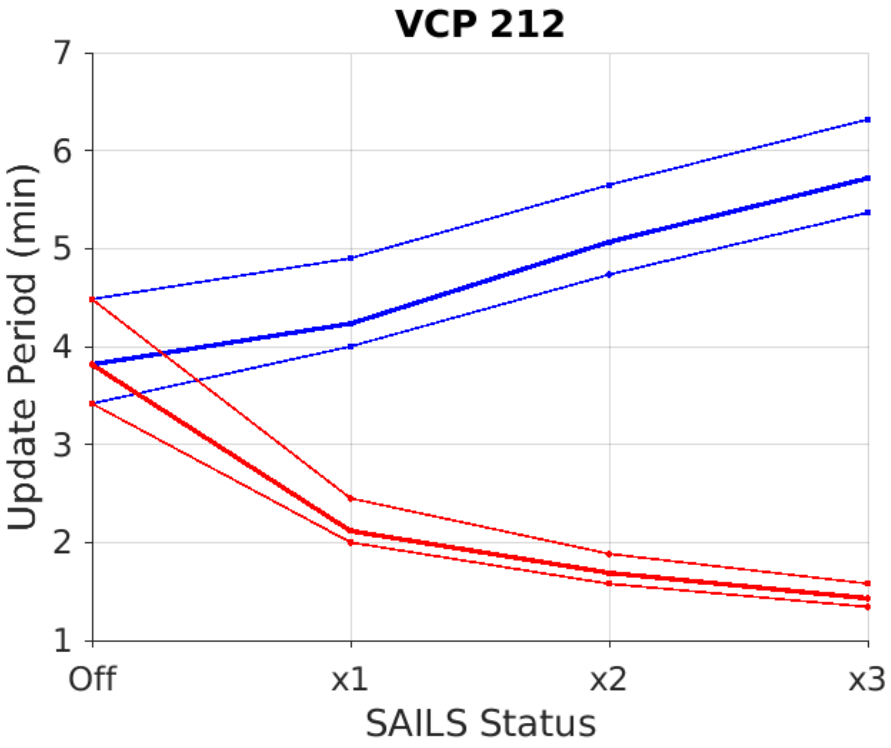

Figure 1. Base scan update period (red) and volume scan update period (blue) vs. SAILS status for VCP 212. The thick lines correspond to the medians and the thin lines denote the 25th and 75th percentile values.

2.1 ANALYSIS METHODOLOGY

The basic idea behind our analysis was to find the scan mode that was operating on the primary WSR-88D used by the forecaster when making the decision to issue or not to issue a severe weather warning. The warning performance metrics—probability of detection (POD), mean lead time (MLT), and false alarm ratio (FAR)—were then computed, parsed by VCP type. We chose mean lead time over median lead time because confidence intervals for the mean are more straightforwardly computed and more commonly agreed upon than confidence intervals for the median, and confidence intervals are crucial in establishing statistically significant differences. Warnings and events were further categorized as being associated with the same event (leading and trailing warnings) or not (solo warnings). This categorization is explained at the beginning of Section 2.2.

The data needed were: 1) storm event data from the National Oceanic and Atmospheric Administration (NOAA) National Center for Environmental Information (NCEI; https://www.ncdc.noaa.gov/stormevents/), 2) storm warning data from the Iowa Environmental Mesonet NWS Watch/Warnings archive (https://mesonet.agron.iastate.edu/request/gis/watchwarn.phtml), and 3) WSR-88D Archive III Status Product (ASP). The ASP data, which contain per-volume-scan information on time, VCP number, SAILS and MRLE status, and volume scan duration, are available on NCEI (https://www.ncdc.noaa.gov/nexradinv/) as well as on Google Cloud (https://console.cloud.google.com/storage/browser/gcp-public-data-nexrad-l3/2019/12?authuser=0&prefix).

On one hand, input data volume should be maximized to reduce statistical uncertainty in the results. On the other hand, background circumstances should be kept constant to reduce unintended biases. Given these opposing exigencies, the analysis period was selected to start on the SAILS deployment date at each WSR-88D site. This varied from 28 February 2014 at KRAX (Raleigh-Durham, NC) to 15 May 2015 at KBYX (Key West, FL). The analysis period end date was 31 December 2022. We set the geographic coverage to be the contiguous United States (CONUS).

To determine the scan mode used at the time of a warning decision, we first matched each severe weather event and warning polygon to the nearest WSR-88D. This procedure assumes that the closest WSR-88D was the one being relied upon most by the forecaster when the warning decision was made. This is not necessarily true, as the closest radar may have been not operating or perhaps a radar farther away had less terrain blockage; also, data from multiple radars may have been consulted. It is impossible to be certain of the "primary" radar that was used without forecasters' logs recording this information. However, because of the large data quantity that we processed, we expect deviations from the assumption (nearest radar being most important) would be fairly small "noise" components in the statistical results.

We then found the ASP volume scan timestamp that was closest to and before the warning issuance time. However, if the difference between the warning issuance time and the ASP timestamp was greater than 11 minutes, the match was discarded. This was necessary to filter out instances where the nearest radar was not in operation or its ASP record was not available (11 minutes marks the longest possible normal

volume scan duration, corresponding to VCPs 31 and 32). For a missed detection, there was no associated warning; it is impossible to know when the decision not to issue a warning was made. In fact, it may be more accurate to say that there was a range of time during which the decision was made not to issue a warning. To account for this spread of time during the assessment period, we subtracted the median warning lead time for that event type (SVR, FF, or TOR) from the initial event-occurrence time, with the idea that this would approximate when the decision not to issue a warning was made. The medians were computed over detected events parsed by warning category (lead, trailing, solo) and enhanced Fujita (EF) scale number groupings (EF0–1, EF2, EF3–5). The median was chosen for this purpose rather than the mean because the median is less sensitive to outliers. Although median lead times also vary with WFO, we did not subdivide the data further in this way, since this would have led to significantly higher variance in the lead-time estimates. This approximate decision time was then used for matching with the ASP scan timestamp.

For FF events, instead of using the event locations directly to find the nearest radar, we first mapped the locations to the corresponding catchment basin polygons—see Cho and Kurdzo (2020a) for details on how this was done. This process more accurately places the radar observations most relevant for FF warning decisions, i.e., where the rain was falling, not where the flooding occurred.

Since a warning decision is not made instantly, one may wonder whether the single scan mode that was being used shortly before the warning issuance time was truly representative of the scan modes operating throughout the decision process. To probe this question, we computed how often the scan modes were changed during the last hour leading up to the warning issuance time. The results are shown in Figure 2. We see that, for the vast majority of cases, the VCP number, SAILS on/off status, and SAILSxN were held constant during that hour. This gives us confidence in the validity of the single, matched scan mode in computing warning performance dependence on scan usage statistics.

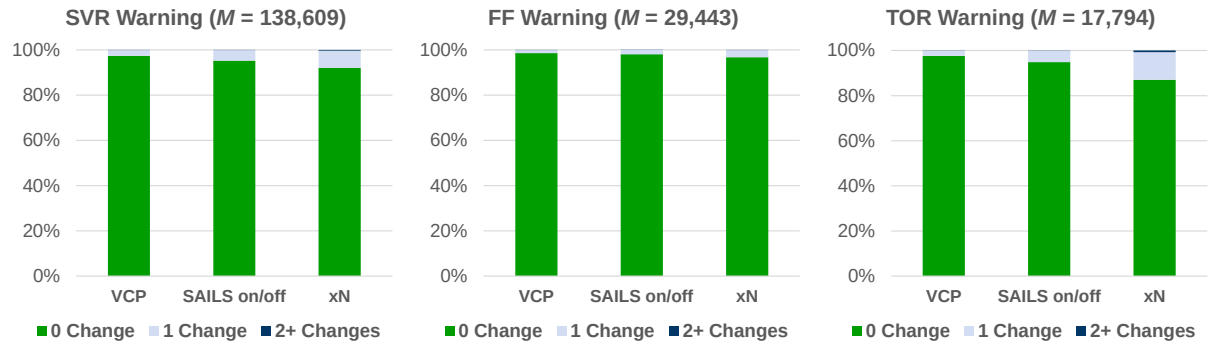

Figure 2. Percentage of cases during one hour prior to when a warning decision was made that a scanning mode (VCP number, SAILS on/off, and SAILSxN) was not changed, changed once, or changed two or more times. M is the number of samples for each warning type.

SAILS usage is restricted to five VCPs: 12, 35, 112, 212, and 215. VCP 35 is a "clear air" mode with a volume update period of ~7 minutes that is rarely employed for non-winter severe weather observation. VCP 215 is a general precipitation surveillance mode with dense upper-elevation sampling and a volume update period of about 6 minutes. VCP 112, which replaced VCP 121 in 2020, is used for large-scale systems with widespread high velocities, and has a volume update period of about 5.5 minutes. VCPs 12 and 212 trade off upper-elevation sampling density in favor of faster volume update periods (about 4 and 4.5 minutes, respectively); the only difference between these two VCPs is that VCP 212 uses pulse-phase coding and processing for second-trip recovery (Sachidananda and Zrnic 1999), whereas VCP 12 does not. The second-trip recovery scheme requires slightly longer scan times, but increases Doppler data coverage to longer ranges. (The approximate volume update periods given above are for when AVSET does not skip any high-elevation scans and SAILS is off.) Furthermore, VCPs 112 and 215 allow only SAILSx1. In order to maintain uniform conditions as much as possible while not discarding too much data, we decided to keep only VCPs 12 and 212 for the SAILS analysis. These two VCPs were used in the overwhelming fraction of warning decisions for all event types (Figure 3): 93% for SVR, 84% for FF, and 96% for TOR.

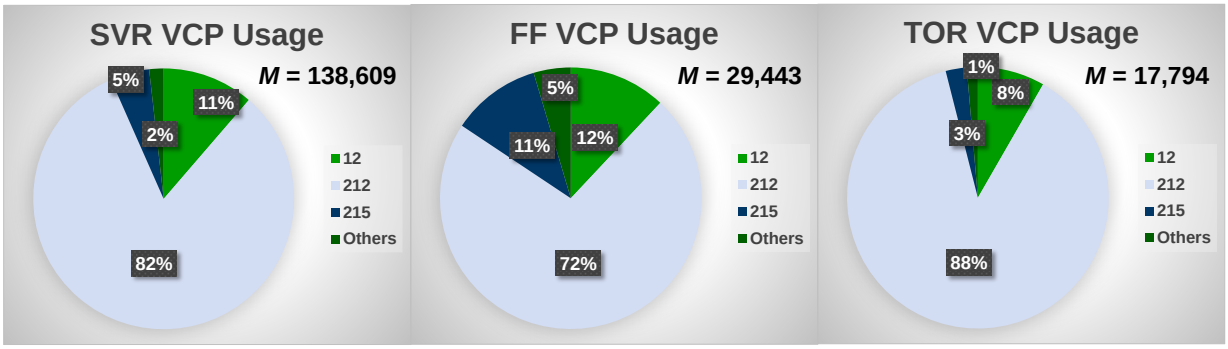

Figure 3. VCP usage frequency by severe weather warning type.

Finally, we know from our past studies that radar coverage quality around the storm location is statistically related to warning performance for TOR (Cho and Kurdzo 2019a,b), FF (Cho and Kurdzo 2020a), and SVR (Cho and Kurdzo 2020b). If there is a strong positive correlation between SAILS usage and radar coverage, e.g., fraction of vertical volume observed (FVO), around the storm of interest, then the statistics of warning performance dependence on SAILS usage could be biased by that correlation. Therefore, we computed the FVO distributions for SAILS off vs. SAILS on for each warning type to check for significant statistical differences. As we did not find such notable differences, we felt confident in proceeding with the SAILS impact analysis.

Regarding the warning performance metrics, we defined a detection when a point event was inside the warning polygon or a polygon-delineated event was inside or intersected the warning polygon, and if any portion of the event duration overlapped the warning-valid interval in time; otherwise, the warning was classified as a false alarm. This definition is consistent with NWS severe convective weather verification

procedures (NWS 2009). For a detection, the lead time was computed as the event's start time minus the initial warning issuance time. By this definition, negative lead times were included in the POD and MLT calculations. Negative lead times consist of a small fraction of all lead times; see, e.g., Figure 7 in Cho and Kurdzo (2020b) for a SVR warning lead time distribution. Including negative lead times increases the number of qualifying events for average lead time calculations, which helps decrease the statistically meaningful confidence interval. POD was calculated as the number of detections divided by the number of events. FAR was computed as the number of false alarms divided by the number of warnings. Multiple events can occur within the same space and time boundaries of a single warning, which implies that even if there were no missed detections, the number of events can be more than the number of warnings.

2.2 SAILS IMPACT RESULTS

NWS forecasters often initially select VCPs (including SAILS modes) based on the expected threat. There may be multiple threat types over disparate geographic areas or over the same area (e.g., coincident severe thunderstorm and flash flood threats), and their relative priorities may evolve with time. The choice between the different levels of SAILS (x1, x2, x3) is a complex decision because one must trade off base scan update rate with volume update rate. Thus, even though the perceived optimal VCP mode may vary over time, in this complex operational forecast and warning environment, the meteorologists' heavy workload may prevent them from changing VCP modes frequently. Therefore, forecasters may tend to default to SAILS-off or SAILSx1 mode until an initial threat detection is made.

With these potential human factors in mind, we computed results in four categories, wherever possible: (1) all data, (2) data associated with warnings that did not overlap with other warnings in space and time (dubbed "solo" warnings), (3) data associated with lead warnings, and (4) data associated with trailing warnings. We tagged a warning as "trailing" if there was any overlap in its valid period with the valid period of a warning issued earlier, and if there was also any overlap in their geographic polygons. This left "lead" warnings as warnings that had at least one space-time overlap with a trailing warning but were the first ones to be issued. SVR, FF, and TOR warnings were each handled separately. In practice, there is sometimes a delay (~1–4 minutes) in the issuance of a follow-up warning, especially during periods of high workload, resulting in a short time gap between the expiration of the earlier warning and the beginning valid time of the trailing warning. To account for this, we allowed up to a four-minute gap in the definition of time overlap. Likewise, there may also be a small spatial gap between an earlier warning polygon and a follow-up polygon. To account for this contingency, we filled out the polygons to their convex hulls and expanded them by 0.05° in latitude-longitude space using the MATLAB function "polybuffer." This procedure allowed angular spatial gaps between polygons of up to 0.1° in the definition of spatial overlap, which is on the order of 10 km at mid-latitudes. The top plot in Figure 4 shows the percentages of warnings in each category. Note that a proposed concept, Threats-in-Motion, seeks to mitigate such gaps by continuously updating polygons that move forward with the storm (Stumpf and Gerard 2021).

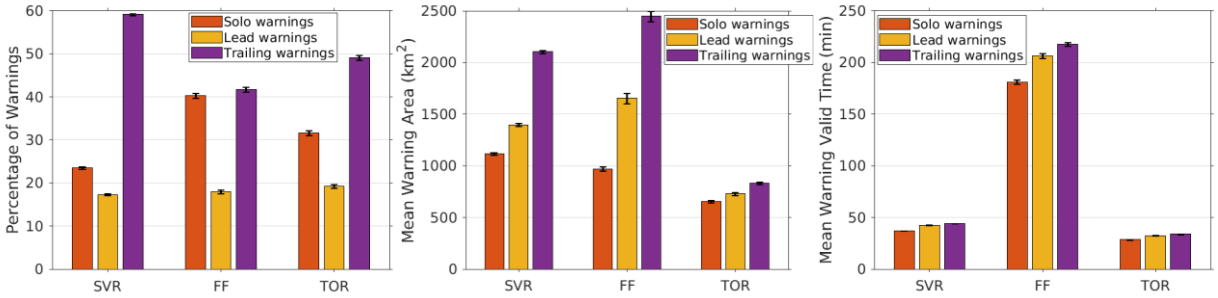

Figure 4. Warning statistics by category: (left) issued percentage, (middle) mean warning area, (right) mean warning valid time. Total data counts were 138,609 for SVR, 29,443 for FF, and 17,794 for TOR. Vertical error bars correspond to 95% confidence intervals (see Section 2.2.1 for details on confidence intervals).

In our earlier paper (Cho et al. 2022), we had parsed the warning categories based on the WFO of warning issuance. For this report, we performed the categorizations regardless of issuance source. This change allows the grouping of warnings that crossed WFO areas of responsibility, and, thus, more accurately reflects the storm phenomenology. The main effect that this change had on the warning statistics was that larger fractions of warnings were categorized as trailing compared to before. The overall results (and conclusions drawn) in the following sections were not impacted in any substantive way.

The FAR for these four categories was calculated directly from the parsed warning data. For MLT, we classified all detected events according to the matching warning. (An event that was successfully predicted by multiple warnings was assigned to the warning with the earliest issuance time.) It was not possible to compute POD separately for solo, lead, and trailing warnings, because its calculation requires knowledge of the number of unwarned events for each category, which cannot be determined.

In operational practice, the event type for which an initial (lead) warning is issued may change for what may be called the trailing warning. Just to give one example, after a TOR warning was issued, a subsequent warning for the same area may be revised to a SVR warning based on a rapidly weakening radar tornado signature. Such “crossover” phenomena are not captured by the event-based warning categories that we used.

Figure 5 displays SAILS usage by warning type. SAILSx1 is the most prevalent scan mode for all warning types, except for TOR trailing warnings where SAILSx3 is most commonly used. This is partly explained by the fact that MESO-SAILS (SAILSx2 and SAILSx3) did not start being deployed until January 2016. However, year-by-year usage plots (Figure 6) indicate that the preference for SAILSx1 has continued in more recent years. Overall usage of SAILS for severe weather warning decisions has also declined somewhat after reaching a peak in 2016. It is also clear that forecasters use SAILS more aggressively in making TOR warning decisions.

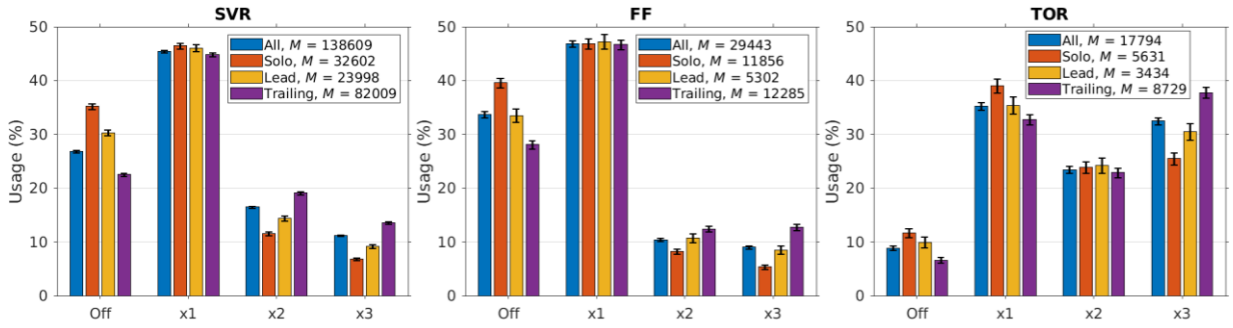

Figure 5. SAILS usage frequency by severe weather warning type and category.

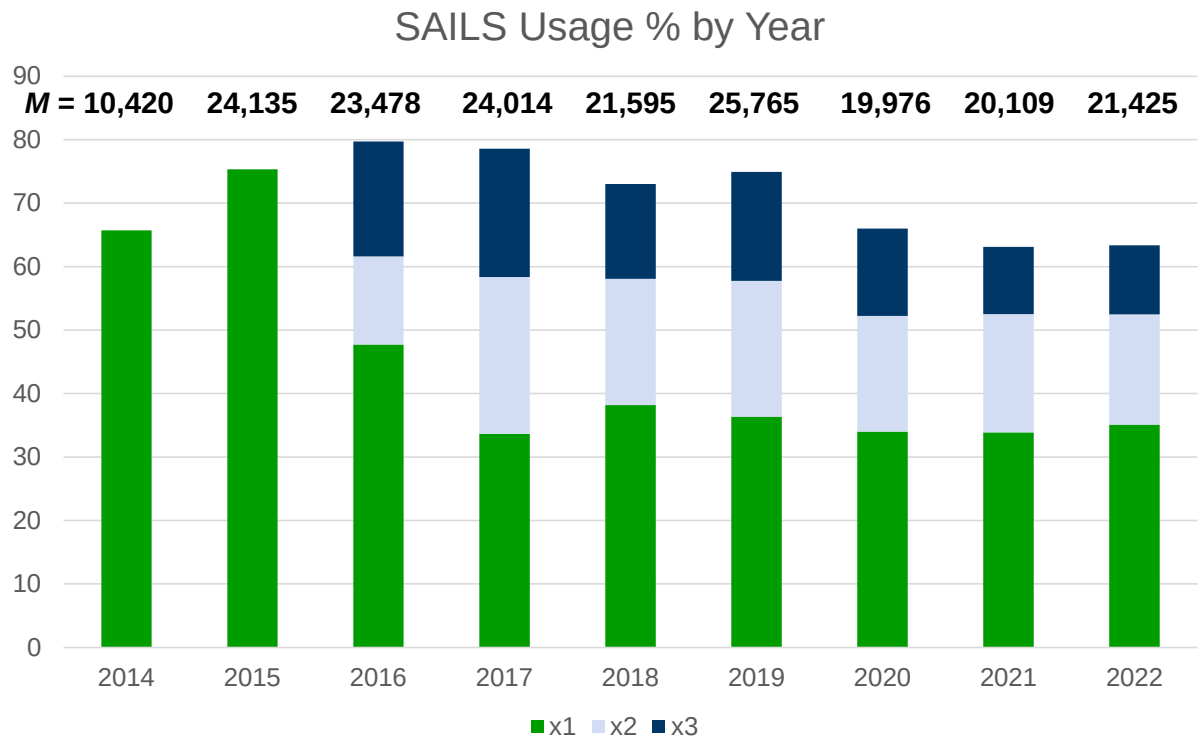

Figure 6. SAILS usage frequency by year for SVR, FF, and TOR warning decisions.

There is a trend of increasing SAILS usage in the order of solo, lead, then trailing warnings, which can be deduced from the fact that SAILS off usage decreases in this order in Figure 5. The same order applies to SAILSx3 usage. It must be noted that this report does not evaluate observed storm mode relative to SAILS usage, only warning type and associated SAILS selections. This precludes the ability to directly assess the nature of the convection in terms of mode, area coverage, and storm motion relative to SAILS trends. Nonetheless, we cautiously surmise that solo warnings tend to be associated with narrower footprint, more transient or faster passing events, e.g., air-mass storms, seen as posing lower threat levels. Lead and trailing warnings, by definition part of multiple linked warnings, may tend to be associated with larger, more persistent storms, e.g., mesoscale convective systems (MCSs) and supercells. This proposition is consistent with the mean warning area being smallest, and the mean warning-valid period shortest (to a lesser extent), for solo warnings (middle and bottom plots in Figure 4).

Because there are many potential factors that influence SAILS usage, we urge caution with drawing too many conclusions here. Nonetheless, one of the possibilities is that the continued preferred usage of SAILSx1 (versus the MESO-SAILS options) is due to forecasters not wanting to overly increase the length of the volume scan. Though this is relevant for all severe weather warning types, it is of particular importance for some wind and most hail events. Given that damaging wind events such as microbursts and large hail events are often warned by observing descending reflectivity cores and observations of mid-level reflectivity convergence (Roberts and Wilson 1989; Schmocker et al. 1996), it makes intuitive sense that increasing the volume update time too much can be seen as a detriment. (We attempt to separate the effects of base vs. volume scan update rates in Section 3.)

Additionally, automated hail algorithms such as MESH (maximum estimated size of hail; Witt et al. 1998) also utilize full-volume data and are frequently used by WFO forecasters as real-time warning guidance for both hail and summer wind warnings (due to the fact that melting hail with high freezing-level environments can enhance downdraft magnitudes; Straka and Anderson 1993). MESH is generated as a function of the frequency of volume scan updates, meaning that heavier MESO-SAILS usage effectively slows down the update rate of volumetric products such as MESH. Given that MESH is heavily used for many summer hail and wind warnings, especially in the southern and eastern U.S., less-frequent selection of MESO-SAILS in these situations would make sense.

2.2.1 SVR Warnings

Figure 7 shows POD, FAR, and MLT for SVR warnings vs. SAILS usage status at the estimated time of warning decision—SAILS off and SAILS on, with the latter further subdivided into SAILSx1, x2, and x3. The short horizontal bars indicate the mean values, and the solid vertical bars are the 95% confidence intervals. For POD and FAR, which are binomial proportion calculations with scores ranging from zero to one, the confidence intervals were estimated by the Wilson score method (Wilson 1927). We chose this formulation due to its conservativeness (on average), coverage probability being consistent and close to the nominal level, and relatively good accuracy even for small sample sizes (Pobocikova 2010). For MLT, the confidence intervals were calculated from $\pm t_{95}\sigma M^{-1/2}$, where M is the number of samples, σ is the standard deviation, and t_{95} corresponds to the number of standard deviations from the mean needed to encompass

95% of the Student's t distribution with $M - 1$ degrees of freedom (e.g., Rees 2001). As M grows large, this formula converges to the familiar 95% confidence interval for the mean of a normal distribution with known standard deviation, $\pm 1.96\sigma M^{-1/2}$.

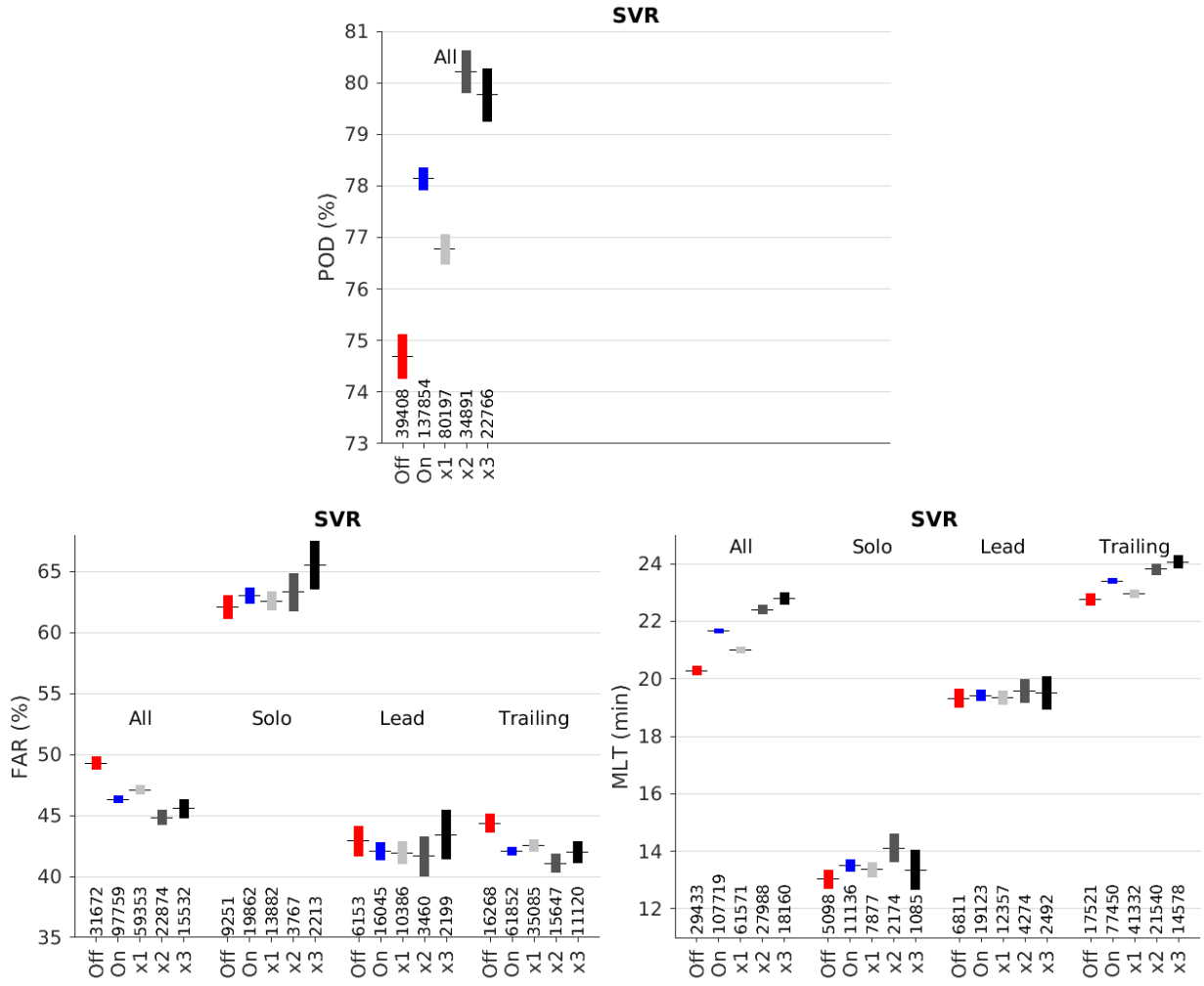

Figure 7. SVR warning performance metrics vs. SAILS usage status. The number of samples per category is displayed at the bottom of each plot. (Colors are used to provide additional visual differentiation between the status categories.) The short horizontal lines denote the mean, and the solid vertical bars are the 95% confidence intervals. (See text for details.)

For the all-warning category in Figure 7, the improvement in SVR warning performance was statistically significant with SAILS on vs. SAILS off—POD was higher, FAR was lower, and MLT was longer. (Differences in performance metrics are statistically significant if the confidence intervals of the

metrics do not overlap.) Furthermore, the SAILSx2 and x3 results exhibited higher skill than the SAILSx1 results, with no statistically significant difference between x2 and x3. One possible explanation for this result is that, for SVR warning decisions, the benefit of adding extra base scans in the VCP reached saturation with SAILSx2. This is because the volume scan update time also increases with the added base scans (a factor that is analyzed further in Section 3). This suggests that the slower volume updates negated any performance boost provided by the third added base scan.

If we only had the all-warning results, one might argue that the apparent gain obtained by using SAILS could have been caused by a correlation between low SAILS usage and worse warning performance for a given warning category. In fact, such a correlation exists—solo warnings have worse FAR and MLT performance relative to lead and trailing warnings, and they are also associated with lower SAILS usage rates (Figure 5). Thus, some of the SAILS benefit apparent in the all-warning results may have contributions from this correlation. However, that correlation cannot explain the fact that the use of SAILS is associated with significantly better FAR and MLT performance *within* the trailing warning category. We conclude that SAILS helps SVR warning decisions, at least for trailing warnings (which form the largest share of SVR warnings). Perhaps for solo and lead warnings, a 3D volumetric awareness of the evolving storm and/or increased assessment of cutting-edge storm features (e.g., ZDR arc) are more critical than just more frequent base scan updates in deciding whether or not to pull the trigger on an initial warning.

Because storm morphology and occurrence rate vary by geographic region and season, and warning methodology and culture can differ between WFOs (Andra et al. 2002; Smith 2011), the relationship between SAILS usage and warning performance can vary from office to office. We checked for such an effect by computing the warning performance metrics separately for each of the 115 CONUS WFOs. Only 29 had statistically significant (at the 95% confidence level) differences in POD between the SAILS-off and -on cases. For 25 out of those 29 WFOs, POD was higher with SAILS on. For FAR, the number of WFOs with statistically significant differences was 15, with 13 having lower FAR with SAILS on. For MLT, the number of WFOs with statistically significant differences was 27, with 23 having longer MLT with SAILS on. Thus, even though we are focusing on the overall CONUS results in this section, it is clear that there is substantial heterogeneity at the WFO level, which we will show in more detail in section 4.

SVR warnings are verified by the presence of a thunderstorm wind or hail event (NWS 2009), which means that POD and MLT (but not FAR) can be computed separately for each event type. Figure 8 shows the consequent POD and MLT results for hail and thunderstorm wind. The overall statistical trends were similar to the aggregate results of Figure 7; however, the improvements in SVR POD and MLT performance that were associated with SAILS usage were noticeably greater for thunderstorm wind compared to hail. In fact, while the SAILS benefit for thunderstorm wind is apparent within the solo and trailing warning categories for MLT, there is no statistically significant SAILS advantage within any of the warning categories for hail MLT. A possible factor is that volumetric update rates are more critical for descending hail cores and automated hail detection algorithms than rapid base scan updates. Large hail is often observable at mid-levels, manifesting as a descending reflectivity core before reaching the ground (e.g., Donavon and Jungbluth 2007). When combined with a forecaster's knowledge of the environmental

freezing levels, this can become more important during the warning process than rapidly updating base scans. These results agree well with earlier findings from PAR-based severe thunderstorm case studies (Bowden and Heinselman 2016). In short, this is a strong argument for rapid volumetric updates (e.g., via MRLE or a future PAR system) rather than simply rapid base scan updates. However, it should also be noted that warning for hail *can* be somewhat automated by diagnostic, algorithmic-based guidance such as MESH, probability of severe hail (POSH), etc. Although these incorporate volumetric data, SAILS data *could* decrease the effective algorithmic update rate due to slower higher-elevation update rates. It is important to remember, though, that wind hazards do not have the same diagnostic parameters available to forecasters as hail, making the SAILS updates possibly more useful for SVR wind warnings. Note that, for hail, the results for MRLE (which is a compromise between low-level scan update rate and vertical coverage) in Section 2.3 show a greater potential benefit over SAILS.

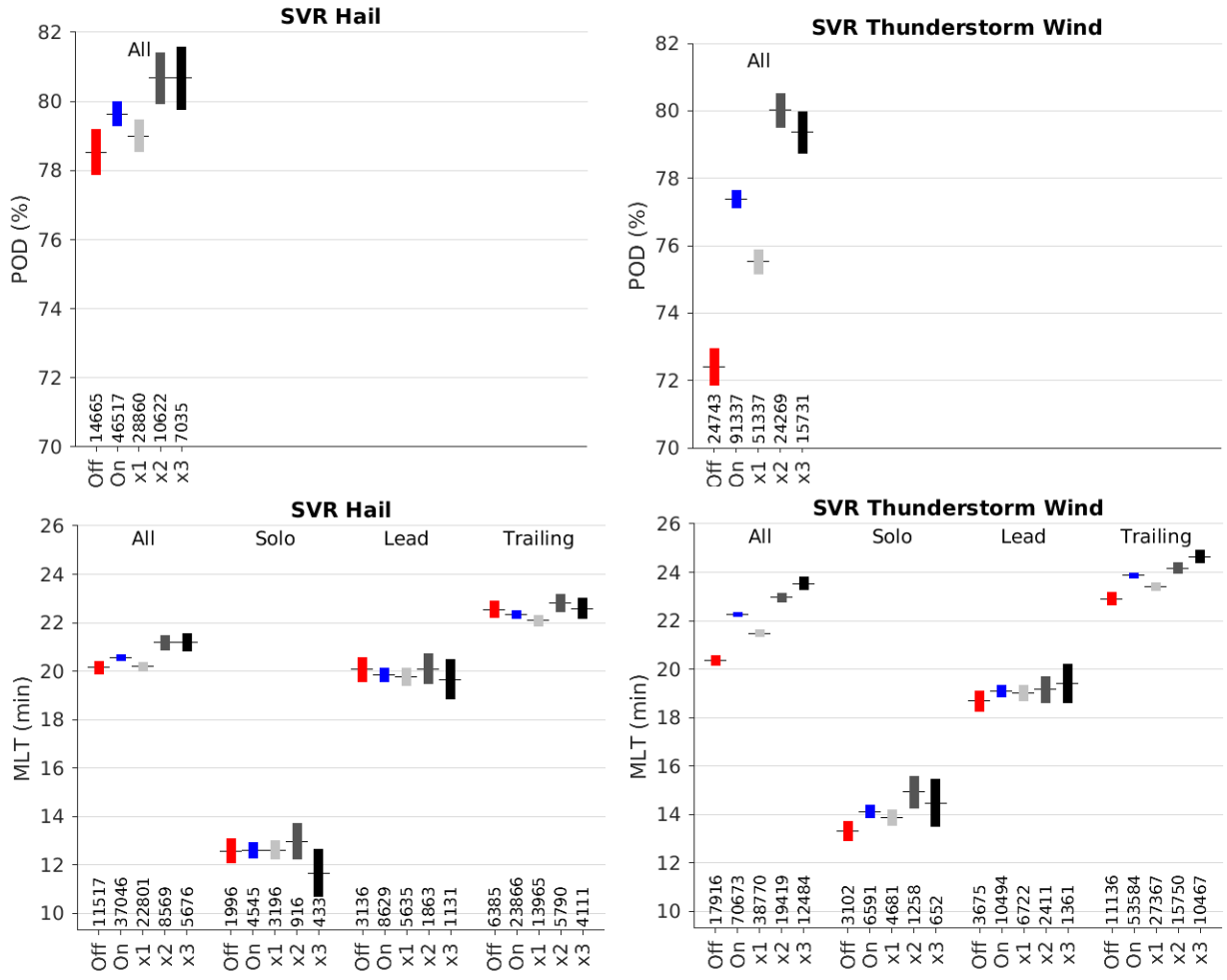

Figure 8. SVR POD and MLT performance vs. SAILS usage status, separated by event type.

Severe winds, on the other hand, can manifest in several different ways. For example, in a pulse storm microburst situation, a descending reflectivity core can be equally useful for a wind threat as it is in other scenarios for hail threats, depending on the thermodynamic environment. However, there are other situations where severe winds can be assessed at the base scan level without as much of a need for rapid volumetric scanning. These scenarios are often prevalent in rapidly moving bow echoes and forward-propagating quasi-linear convective systems (QLCSs) where a rear inflow jet is forcing mesoscale severe winds at the surface, either with the onset of precipitation or as part of a gust front (Markowski and Richardson 2010). In these cases, rapid base scan updates can be particularly useful for a forecaster.

2.2.2 FF Warnings

Figure 9 displays POD, FAR, and MLT for FF warnings vs. SAILS usage status at the estimated time of warning decision. As with SVR warnings, SAILS utilization corresponded with improved warning performance in the all-warning category. SAILSx2 and SAILSx3 did significantly better than SAILSx1 for FAR in the all-warning category. SAILSx3 did significantly better than SAILSx1 and SAILSx2 for MLT, although this difference comes entirely from the trailing warning category. Thus, although there are hints in these results that the fastest base scan updates provided by SAILSx3 may be beneficial for FF warning decisions, it may not be the optimal choice in all cases. The best balance between faster base scan updates and slower volume scan updates may be situation dependent. Note that a recent flash flood model study showed that the peak stream discharge estimate was 10% lower using 5- vs. 1-minute radar volume updates (Wen et al. 2021); it would be valuable to deconvolve the effects of faster base scan updates from those of faster volume scan updates in future studies.

As with the SVR results, the solo warning category showed noticeably worse warning statistics compared to the lead and trailing warning categories. And since SAILS is used more often with the latter warning categories, these correlations could have accounted for the apparent SAILS performance boost in the overall results. However, because even within these warning categories (all three for FAR and trailing for MLT), SAILS-on was associated with better warning performance relative to SAILS-off, we can be confident that the SAILS usage benefit for FF warnings is real and not just the product of the above-mentioned correlations, just like in the SVR warning case.

Interestingly, in the trailing warning MLT sub-category for both SVR thunderstorm wind and FF, SAILSx3 significantly outperformed the other options. Perhaps once a storm is already established as being a threat for these hazards, more frequent updates of the phenomenon itself (near-surface wind and rainfall) become more useful for prediction.

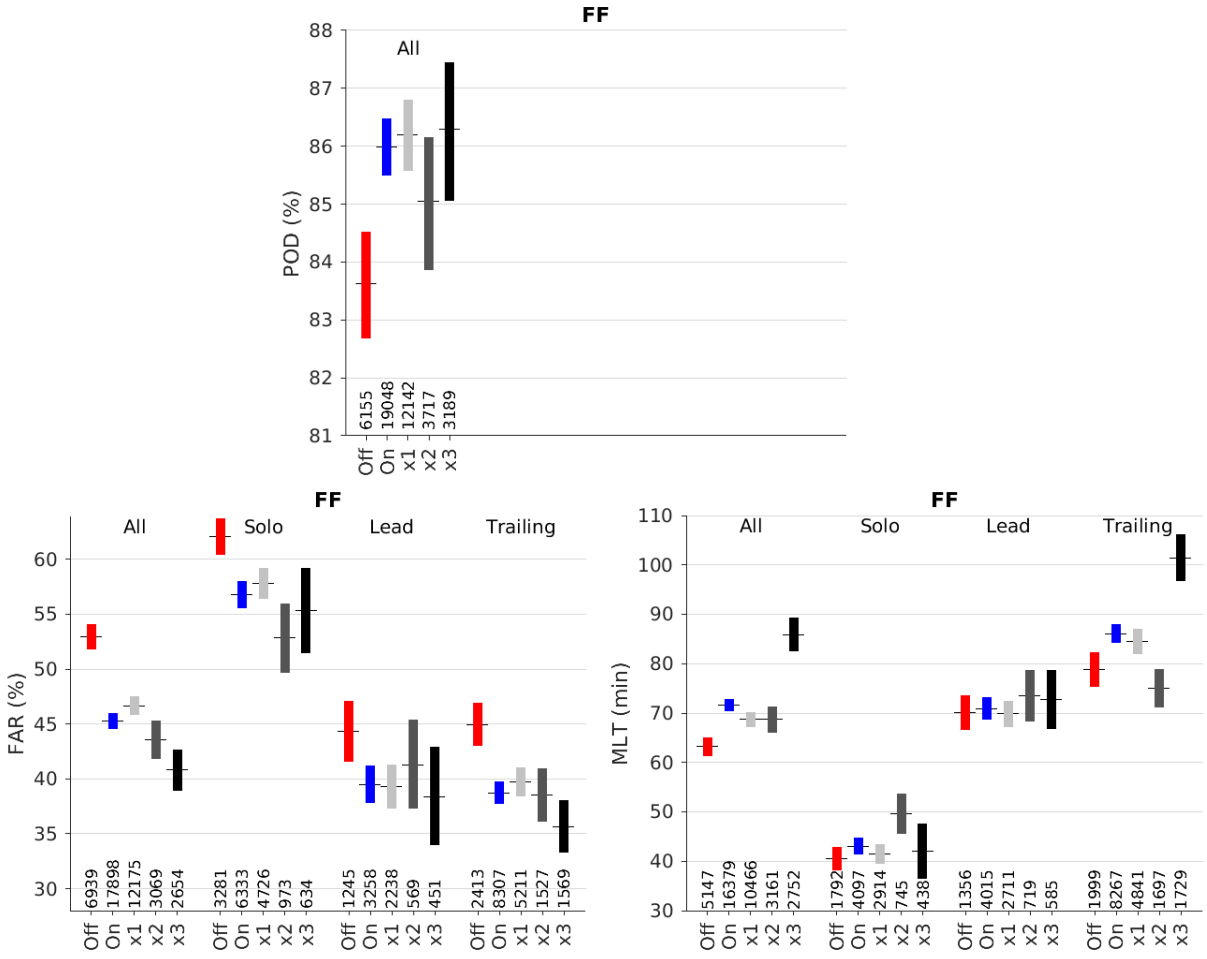

Figure 9. FF warning performance vs. SAILS usage status.

In a parallel study on the effects of SAILS on quantitative precipitation estimation (QPE; Kurdzo et al. 2021), we found that SAILSx3 was a statistically significant indicator for more accurate QPE compared with SAILS-off and other SAILS/MESO-SAILS modes. This was true across several QPE methods, which points to the possibility that faster base scan updates than provided by SAILSx3 might lead to even more accurate QPE. The importance of the base scan cannot be overstated for QPE and FF warnings, since QPE on the WSR-88D is calculated using the hybrid base scan only (Fulton et al. 1998). In a dynamic, rapidly evolving heavy rainfall situation, the faster base scan updates allow for shorter integrations of a given rainfall rate, effectively increasing the spatial resolution of rainfall rate estimation along with the obvious improvement in temporal resolution. Additionally, convective heavy rainfall is often caused by "training" storms over a given area. These cases would also conceivably benefit from faster base scan updates for QPE totals because of the expected faster forecaster recognition of FF potential.

With increased QPE accuracy, we would expect to see better FF warning performance. This argues that faster base scan updates could conceivably further improve FF warning statistics. Additionally, assuming FF warning performance is related to QPE accuracy, use of the vertical profile of reflectivity (VPR; e.g., Kirstetter et al. 2010) technique in future operational scenarios would conceivably also increase the performance of both. However, VPR benefits would only be realized in the event of rapid volumetric scan updates; again, an argument for the benefits of PAR weather radar architectures in the future.

2.2.3 TOR Warnings

Figure 10 shows POD, FAR, and MLT for TOR warnings vs. SAILS usage status at the estimated time of warning decision. In the all-warnings category, SAILS utilization was associated with significantly improved POD and FAR. Furthermore, POD significantly increased monotonically with SAILSx1, x2, and x3, while for FAR and MLT, SAILSx3 was associated with statistically better performance compared to SAILSx1 and x2. Nonetheless, the SAILSx1 and x2 cases were statistically indistinguishable for FAR and MLT, which raises the question of whether there is utility in selecting SAILSx2 over x1 in TOR warnings given that skipping over x2 to x3 showed the best statistical performance.

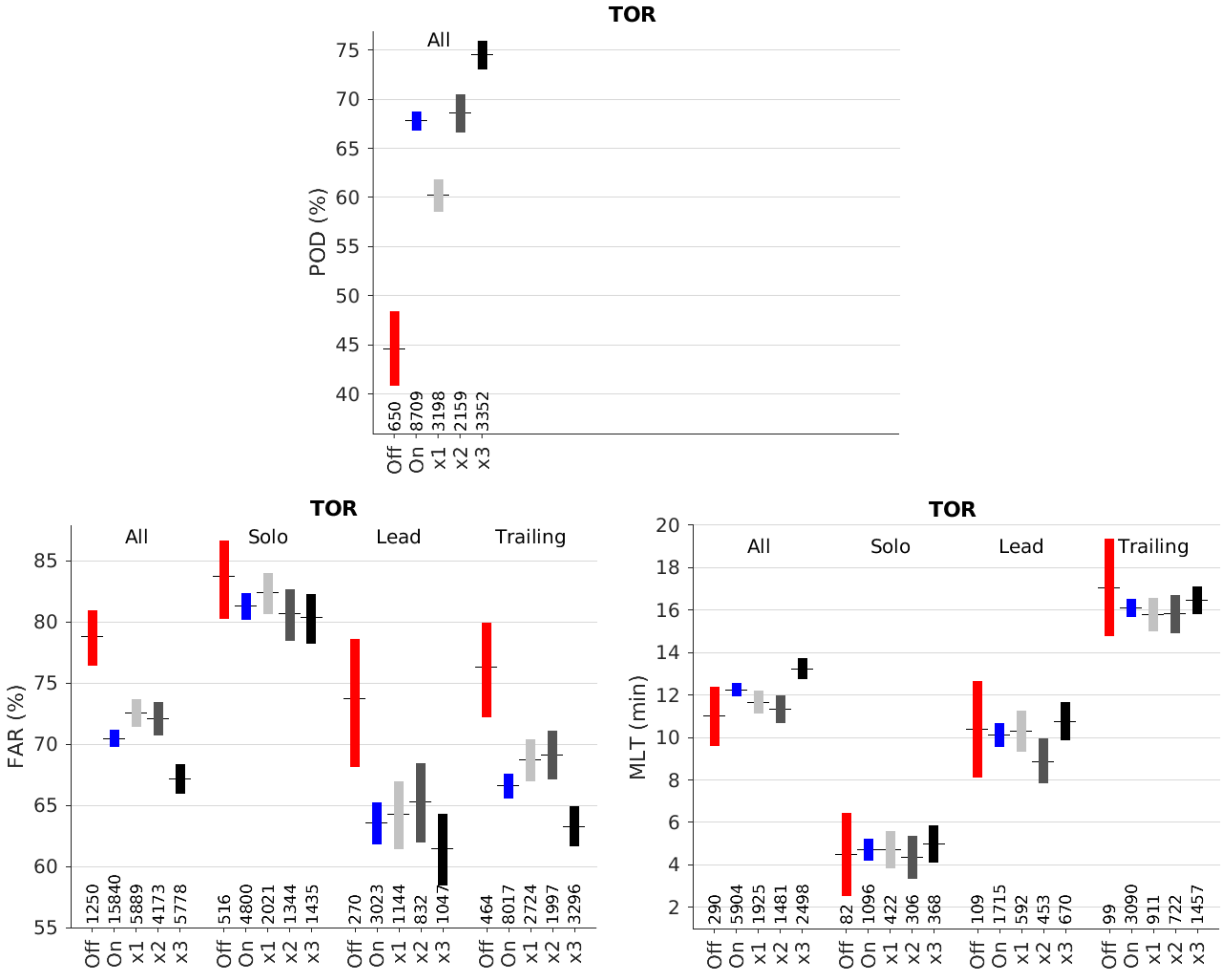

Figure 10. TOR warning performance vs. SAILS usage status.

As with SVR and FF, the FAR and MLT performances were significantly worse for solo TOR warnings relative to lead and trailing warnings. As we discussed earlier, this may be due to solo warnings tending to be associated with faster passing, more transient events. This is consistent with TOR warning performance being worse for disorganized storms and QLCSs compared to supercells (Brotzge et al. 2013; Anderson-Frey and Brooks 2021). (Note that the solo warning category could also include situations where a TOR warning transitioned directly to a SVR warning following a spotter report of no low-level rotation and/or a noticeable weakening in the radar velocity signature.) Thus, since SAILS is used less often for solo warnings, these correlations could have accounted for some of the apparent SAILS performance boost for FAR. Nevertheless, the significantly better FAR performance with SAILS on *within* the lead and trailing

warning categories gives us confidence that these apparent SAILS benefits for FAR are not just due to such correlations.

For MLT, the situation was more ambiguous. There was no clear statistical separation between the SAILS-off and -on cases. However, under the all-warnings category, the SAILSx3 case yielded a statistically significant increase in MLT compared with all of the other modes.

Taken overall, the Figure 10 results indicate that providing forecasters with more frequent base scan updates than given by SAILSx3 might help improve TOR warning performance further. This agrees, at least conceptually, with the multitude of studies utilizing experimental mobile rapid-scan radar systems for observations of tornadoes and tornadogenesis (e.g., Bluestein et al. 2007; Wurman et al. 2007; Kosiba et al. 2013; Kurdzo et al. 2017). The incredibly rapid changes that can occur in the low-level mesocyclone, the rear-flank downdraft, and the surrounding wind field seen in several rapid-scan radar studies suggests that ~90-s updates of the base scan do not provide enough detail to forecasters issuing warnings (Wilson et al. 2017). These update rates are particularly critical in the most rapidly forming and shorter-lived tornadoes, such as those in QLCS or tropical environments. Rapid tornadogenesis can also occur in supercells, especially recently developed supercells in environments primed for tornadoes, as well as in cases of frequent, cyclic tornadogenesis. The precursors to tornadogenesis in these scenarios can be short-lived and subtle (e.g., Sessa and Trapp 2020)—in these situations, the QLCS mesovortex three ingredients method (Schaumann and Przbylinski 2012) can be useful; however, faster scan updates would likely be even more helpful. To investigate the impact of SAILS on TOR warning performance for different background weather situations, we parsed the results according to storm type in Section 2.2.3.1.

We know from past studies that TOR warning performance is strongly related to the tornado's EF damage rating number, with greater warning skill associated with higher EF-scale ratings (e.g., Simmons and Sutter 2005). Therefore, we tried parsing our POD and MLT results in this way. (Such parsing is not possible for FAR, since false alarms do not have associated tornado events.) From past experience (Cho and Kurdzo 2019a,b), we knew that EF0 and EF1 tornadoes tend to have similar POD and MLT statistics, whereas the occurrence rates for EF3-and-above tornadoes dwindle rapidly. Thus, we divided the results according to three groups—EF0–1, EF2, and EF3–5. The results are shown in Figure 11.

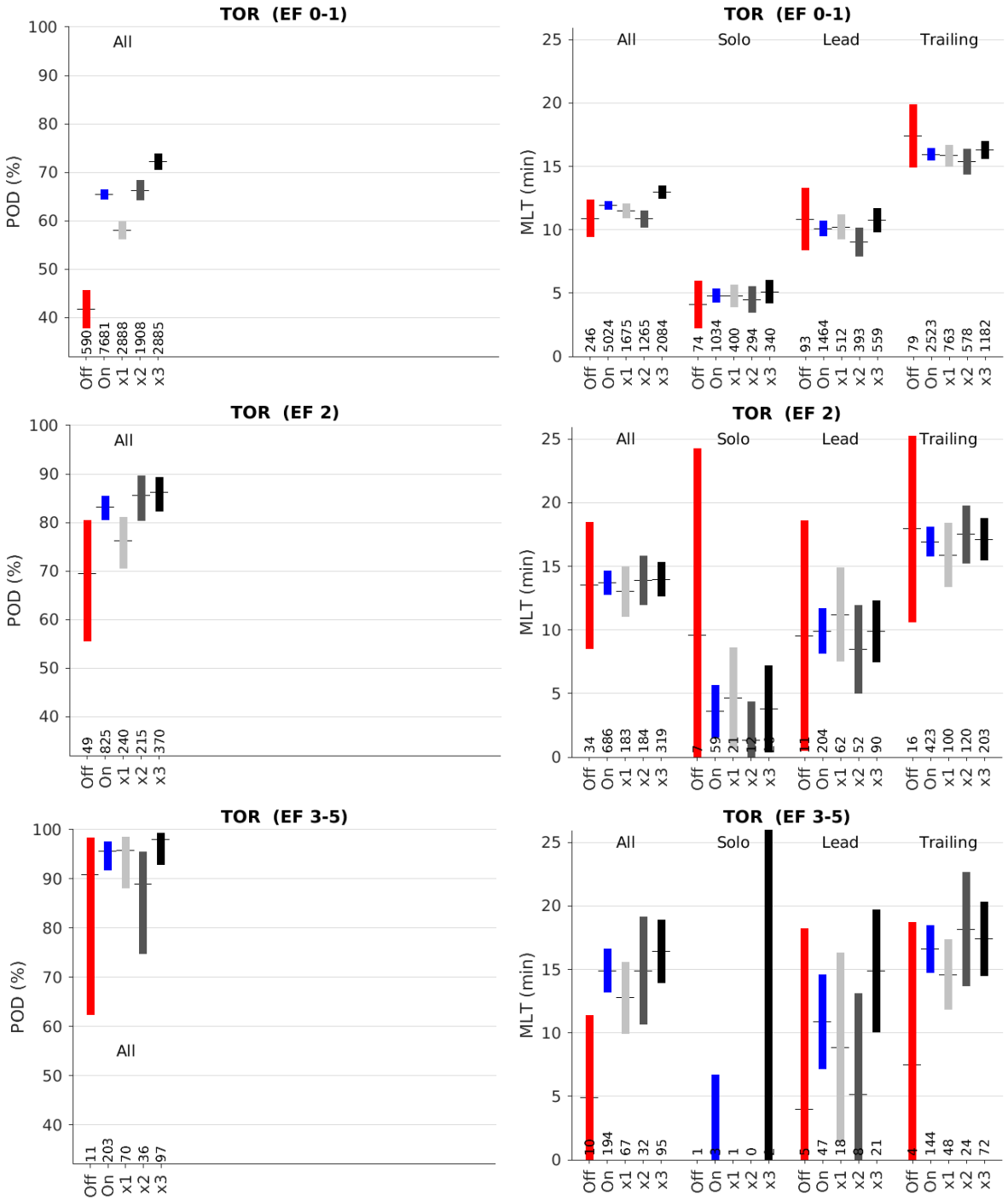

Figure 11. TOR POD and MLT performance vs. SAILS usage status, separated by EF number groups. Results with sample size less than two were not plotted.

The EF0–1 results were quite similar to the overall results in Figure 10, which is to be expected since this group encompassed most (88%) of the tornado events. As for EF2, the only clear difference amongst the various SAILS usage statuses was that the SAILS-on case yielded significantly higher POD than the SAILS-off case, and SAILSx3 was associated with a higher POD than SAILSx1. With EF3–5, the only statistically significant result was that the SAILS-on case was associated with longer MLT than the SAILS-off case. Although the sample size was relatively small, this last result is noteworthy, since increasing the lead time for these deadliest tornadoes is one of the most important goals for the NWS.

2.2.3.1 TOR Warning Results Parsed by Storm Type

Tornadoes are generated by different types of convective storms, and the optimal radar scanning strategy may vary for these different situations. Although we have now seen that SAILS is an effective scanning option when making tornado warning decisions, it would be even more helpful to know whether this result varies with convective mode. In order to probe this question, we utilized a tornado events database from the NWS Storm Prediction Center (SPC) that assigned the parent storms to various categories. For this analysis, we took a subset of those categories that contained enough data points for deriving statistically meaningful impact results for TOR warnings. These categories are listed in the left-hand column of Table 1, together with the shorthand label that are used in subsequent figures. Table 1 also shows the mapping of these categories to the three major convective modes and their subtypes as defined by Smith et al. (2012). Note that there were so few left-moving supercell instances that we omitted those cases from the supercell subcategories as indicated in Table 1.

Figure 12 shows the SAILS mode usage rates by tornadic storm type. For this graph, the tropical cyclone ("TropCyc") category was included, even though it did not have enough data points for the SAILS impact analysis, because the SAILS usage rates were markedly different. According to this plot, forecasters appear to utilize SAILS more aggressively for rapidly developing storm types, such as supercell/cell in line, QLCS, and tropical cyclones. It makes sense that they would seek to obtain faster updates of at least the base scan in these situations.

TABLE 1
Tornadic Storm Classification and Labeling Scheme

Study Category [Label]	Supercell (RM and LM)*			QLCS		Disorganized		
	Cell in Line	Cell in Cluster	Discrete Cell	Line	Bow Echo	Cluster	Cell in Cluster	Discrete Cell
RM supercell [RMSup]	RM	RM	RM					
RM supercell/cell in line [RMSupLine]	RM							
RM supercell/cell in cluster [RMSupClust]		RM						
RM supercell/discrete cell [RMSupDisc]			RM					
QLCS [QLCS]				All	All			
Disorganized [Disorg]						All	All	All
Supercell/cell in Line + QLCS [AnyLine]	All			All	All			
Supercell/discrete + disorganized/ discrete [Discrete]			All					All

*RM = right-moving, LM = left-moving

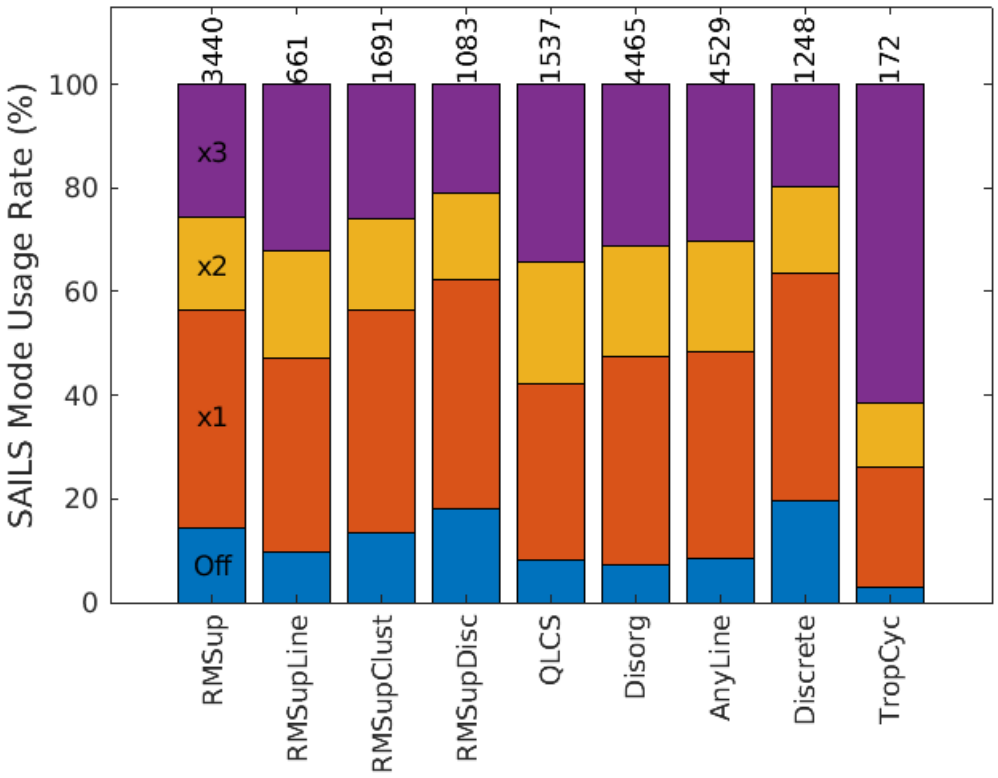

Figure 12. SAILS mode usage rate by tornadic storm type. Number of data points per type is listed at the top.

Brotzge et al. (2013) computed TOR POD and lead time parsed by storm type. Their results showed that these TOR warning performance metrics were best for the supercell/discrete cell category followed by, in descending order, supercell/cell in cluster, supercell/cell in line, QLCS, and disorganized. Interestingly, this is exactly the opposite order of SAILS usage rate in Figure 12. The implication is that forecasters are choosing to use SAILS more during situations that have historically been harder for TOR warnings decisions.

Figure 13 shows the dependence of TOR POD on SAILS mode and storm type. For all except the supercell/cell in line category (for which the sample size is smallest), SAILS-on was associated with significantly higher POD than SAILS-off. Furthermore, SAILSx3 performed significantly better than SAILSx1 and SAILSx2 for most of the storm types. Therefore, SAILS (especially SAILSx3) seems to be a good choice for TOR warning decisions in virtually any type of convective mode.

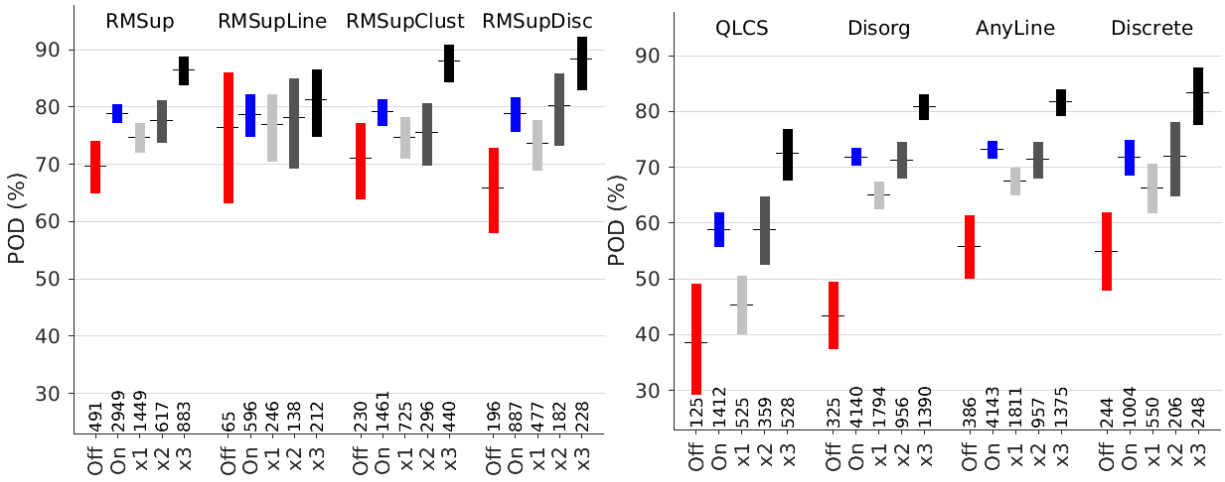

Figure 13. TOR POD vs. SAILS usage status, parsed by storm type.

For the hardest-to-warn TOR storm categories, the historical detection probabilities from the pre-SAILS era were: POD of 48.6 ± 6.2% for QLCS and 44.2 ± 4.7% for disorganized (Brotzge et al. 2013). Comparison with Figure 13 shows that these values are essentially equal to the current values with SAILS off. Thus, the significantly higher detection probabilities we see today with SAILS on for QLCS and disorganized storms form a strong case for claiming a tangible, likely life-saving, benefit of SAILS.

The historical TOR detection probabilities for the supercell sub-categories from the pre-SAILS era were: POD of 80.5 ± 5.1% for cell in line, 84.6 ± 2.4% for cell in cluster, and 87.9 ± 2.4% for discrete cell (Brotzge et al. 2013). The latter two figures are actually higher than the current POD values for those supercell sub-types, although they are matched by the SAILSx3 results. This is likely due to the fact that there was a sharp decline in TOR POD between 2011 and 2014 that has been attributed to a concerted effort to reduce FAR (Brooks and Correia 2018). It is, thus, even more remarkable that the TOR detection probabilities for the QLCS and disorganized storm types have made such great strides with SAILS.

Figure 14 shows the dependence of TOR MLT on SAILS mode and storm type. We do not observe any statistically significant benefit for SAILS except for QLCS, where SAILSx3 performed better than SAILS-off. The pre-SAILS TOR warning MLT for QLCS was 12.3 minutes (Brotzge et al. 2013), which falls within the current SAILS-off range. Therefore, the longer MLT with SAILSx3 for QLCS could be claimed as a SAILS benefit. As with POD, the supercell/cell in line category is an anomaly, likely due to the small sample size. These ambiguous results may be a reflection of just how difficult it is to increase TOR warning lead time beyond about 15 minutes, simply due to the limits in our understanding of why one storm spawns a tornado and a similar-looking one does not.

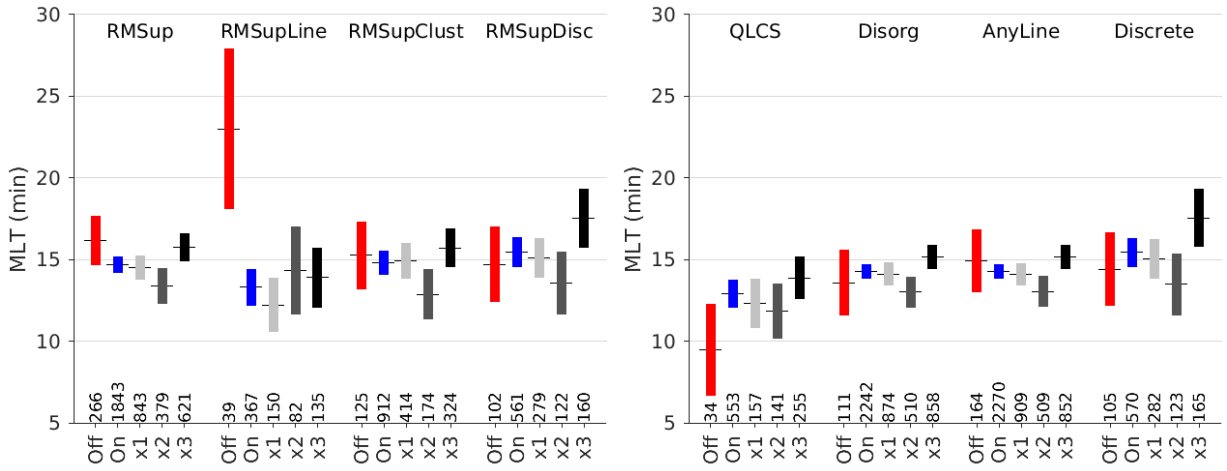

Figure 14. TOR MLT vs. SAILS usage status, parsed by storm type.

Note that FAR statistics could not be parsed by storm type because false alarm cases (non-tornadic storms) were not catalogued in the storm classification database.

2.3 MRLE IMPACT RESULTS

MRLE was introduced after the deployment of SAILS in order to provide WSR-88D operators with the choice of more frequent updates of not just the base scan, but successively higher angle scans as well. SAILSx1 adds a base (0.5° elevation angle) scan in the middle of a VCP; on top of that starting point, MRLE adds progressively higher angle scans in the middle of a VCP. Let us label these options as MRLE+L, where *L* is the number of scans added in the middle of the VCP. Then MRLE+2 revisits the 0.5° and 0.9° cuts in the middle of the VCP, MRLE+3 revisits the 0.5°, 0.9°, and 1.3° in the middle of the VCP, and MRLE+4 revisits the 0.5°, 0.9°, 1.3°, and 1.8° in the middle of the VCP. Currently, these are the three options available for MRLE. (Note that by this definition, MRLE+1 equals SAILSx1, so we will not use the former term to avoid confusion and redundancy.)

As with SAILS, there is a price to pay for adding these extra scans in the middle of the VCP—the volume scan update time will increase. Furthermore, the base scan update period will also increase with higher *L*, but not to the same extent. These effects are shown in Figure 15. The radar operator must take these trade-offs into consideration when choosing SAILS and MRLE options.

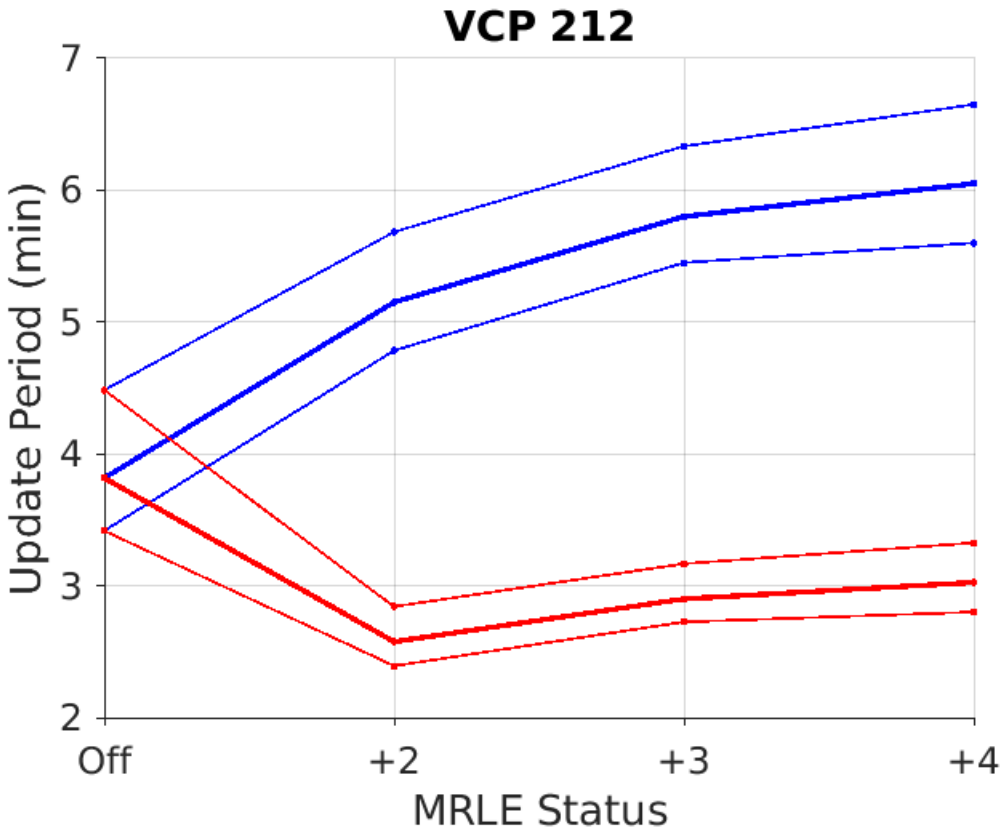

Figure 15. Base scan update period (red) and volume scan update period (blue) vs. MRLE status for VCP 212. The thick lines correspond to the medians and the thin lines denote the 25th and 75th percentile values.

Figure 16 shows MRLE usage rates during SVR, FF, and TOR warning decisions. The rates are much lower than SAILS usage rates (Figure 5). For SVR warnings, there is a clear trend of more frequent usage with solo, lead, and trailing warnings, in that order. There is no such clear trend for FF and TOR warnings. For SVR and FF warnings, there is decreasing usage in the order of MRLE+2, +3, and +4, whereas for TOR warnings, MRLE+2 and +3 have comparable usage rates that are greater than for MRLE+4. The overall low usage rate for MRLE may partly be explained by its newness, i.e., the unfamiliarity of this option to the radar operator. The year-to-year record (Figure 17) indeed shows that during the initial two years in which MRLE was being rolled out nationally, its usage was extremely limited. However, after a sharp rise to a peak in 2021, the MRLE usage rate seems to have settled back down in 2022 at a level that is still an order of magnitude lower than the SAILS usage rate. Thus, it is clear that SAILS is the favored option under most severe weather warning situations, whereas MRLE is chosen on more restricted occasions.

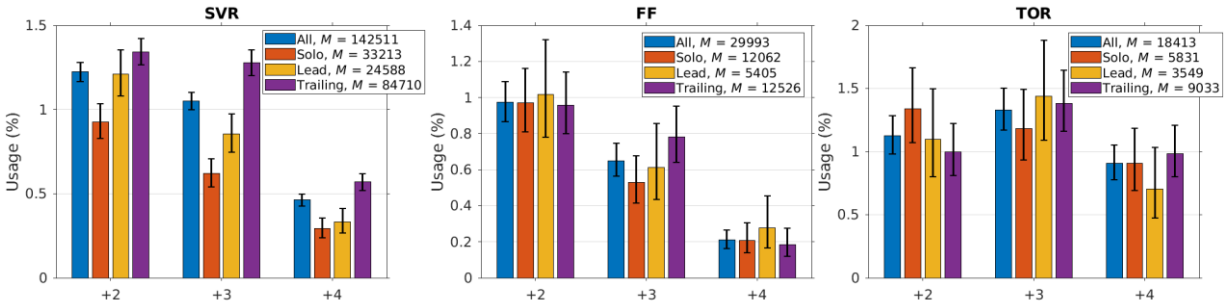

Figure 16. MRLE usage frequency by severe weather warning type and category.

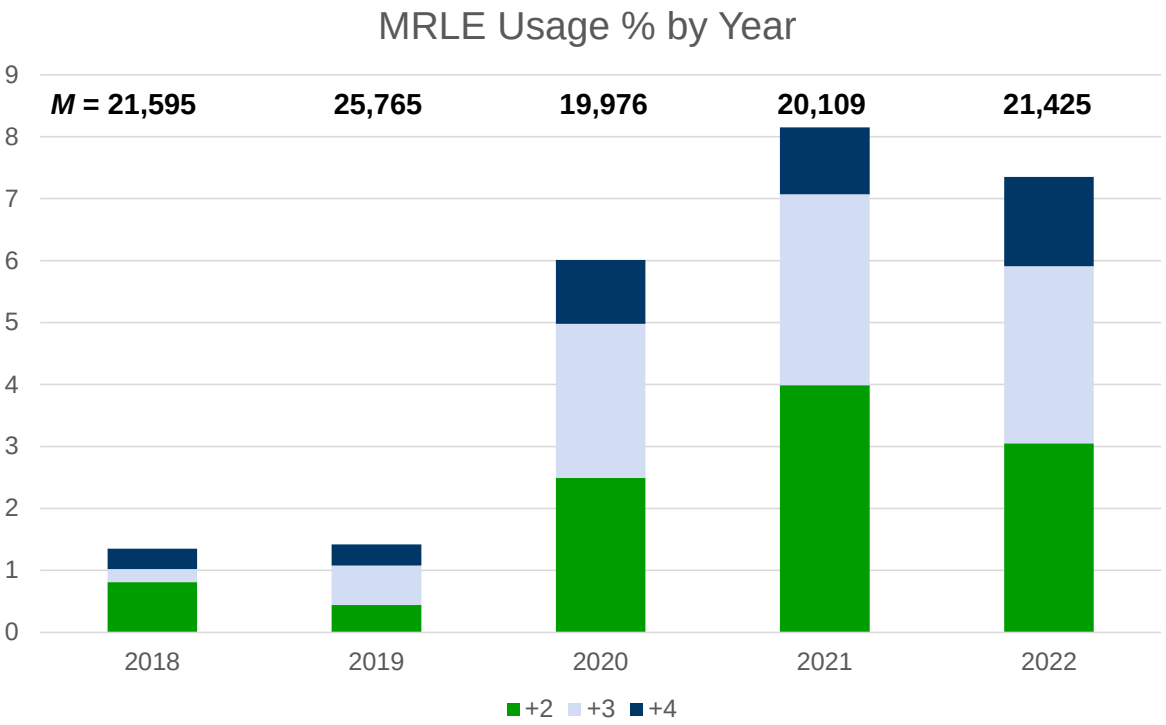

Figure 17. MRLE usage frequency by year for SVR, FF, and TOR warning decisions.

2.3.1 SVR Warnings

Figure 18 shows POD, FAR, and MLT for SVR warnings vs. MRLE usage status at the estimated time of warning decision. The uncertainty bars for the MRLE-on cases are much longer relative to SAILS

results due to the much smaller sample numbers. For the MRLE-off cases, we used the same data span as for the SAILS-off cases in order to provide the same "off" baseline for both SAILS and MRLE.

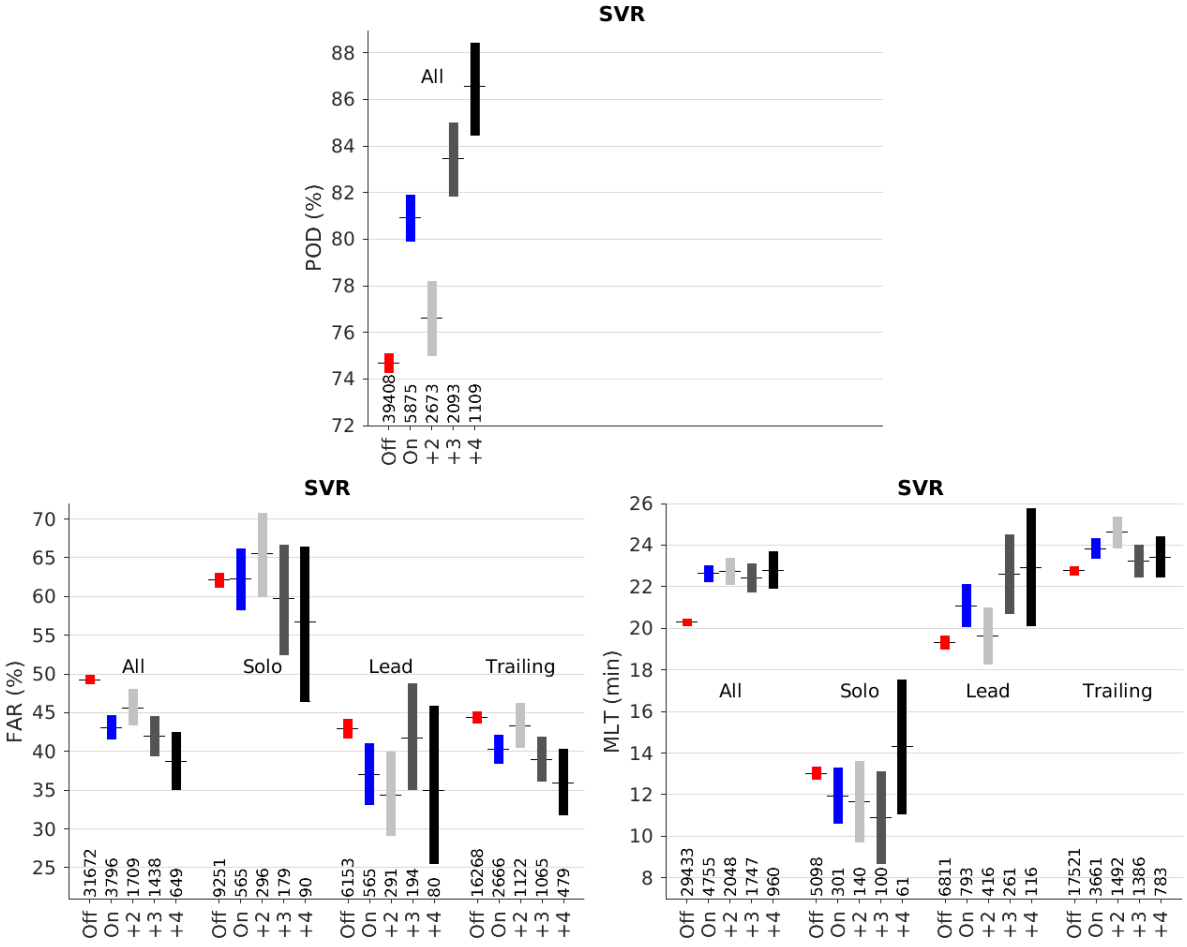

Figure 18. SVR warning performance metrics vs. MRLE usage status. The number of samples per category is displayed at the bottom of each plot. The short horizontal lines denote the mean, and the solid vertical bars are the 95% confidence intervals.

For the all-warning category in Figure 18, the improvement in SVR warning performance was statistically significant with MRLE on vs. MRLE off—POD was higher, FAR was lower, and MLT was longer. For POD, the MRLE+3 and +4 results exhibited higher skill than the MRLE+2 results, with no statistically significant difference between +3 and +4. Also of note is that the FAR and MLT performances were significantly better with MRLE on within the lead and trailing warning categories. As with SAILS, if we only had the all-warning results, one might argue that the apparent gain obtained by using MRLE could have been caused by a correlation between low MRLE usage and worse warning performance for a given

warning category. In fact, such a correlation exists—solo warnings have worse FAR and MLT performance relative to lead and trailing warnings, and they are also associated with lower MRLE usage rates (Figure 16). Thus, some of the MRLE benefit apparent in the all-warning results may have contributions from this correlation. However, that correlation cannot explain the fact that the use of MRLE is associated with significantly better FAR and MLT performance *within* the lead and trailing warning categories. We conclude that the use of MRLE helps SVR warning decisions, at least for lead and trailing warnings.

Figure 19 shows the POD and MLT statistics computed separately for hail and thunderstorm wind events (FAR cannot be parsed by event type, because false alarms are not associated with events). The overall statistical trends were similar to the all-events results of Figure 18, with POD and MLT showing better performance with MRLE on for both hail and wind events. POD for thunderstorm wind, however, shows progressively better performance with MRLE+2, +3, and +4. And for solo warnings, MRLE does not appear to provide a benefit—in fact, for hail MLT, it is associated with worse performance.

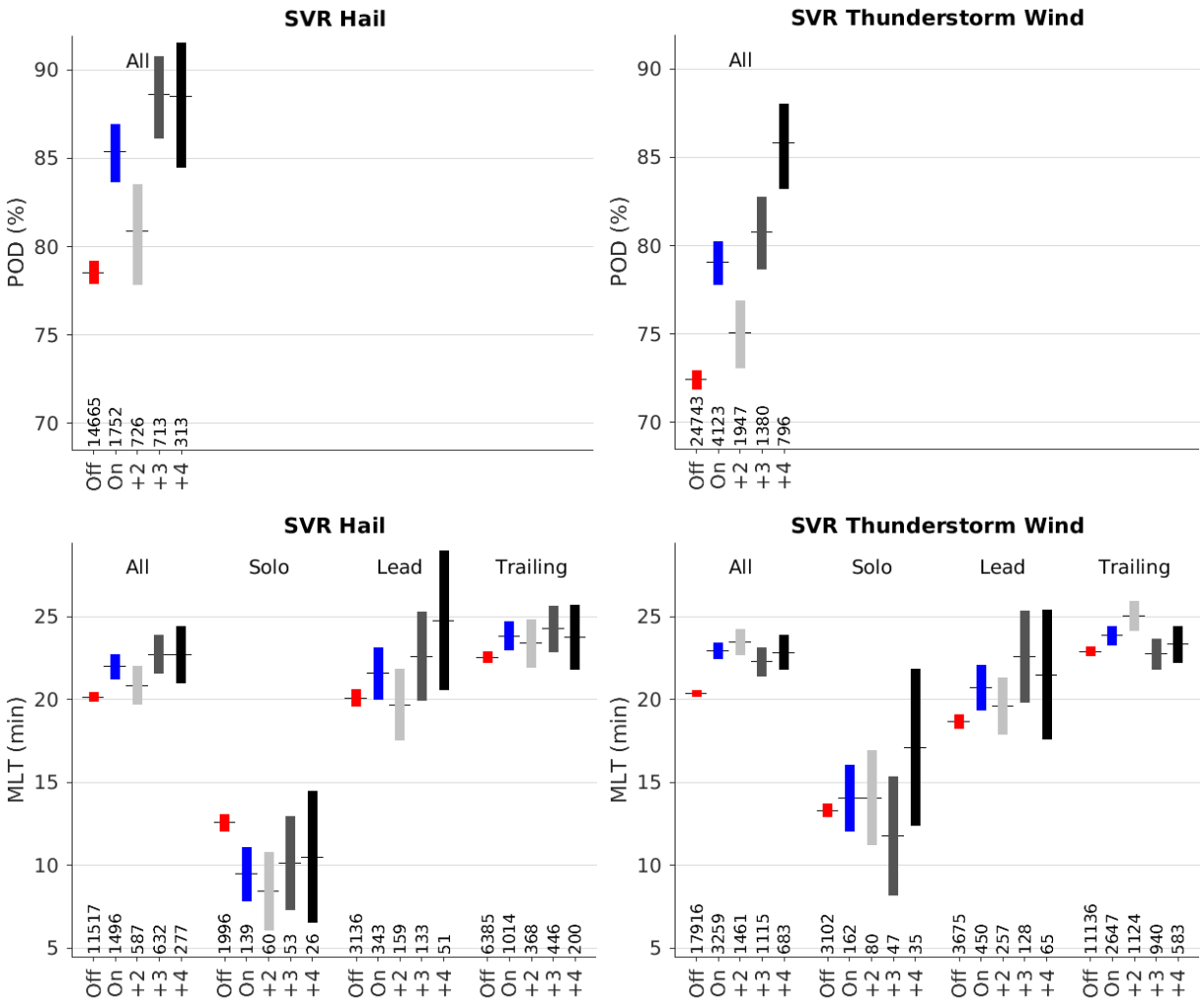

Figure 19. SVR POD and MLT performance vs. MRLE usage status, separated by event type.

2.3.2 FF Warnings

Figure 20 displays POD, FAR, and MLT for FF warnings vs. MRLE usage status at the estimated time of warning decision. As with SVR warnings, MRLE utilization corresponded with improved warning performance in the all-warning category. MRLE+4 did significantly better than MRLE+2 for FAR in the all-warning category. In the trailing warning category, MRLE-on performed better than MRLE-off in both FAR and MLT.

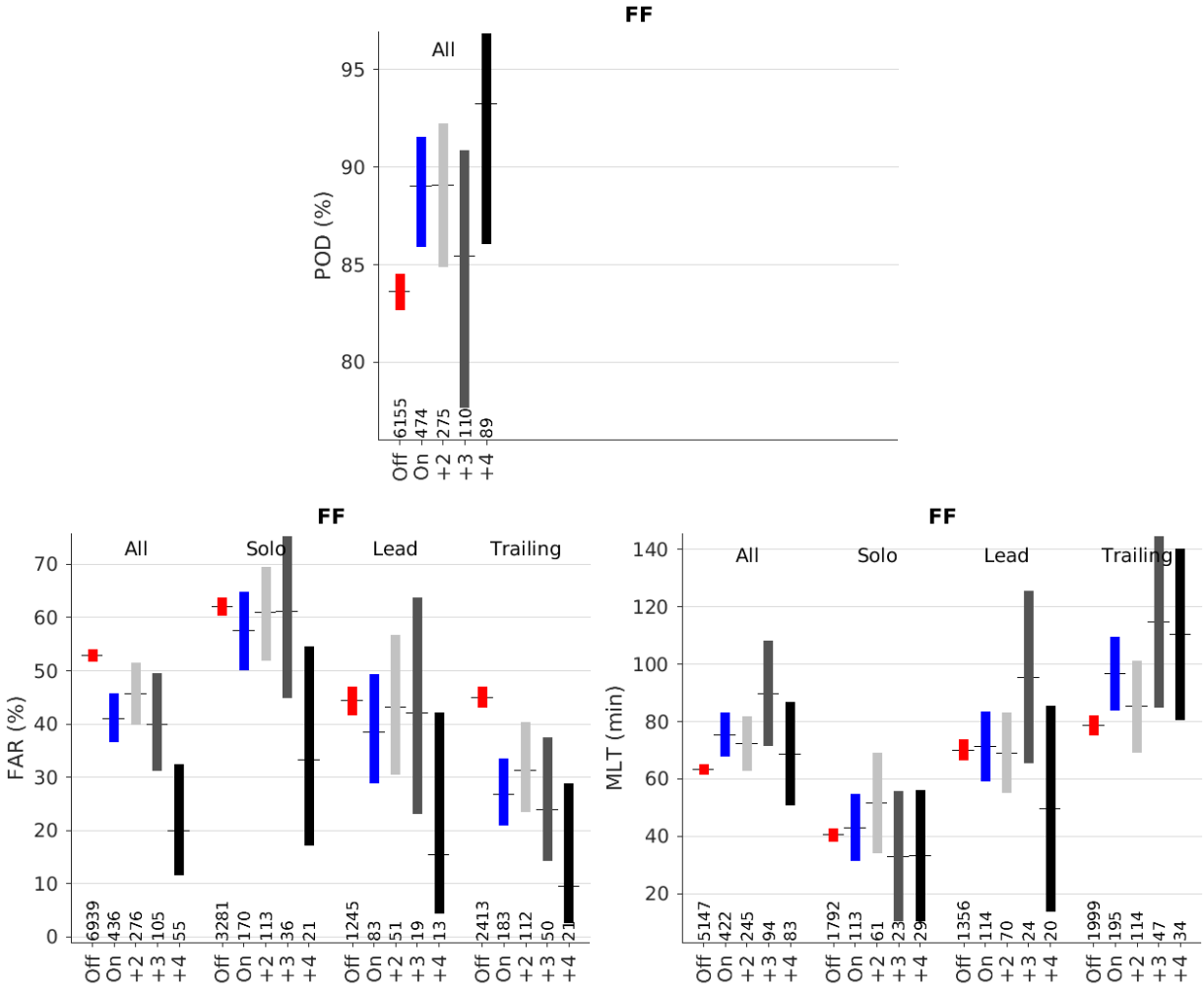

Figure 20. FF warning performance vs. MRLE usage status.

2.3.3 TOR Warnings

Figure 21 shows POD, FAR, and MLT for TOR warnings vs. MRLE usage status at the estimated time of warning decision. In the all-warnings category, MRLE utilization was associated with significantly improved POD and FAR. Within the warning categories, MRLE-on did significantly better than MRLE-off for lead and trailing warnings for FAR, and for trailing warnings only for MLT. No significant differences between MRLE+2, +3, and +4 were observed, possibly due to the very small sample sizes. We do not include plots of results parsed by EF categories here because there were no notable differences that were statistically significant.

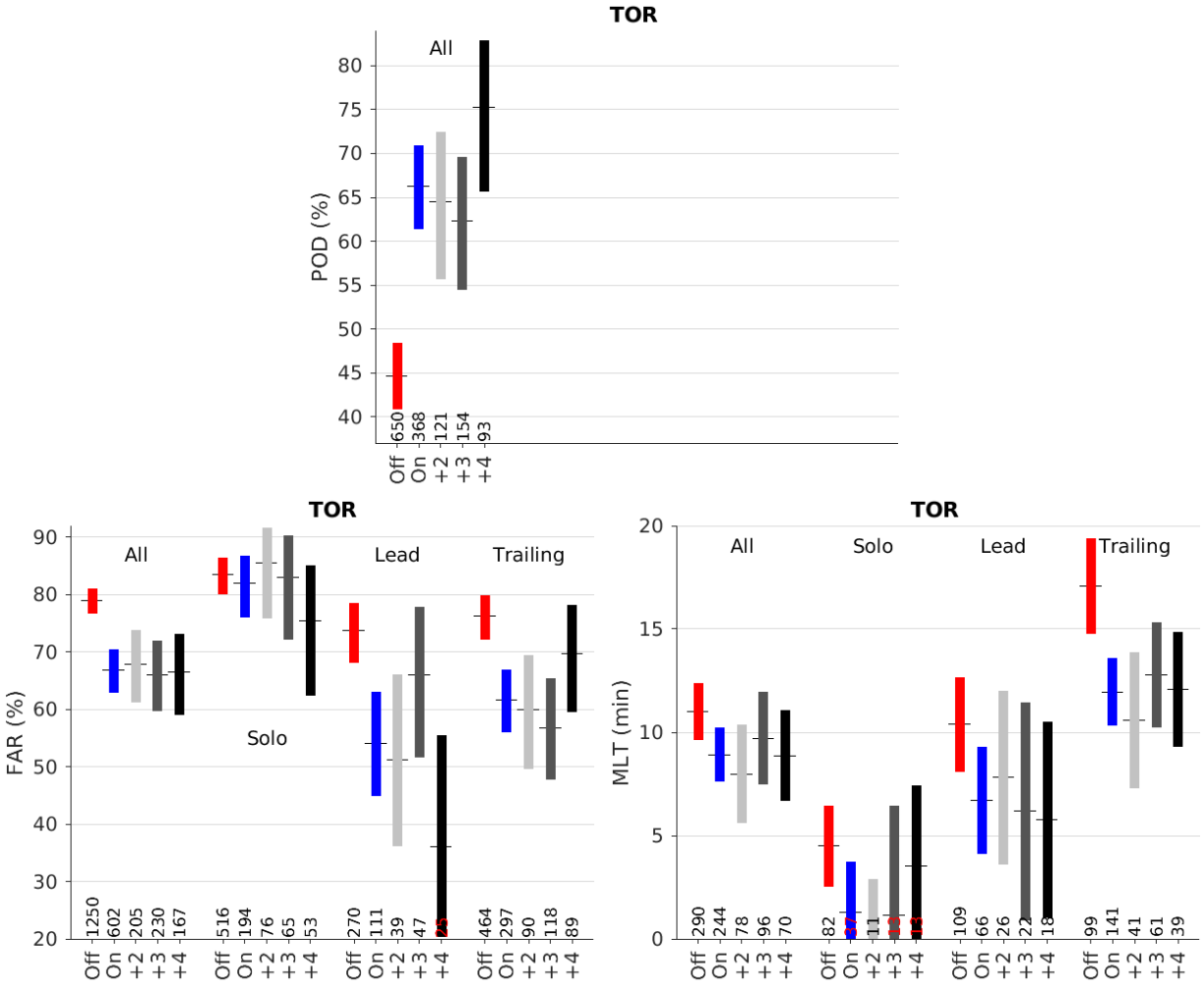

Figure 21. TOR warning performance vs. MRLE usage status.

2.4 SAILS VS. MRLE IMPACTS

We now compare SAILS and MRLE impact results. Figure 22 shows this comparison for SVR warnings. MRLE was associated with better POD, FAR, and MLT performance compared to SAILS. Within the types of SAILS and MRLE scans, MRLE+4 performed the best for POD and FAR, although the sample sizes for MRLE+4 were relatively small. Even parsed by hail vs. thunderstorm wind (Figure 23), MRLE performed better than SAILS. And for POD, MRLE+4 did best (with MRLE+3 doing just as well for hail).

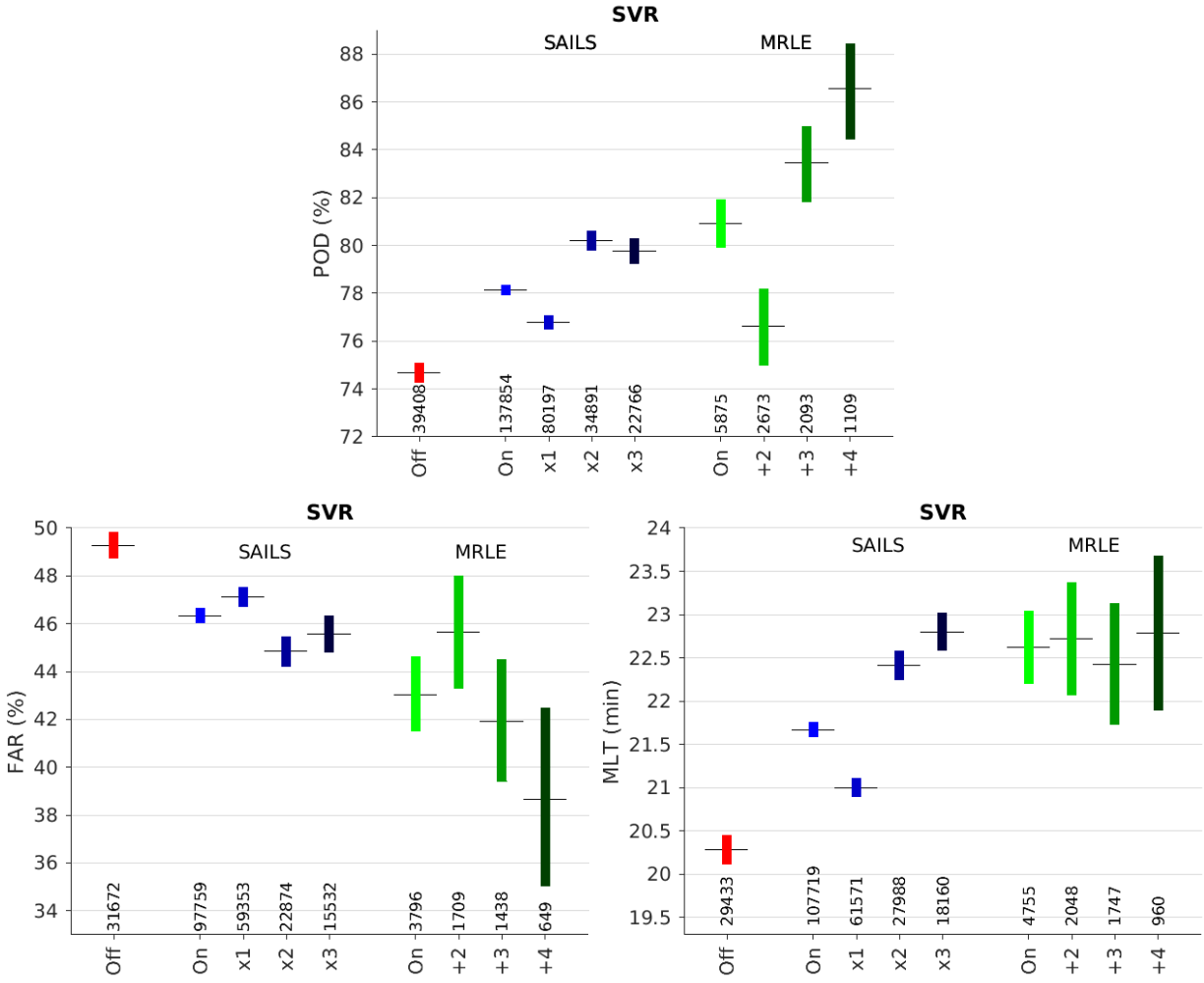

Figure 22. SVR warning performance metrics vs. SAILS and MRLE usage status. Colors are used to help visual differentiation between categories.

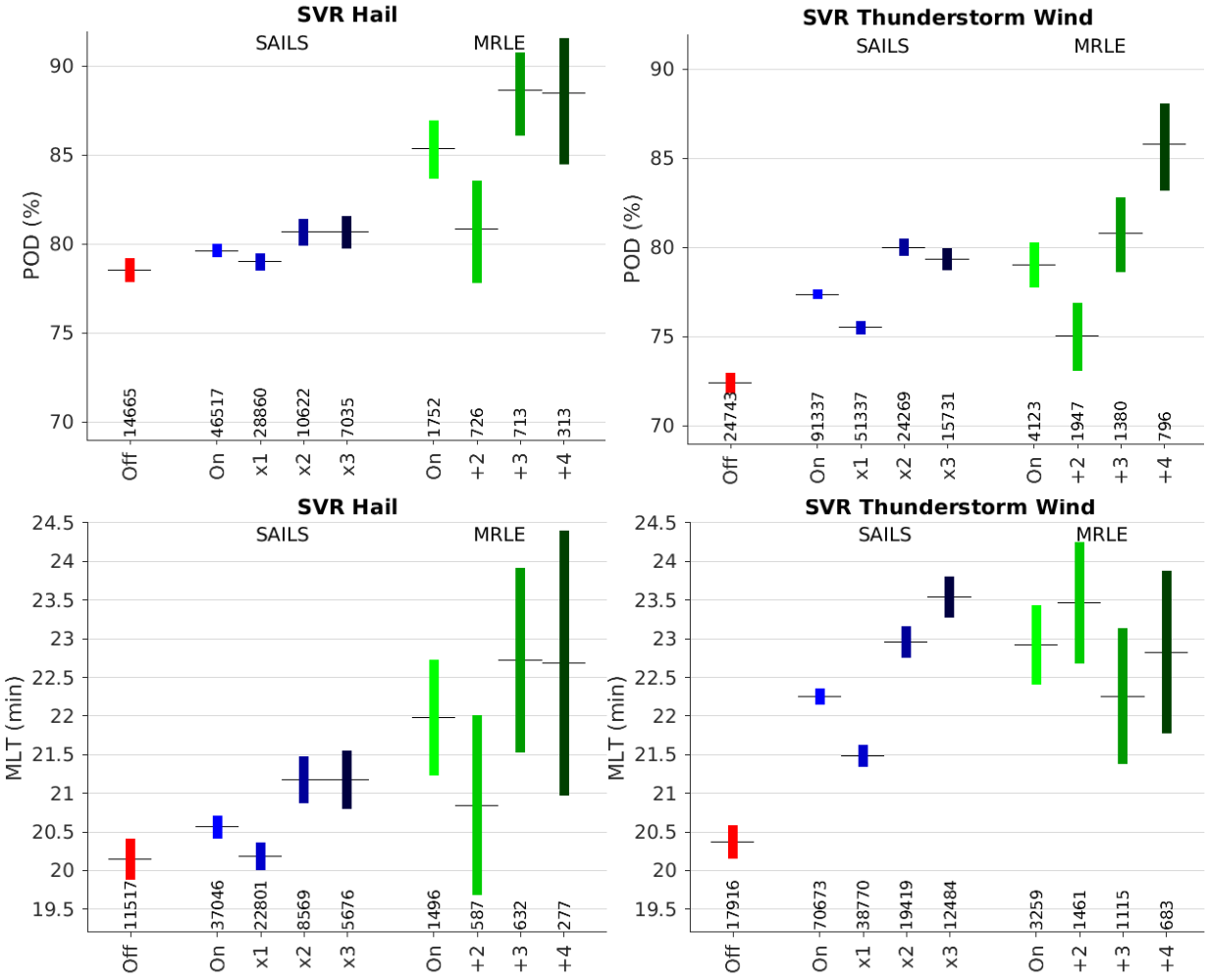

Figure 23. SVR POD and MLT performance vs. SAILS and MRLE usage status, separated by event type.

Figure 24 shows little statistically significant difference between SAILS and MRLE impacts on FF warning performance. The only exception was MRLE+4 outperforming other options in FAR, although one must be cognizant of the small sample size (55).

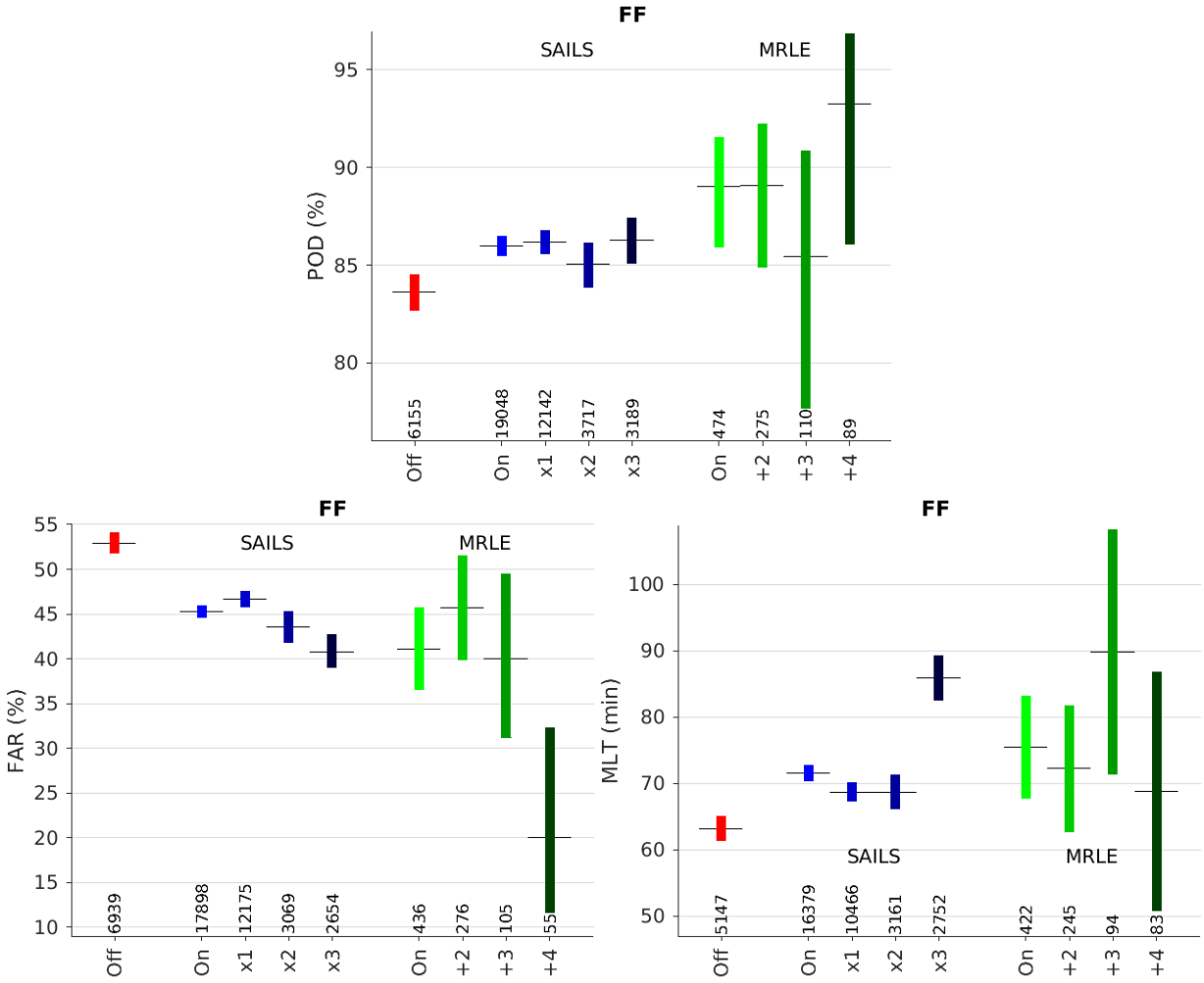

Figure 24. FF warning performance vs. SAILS and MRLE usage status.

With tornadoes (Figure 25), SAILS and MRLE performed similarly, except for MLT where the SAILS options did better than MRLE.

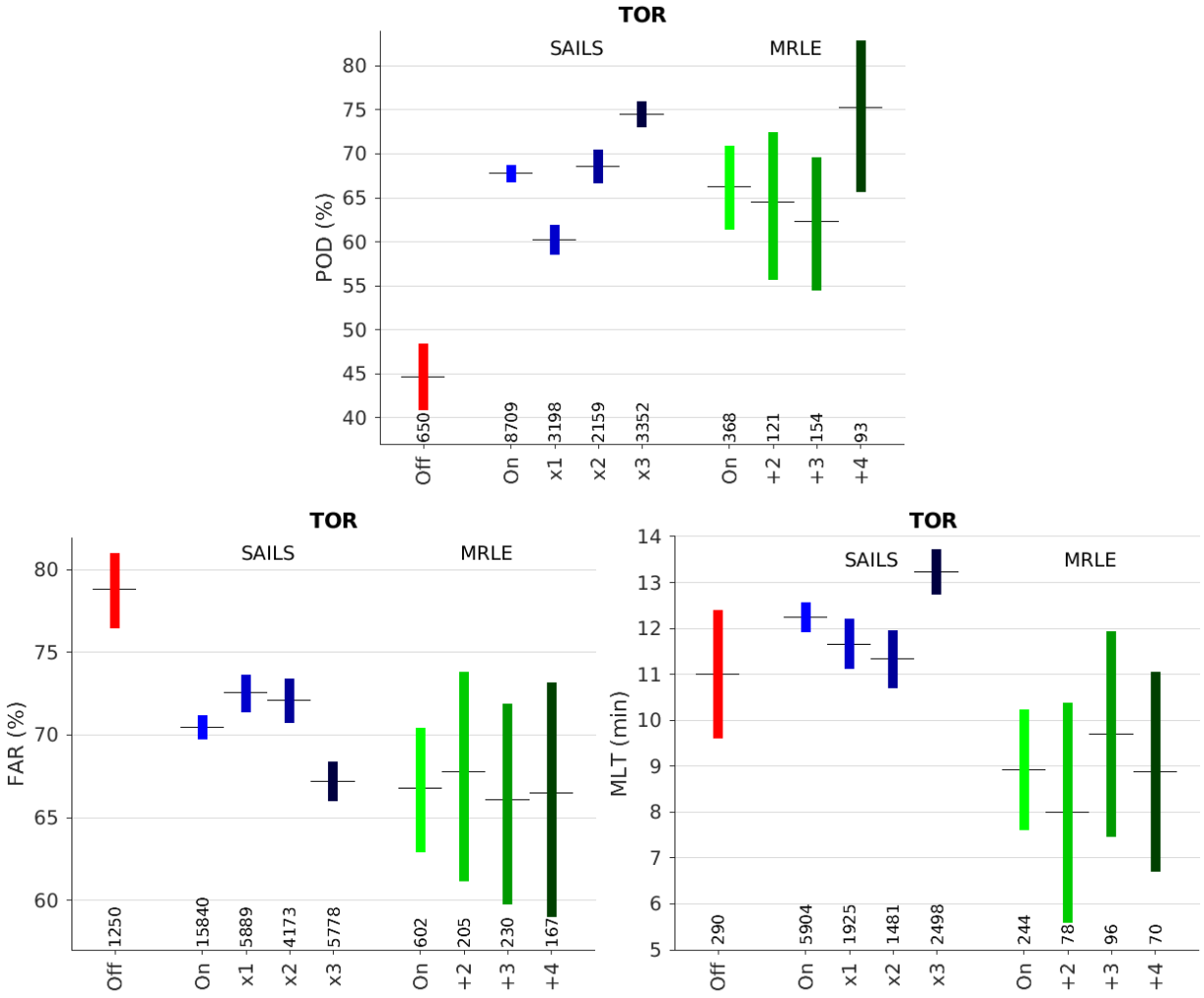

Figure 25. TOR warning performance vs. SAILS and MRLE usage status.

In an effort to provide objective input to the radar operator training program, Table 2 summarizes and compares the historically most used SAILS/MRLE options (including the "off" alternative) with the options that our study showed to be statistically associated with best warning performance. Because the optimal (or best compromise) radar scanning choice in any given situation will be dependent on many factors, such as storm developmental stage and distance from radar, this table is not meant to be used as a rigid basis for decision making. Rather, we would like forecasters to be aware that there is a statistical basis for certain scanning options being associated with best warning performance in the aggregate SVR, FF, and TOR warning categories, and, therefore, that these options should be perhaps considered favorably with that in mind.

TABLE 2
SAILS and MRLE Historical Usage vs. Top Performers

Category	SVR (hail)	SVR (wind)	FF	TOR
Historically most used	SAILSx1	SAILSx1	SAILSx1	SAILSx1
Option associated with top warning performance	MRLE+4	MRLE+4	MRLE+4	SAILSx3
Option(s) associated with second-best warning performance	MRLE+3	SAILSx3	MRLE+3 SAILSx3	SAILSx2

We have already discussed some of the possible physical reasons behind the Table 2 results. For TOR, the latest wind field closest to the surface may be one of the most critical factors in deciding whether or not to issue a warning, which may be why SAILSx3 (followed by SAILSx2) is associated with the best performance. For SVR warnings, the evolution of the convection morphology, including mid-level structures, might be tracked in a timelier manner with MRLE. For FF, the rainfall rate is best estimated by the most frequent base scan updates (SAILSx3), but the short-range prediction for intense rainfall may be more dependent on the amount of water aloft, so MRLE+4 or MRLE+3 might be best for that purpose. Note, however, that results for MRLE are not as robust as those for SAILS, especially for FF and TOR, due to the much smaller sample sizes.

3. VOLUME AND BASE SCAN UPDATE RATE IMPACTS ON WARNING PERFORMANCE

3.1 ANALYSIS METHODOLOGY

In Section 2, we analyzed the effects of SAILS and MRLE usage on severe weather warning performance. Due to the inherent resource limitations of the WSR-88D, given a certain level of data quality and spatial resolution, arbitrarily fast scan update rates cannot be achieved. SAILS and MRLE options represent a range of trade-off points between volume scan update rates and the update rates of the lowest elevation angle scans. In formulating requirements for a potential future replacement of the WSR-88D, it is of interest to disentangle the impacts of volume scan update rate vs. individual elevation angle scan update rates. Taken in aggregate, with the diversity of VCPs, SAILS/MRLE options, and the variation in volume scan periods due to AVSET, we have access to a spread of data points across the 2D base vs. volume scan update period joint distribution (Figure 26). It is thus possible to conduct regression analyses of severe warning performance with these two variables as predictors.

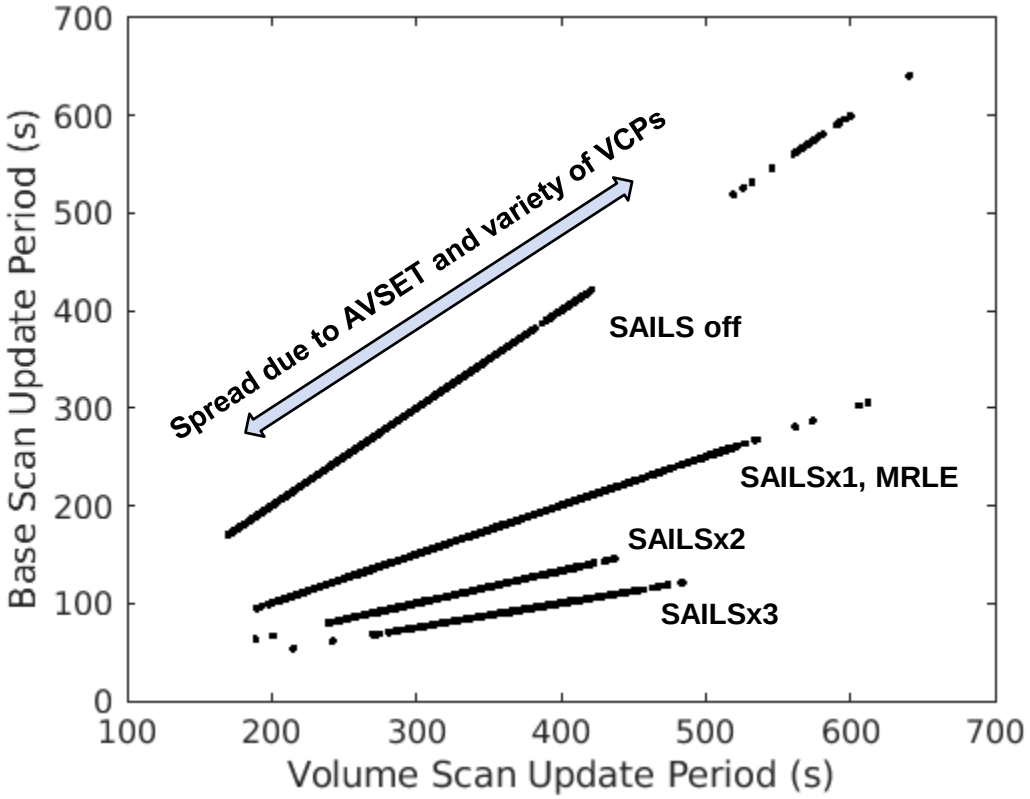

Figure 26. Scatter plot of base scan update period vs. volume scan update period in severe weather warning decision cases.

Previous experiments with a rapid-scan PAR generally showed performance improvements for non-operational SVR and TOR warnings for volume update periods of ~1 minute vs. ~2 and ~5 minutes (Wilson et al. 2017). Our current analysis, which utilizes large sets of operational data for statistical robustness, provides an excellent complement to those earlier studies.

For this analysis, we used data from 2012 to 2022, since AVSET has been on by default at all sites since 2012. For POD and FAR, we employed a binomial logistic (Berkson 1944) regression, as appropriate for events with a binary outcome; the MATLAB fitglm function with the binomial distribution option was used. For lead time, we applied a normal linear regression (MATLAB fitglm function with the normal distribution option). For predictors, in addition to volume and base scan periods (s), we also included event distance from the radar (km), since we knew from past studies that POD is related to event (or source basin for FF) distance from the radar, and that FAR is linked to warning polygon distance from the radar for SVR (Cho and Kurdzo 2020b), FF (Meléndez et al. 2018; Cho and Kurdzo 2020a), and TOR (Brotzge and Erickson 2010; Cho and Kurdzo 2019a,b). Lead time was only found to be linked to distance from radar for FF (Cho and Kurdzo 2020a), so distance from radar was not included as a predictor variable for the SVR and TOR lead time regression analyses.

3.2 IMPACT RESULTS

The regression analysis results for SVR warnings are listed in Table 3. According to the vanishingly small *p* values, all results were statistically significant. The negative signs of the coefficients mean that POD decreased with increasing radar distance, volume scan period, and base scan period, all of which make sense. The larger coefficient magnitude (i.e., steeper slope in the regression fit) implies that a change in base scan period has more leverage than a similar change in volume scan period to impact POD. For FAR, the positive signs of the coefficients mean that FAR increased with increasing radar distance, volume scan period, and base scan period, which also makes sense. In this case, the volume scan period appears to have a bit more impact on FAR than the base scan period. Lead time increased with decreasing volume and base scan periods, with the base scan period having a significantly stronger impact in this case.

Note that Section 2 showed that improved SVR warning performance was associated with SAILS on (longer volume scan periods, shorter base scan periods) vs. SAILS off (shorter volume scan periods, longer base scan periods)—in other words, that shorter volume scan periods had an indirect association with worse SVR warning performance. This means that the multiple regression results of Table 3 where reduction in both volume and base scan periods were significantly correlated with improved warning performance had to work *against* that SAILS influence. That is why these results are a very important addition to the SAILS impact results—we were able to show that despite the SAILS-based anticorrelation between volume and base scan update rates, reducing either or both leads to improved SVR warning performance.

TABLE 3

SVR Warning Performance Regression Fit Results

Warning Metric	*M*	Regression Output	*y* Intercept	Distance from Radar	Volume Scan Period	Base Scan Period
POD	269,480	Coefficient	1.97 ± 0.04	$-1.28 \pm 0.10 \times 10^{-3}$	$-1.28 \pm 0.10 \times 10^{-3}$	$-1.97 \pm 0.07 \times 10^{-3}$
		p value	$<10^{-9}$	$<10^{-9}$	$<10^{-9}$	$<10^{-9}$
FAR	184,052	Coefficient	-0.739 ± 0.043	$2.82 \pm 0.11 \times 10^{-3}$	$7.90 \pm 1.05 \times 10^{-4}$	$5.59 \pm 0.75 \times 10^{-4}$
		p value	$<10^{-9}$	$<10^{-9}$	$<10^{-9}$	$<10^{-9}$
Lead Time	202,284	Coefficient	1480 ± 20	—	-0.227 ± 0.045	-0.655 ± 0.033
		p value	$<10^{-9}$	—	3.7×10^{-7}	$<10^{-9}$

Table 4 gives the regression analysis results for only SVR hail events. Again, POD improvement was associated with decreased volume and base scan periods, with base scan period having more impact. Lead time improvement was associated with decreased volume and base scan period, but in this instance, there was no statistically significant difference in impact between the two predictors, as the coefficient estimate error bars overlapped. Oddly, POD increased with distance from radar in this case. This is difficult to explain physically. Perhaps because at farther ranges, more of the vertical extent of the storm is captured by the rapid-update SAILS/MRLE low-elevation-angle scans, the forecaster is able to make a better evaluation of hail potential. But those factors still have to outweigh the better spatial resolution one obtains at closer range. It is also possible that AVSET effects might have affected these results, i.e., that the tendency for storms farther away to be associated with shorter volume scan periods due to AVSET truncating the highest elevation cuts could have introduced an indirect association between improved POD and distance from radar. However, even with truncated AVSET volume scans omitted from the analysis, increased POD was still associated with increased distance from radar.

TABLE 4
SVR Warning Performance Regression Fit Results (Hail)

Warning Metric	*M*	Regression Output	*y* Intercept	Distance from Radar	Volume Scan Period	Base Scan Period
POD	93,569	Coefficient	1.74 ± 0.07	$8.08 \pm 1.74 \times 10^{-4}$	$-5.59 \pm 1.77 \times 10^{-4}$	$-1.91 \pm 0.12 \times 10^{-3}$
		p value	$<10^{-9}$	3.5×10^{-6}	0.0016	$<10^{-9}$
Lead Time	73,118	Coefficient	1430 ± 30	—	-0.373 ± 0.076	-0.497 ± 0.053
		p value	$<10^{-9}$	—	$<10^{-9}$	$<10^{-9}$

Table 5 gives the regression analysis results for only SVR thunderstorm wind events. POD improvement was associated with decreased volume and base scan periods, with base scan period having more impact. Lead time improvement was associated with decreased volume and base scan periods, with base scan period having more impact also in this case. POD decreased with radar distance, which is what one would expect (and also observed in the past).

TABLE 5
SVR Warning Performance Regression Fit Results (Thunderstorm Wind)

Warning Metric	*M*	Regression Output	*y* Intercept	Distance from Radar	Volume Scan Period	Base Scan Period
POD	175,911	Coefficient	2.02 ± 0.05	$-2.67 \pm 0.13 \times 10^{-3}$	$-1.30 \pm 0.11 \times 10^{-3}$	$-2.10 \pm 0.08 \times 10^{-3}$
		p value	$<10^{-9}$	$<10^{-9}$	$<10^{-9}$	$<10^{-9}$
Lead Time	129,166	Coefficient	1540 ± 20	—	-0.281 ± 0.055	-0.710 ± 0.042
		p value	$<10^{-9}$	—	4.1×10^{-7}	$<10^{-9}$

The regression analysis results for FF warnings are listed in Table 6. We marked the results with *p* values greater than or equal to 0.01 in red, to indicate that they are less statistically reliable and could be ignored. With that in mind, POD improvement was associated with decreasing distance from radar and base scan periods. FAR improvement was associated with decreasing distance from radar and base scan period, but also with increasing volume scan period. Lead time increase was associated with decreasing base scan

period, but also with increasing volume scan period. The FF warning performance improvement with increasing volume scan period is a surprising result that is hard to explain. However, as noted earlier, there is an underlying SAILS-based anticorrelation between volume and base scan update rates that may be counteracting other factors that would lead to a correlation between decreased volume scan period and increased POD. Thus, in this context, we recommend that these results be interpreted to mean that decreasing base scan periods is certainly important for improving FF warning performance, but not form a definite conclusion regarding volume scan period effects.

TABLE 6
FF Warning Performance Regression Fit Results

Warning Metric	*M*	Regression Output	*y* Intercept	Distance from Radar	Volume Scan Period	Base Scan Period
POD	36,779	Coefficient	2.31 ± 0.10	$-4.64 \pm 0.34 \times 10^{-4}$	$4.74 \pm 26.0 \times 10^{-5}$	$-1.04 \pm 0.19 \times 10^{-3}$
		p value	$<10^{-9}$	$<10^{-9}$	0.86	4.7×10^{-8}
FAR	37,793	Coefficient	-0.614 ± 0.071	$5.53 \pm 0.26 \times 10^{-3}$	$-7.83 \pm 1.82 \times 10^{-4}$	$1.34 \pm 0.14 \times 10^{-3}$
		p value	$<10^{-9}$	$<10^{-9}$	1.7×10^{-5}	$<10^{-9}$
Lead Time	31,127	Coefficient	2470 ± 190	1.66 ± 0.66	5.68 ± 0.49	-1.11 ± 0.36
		p value	$<10^{-9}$	0.011	$<10^{-9}$	1.9×10^{-3}

The regression analysis results for TOR warnings are listed in Table 7. POD improvement was associated with decreasing distance from radar and base scan periods, but also with increasing volume scan period. The latter association is, again, surprising. Again, as noted for FF, there is an underlying SAILS-based anticorrelation between volume and base scan update rates that may be counteracting other factors that would lead to a correlation between decreased volume scan period and increased POD. FAR improvement was associated with decreasing distance from radar and base scan period. There were no statistically reliable results for lead time. As with FF warnings, we recommend interpreting the results to mean that decreasing base scan periods is certainly important for improving TOR warning performance, but not form a definite conclusion regarding volume scan period effects.

TABLE 7
TOR Warning Performance Regression Fit Results

Warning Metric	*M*	Regression Output	*y* Intercept	Distance from Radar	Volume Scan Period	Base Scan Period
POD	12,600	Coefficient	0.480 ± 0.169	$-3.17 \pm 0.46 \times 10^{-3}$	$2.28 \pm 0.39 \times 10^{-3}$	$-1.96 \pm 0.31 \times 10^{-3}$
		p value	4.5×10^{-3}	$<10^{-9}$	3.8×10^{-9}	$<10^{-9}$
FAR	23,363	Coefficient	0.618 ± 0.149	$5.00 \pm 0.38 \times 10^{-3}$	$-8.60 \pm 3.34 \times 10^{-4}$	$9.55 \pm 2.62 \times 10^{-4}$
		p value	3.2×10^{-5}	$<10^{-9}$	0.010	2.7×10^{-4}
Lead Time	8235	Coefficient	780 ± 80	—	-1.47 ± 1.89	0.0422 ± 0.159
		p value	$<10^{-9}$	—	0.44	0.79

Because correlation between multiple predictor variables could be problematic in interpreting the regression results, we checked for multicollinearity with the variance inflation factor (VIF). VIF never exceeded 1.73 for any predictor pair, which is below the commonly used threshold of 5 (or a more conservative threshold of 2.5) that indicates a degree of multicollinearity that is problematic for regression analysis (Simon 2009). Thus, interpretation of the regression results should not be impacted by such correlations.

The biggest takeaway message from this section is that even though Section 2 clearly showed that the usage of SAILS and MRLE is associated with improved severe weather warning performance, where the usage of SAILS and MRLE increases the volume scan period, a decreased volume scan period was shown to be independently associated with improved warning performance, at least for SVR warnings. This analysis was made possible by the diversity in volume scan periods generated by AVSET and the range of VCPs used. The implication is that there is likely a benefit for future weather radars if both base and volume scan update rates could be increased without sacrificing one for the other.

4. SAILS AND MRLE USAGE AND WARNING PERFORMANCE BY WFO

WSR-88Ds are operated by the local WFO, of which there are 116 in the CONUS. With multiple forecasters per WFO working in shifts around the clock, there is a very large roster of radar operators that are making VCP, SAILS, and MRLE usage decisions. Although there are regional and national training programs run within the NWS for WSR-88D operations, the range of weather climatology, staff experience, and WFO culture (Smith 2011) may result in a wide range of radar scan option statistics. This section presents the results of investigating such statistics. The results are presented without identifying individual WFOs to maintain their anonymity, and only plots are shown without accompanying tables in Appendix A.

Figure 27 shows POD vs. SAILS usage rate by WFO for SVR warnings. The dataset analyzed is the same as used in Section 2. The error bars were computed as $\pm t_{95}$ times the standard error for proportional data, representing the 95% confidence intervals in both dimensions. We used this metric instead of the Wilson score employed in the earlier sections because we needed symmetrical error estimates for input to the regression fit function. There is a wide range of both SAILS usage rate and POD among the WFOs. Unusually low PODs are generally associated with WFOs that generated few SVR warnings (i.e., long vertical error bars), so that is somewhat of a small-sample-size issue. However, there are some unusually low SAILS usage rates that are associated with WFOs large numbers of SVR warnings (i.e., short horizontal error bars) that cannot be attributed to small-sample-size statistical unreliability. So, for whatever reasons, there are some WFOs that have historically tended not to choose SAILS when making SVR warning decisions.

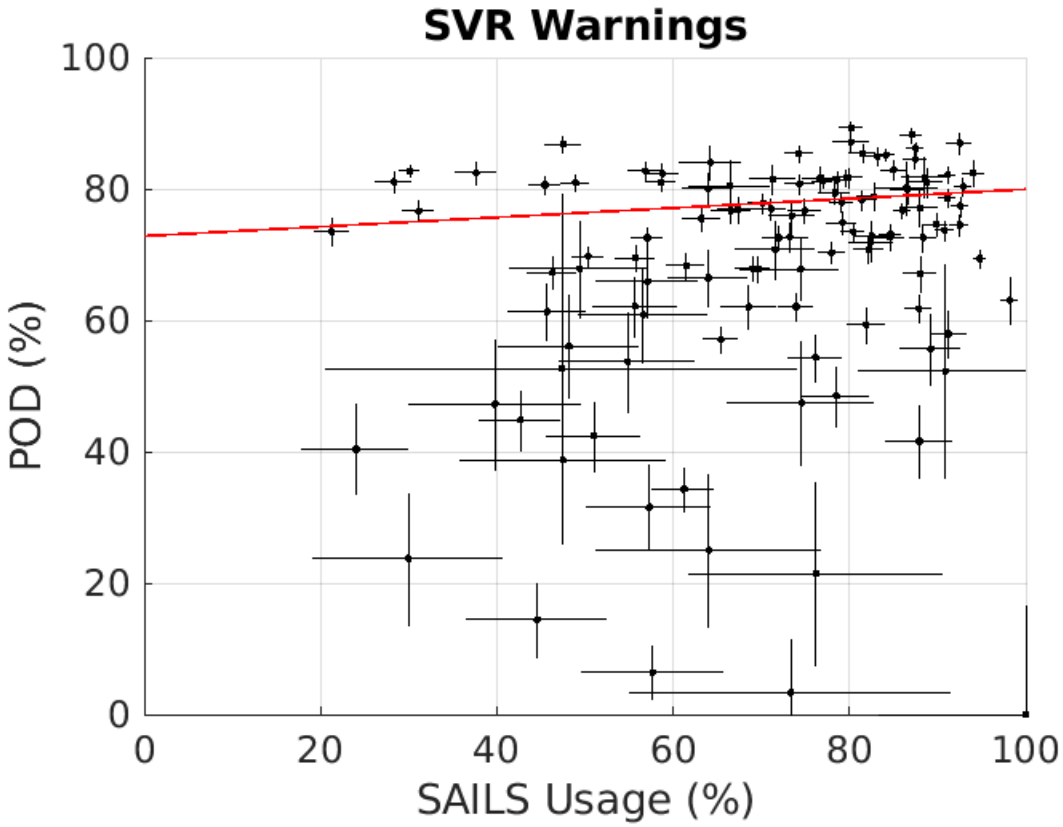

Figure 27. Scatter plot of POD vs. SAILS usage rate by WFO for SVR warnings. Horizontal and vertical bars denote 95% confidence intervals. The red line is a linear least-squares fit to the data. See main text for details.

In Figure 27, one can see that there is some positive correlation between POD and SAILS usage rate. To bolster this visual impression, the red line is the result of a least-squares straight line fit to the data with input uncertainty in two dimensions using the Numerical Recipes function fitexy (Press et al. 1992). The parameter estimates from the fit were: *y* intercept = 72.8 ± 1.0 and slope = 0.0712 ± 0.0129, but with a large chi-squared residual of 2390. Thus, the fit values should not be taken too seriously, but the positive sign of the slope is some added evidence that SVR POD benefits from SAILS usage.

Figure 28 shows FAR vs. SAILS usage rate by WFO for SVR warnings. Similar comments apply as for Figure 27: There is a wide range of both SAILS usage rate and FAR among the WFOs. Unusually high FARs tend to be associated with WFOs that generated few SVR warnings (i.e., long vertical error bars), which could at least be partly attributable to a small-sample-size issue. However, there are some unusually low SAILS usage rates that are associated with WFOs large numbers of SVR warnings (i.e., short horizontal error bars). Again, the linear fit to the data supports the Section 2 conclusion that usage of SAILS generally

benefits SVR warning performance. For reference, the estimated values were: *y* intercept = 74.8 ± 1.7 and slope = -0.374 ± 0.023, with a chi-squared residual of 4460.

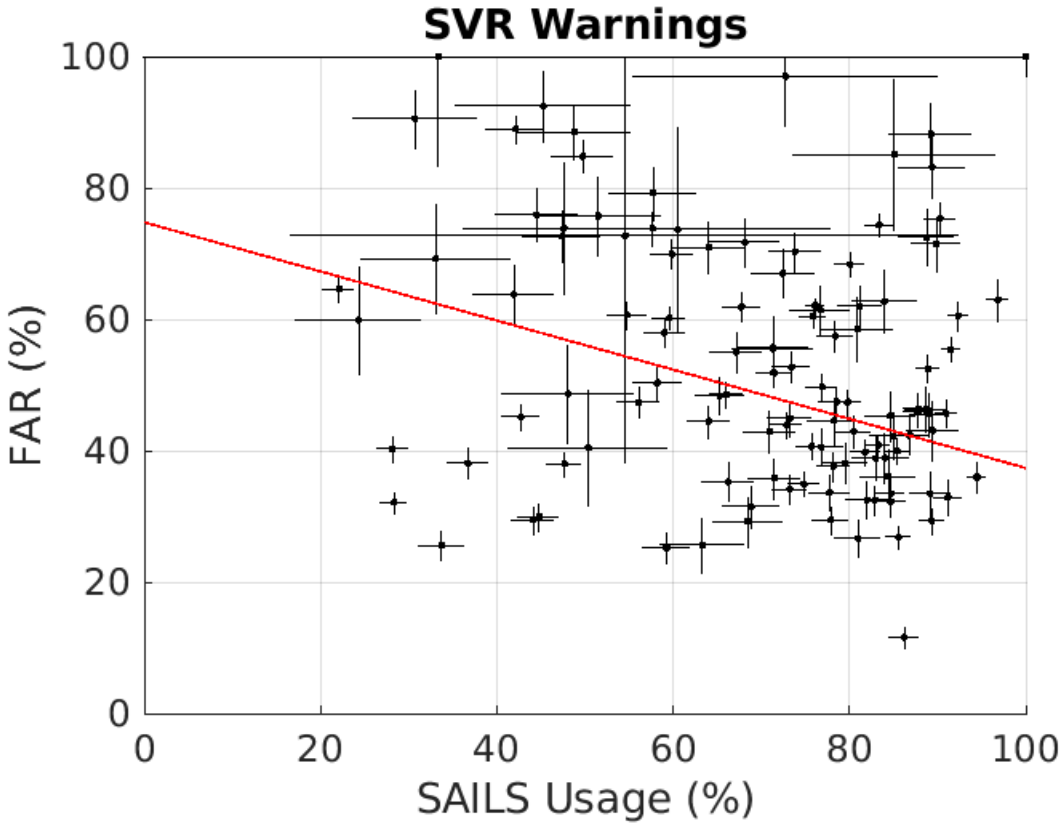

Figure 28. Scatter plot of FAR vs. SAILS usage rate by WFO for SVR warnings. Horizontal and vertical bars denote 95% confidence intervals. The red line is a linear least-squares fit to the data.

Figure 29 shows MLT vs. SAILS usage rate by WFO for SVR warnings. Again, one can discern a positive correlation between the two variables, as with POD vs. SAILS usage rate, especially when focusing on the data points with small errors. The corresponding linear fit parameter estimates were: *y* intercept = 17.7 ± 0.3 and slope = 0.0426 ± 0.0044, with a chi-squared residual of 1610.

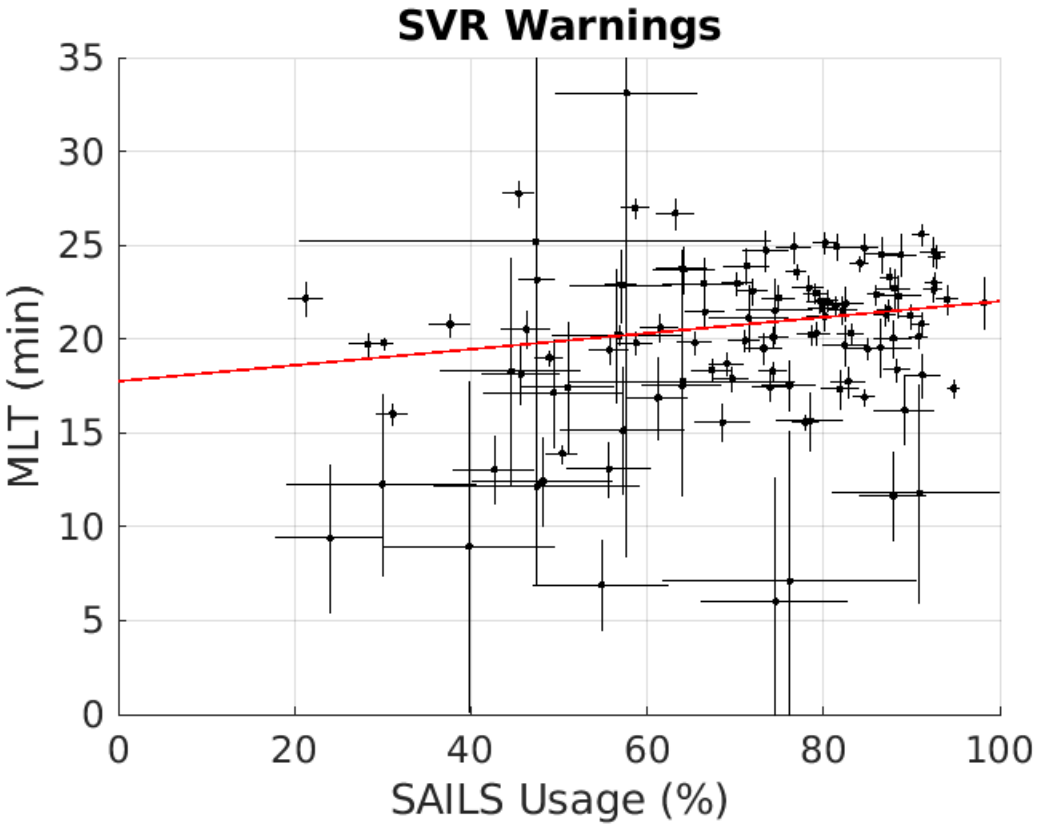

Figure 29. Scatter plot of MLT vs. SAILS usage rate by WFO for SVR warnings. Horizontal and vertical bars denote 95% confidence intervals. The red line is a linear least-squares fit to the data.

Figure 30 shows POD vs. SAILS usage rate by WFO for FF warnings. The dataset analyzed is the same as used in Section 2. With fewer data points compared to the SVR warning results, the error bars are longer and a trend is harder to discern. The linear least-squares fit does yield a positive slope, implying a SAILS usage benefit: *y* intercept = 84.7 ± 1.8 and slope = 0.040 ± 0.026, with a chi-squared residual of 384.

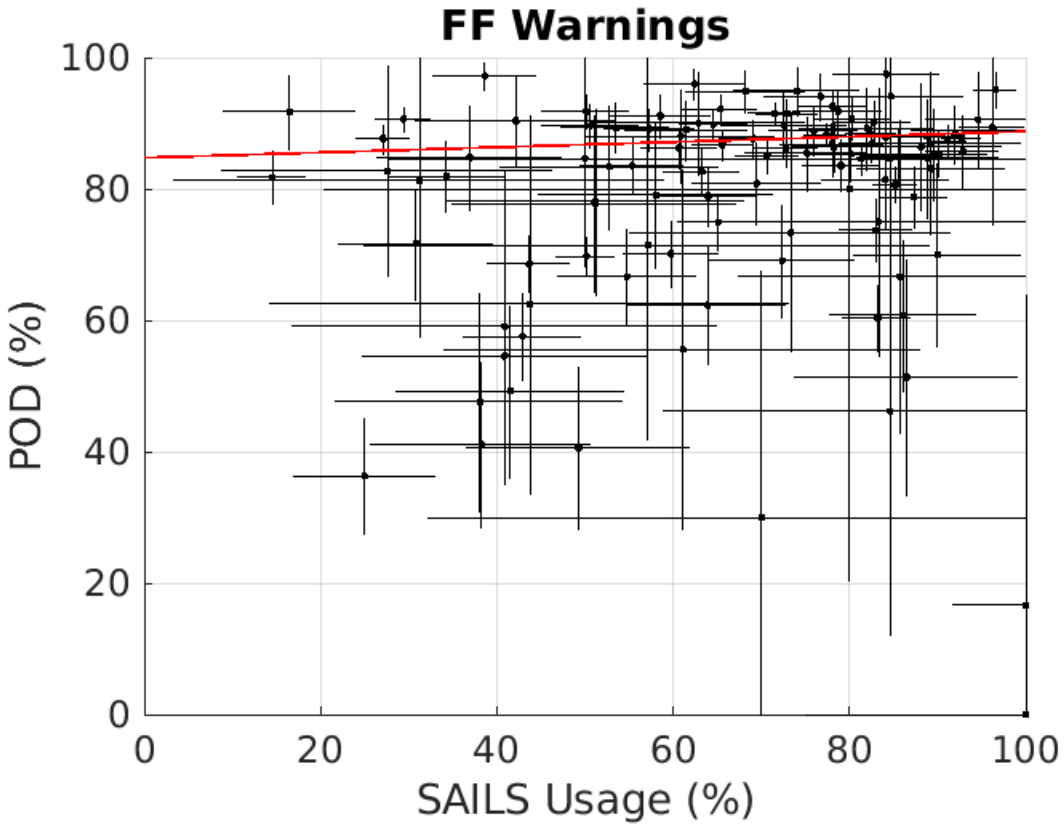

Figure 30. Scatter plot of POD vs. SAILS usage rate by WFO for FF warnings. Horizontal and vertical bars denote 95% confidence intervals. The red line is a linear least-squares fit to the data.

Figure 31 shows FAR vs. SAILS usage rate by WFO for FF warnings. The linear fit parameter estimates were: *y* intercept = 87.9 ± 2.6 and slope = -0.599 ± 0.038, with a chi-squared residual of 637.

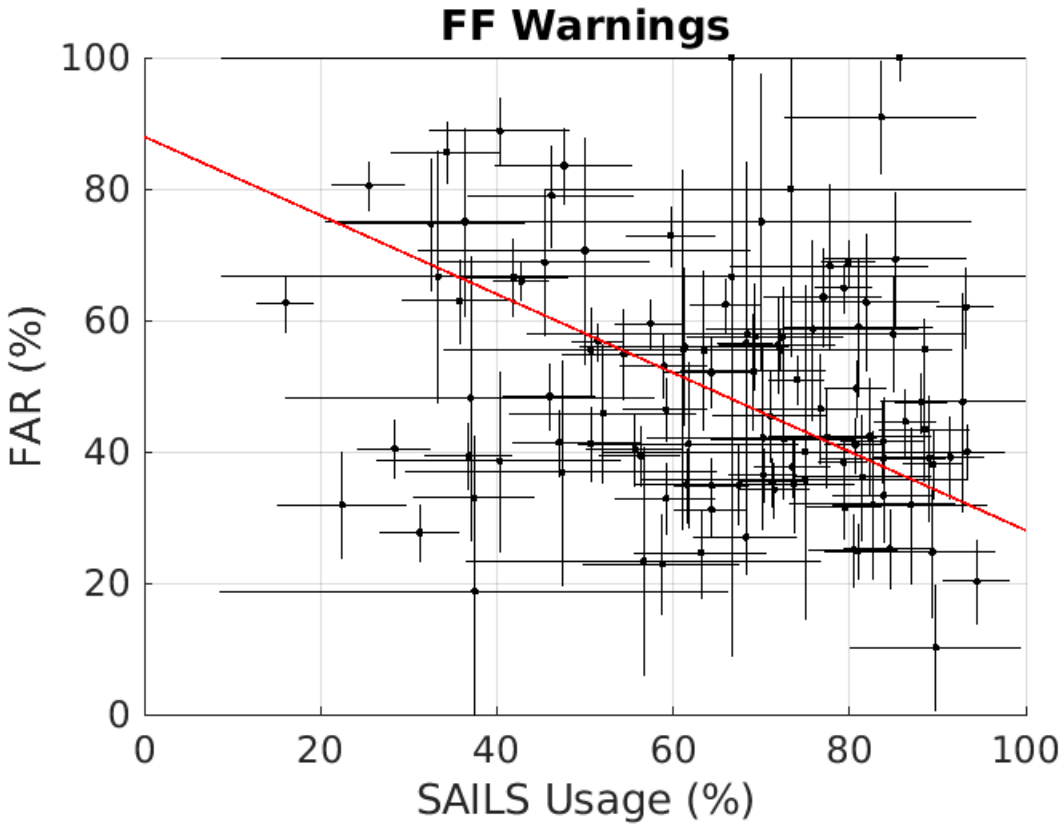

Figure 31. Scatter plot of FAR vs. SAILS usage rate by WFO for FF warnings. Horizontal and vertical bars denote 95% confidence intervals. The red line is a linear least-squares fit to the data.

Figure 32 shows MLT vs. SAILS usage rate by WFO for FF warnings. The linear fit parameter estimates were: *y* intercept = 44.8 ± 3.7 and slope = 0.258 ± 0.055, with a chi-squared residual of 556.

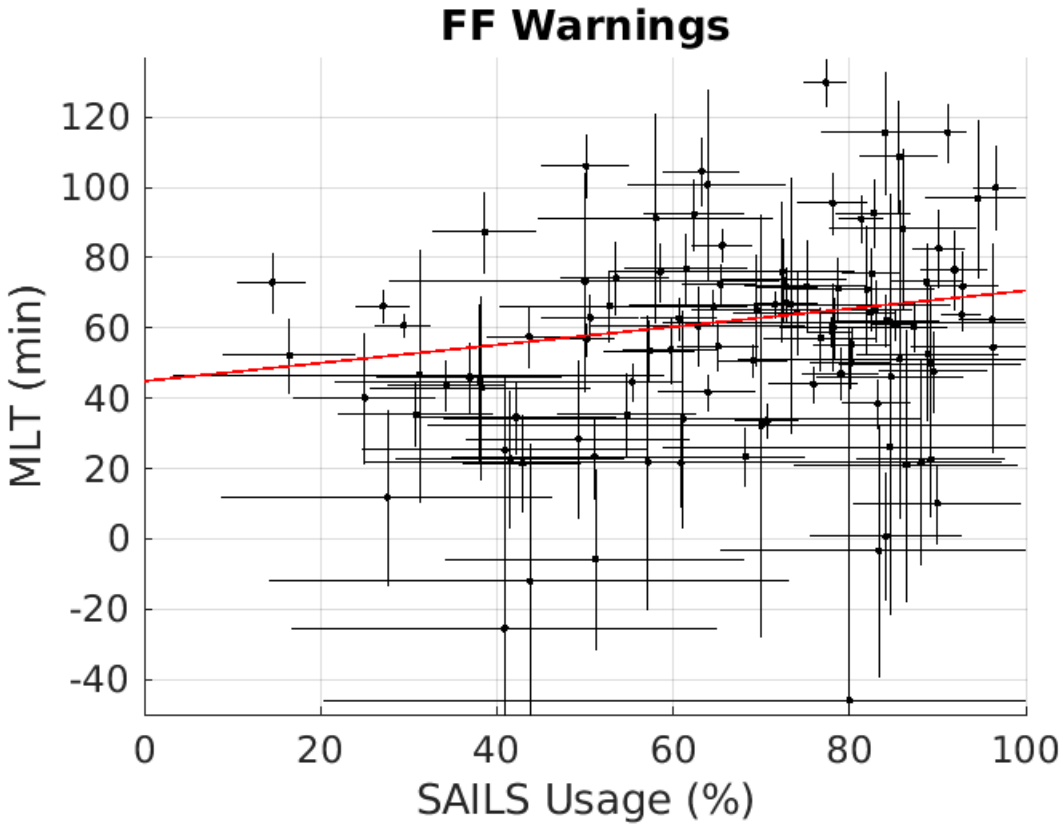

Figure 32. Scatter plot of MLT vs. SAILS usage rate by WFO for FF warnings. Horizontal and vertical bars denote 95% confidence intervals. The red line is a linear least-squares fit to the data.

Figure 33 shows POD vs. SAILS usage rate by WFO for TOR warnings. The dataset analyzed is the same as used in Section 2. With even fewer data points than for FF warnings, the error bars are very large for most WFOs, especially since tornadoes tend to occur in more concentrated areas of the CONUS. Nevertheless, there is still a hint of a positive correlation, which also shows up in the least-squares fit results: *y* intercept = -18.5 ± 7.9 and slope = 0.952 ± 0.088, with a chi-squared residual of 165.

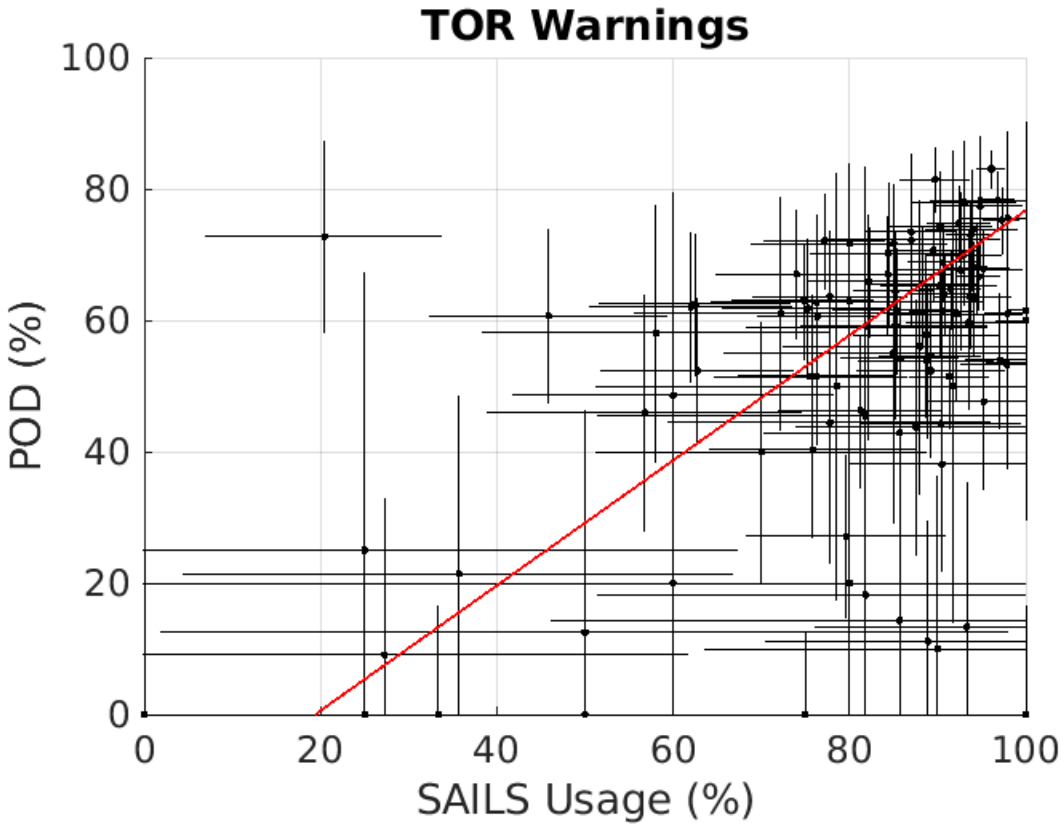

Figure 33. Scatter plot of POD vs. SAILS usage rate by WFO for TOR warnings. Horizontal and vertical bars denote 95% confidence intervals. The red line is a linear least-squares fit to the data.

Figure 34 shows FAR vs. SAILS usage rate by WFO for TOR warnings. The linear fit parameter estimates were: *y* intercept = 129 ± 8.0 and slope = -0.616 ± 0.091, with a chi-squared residual of 327.

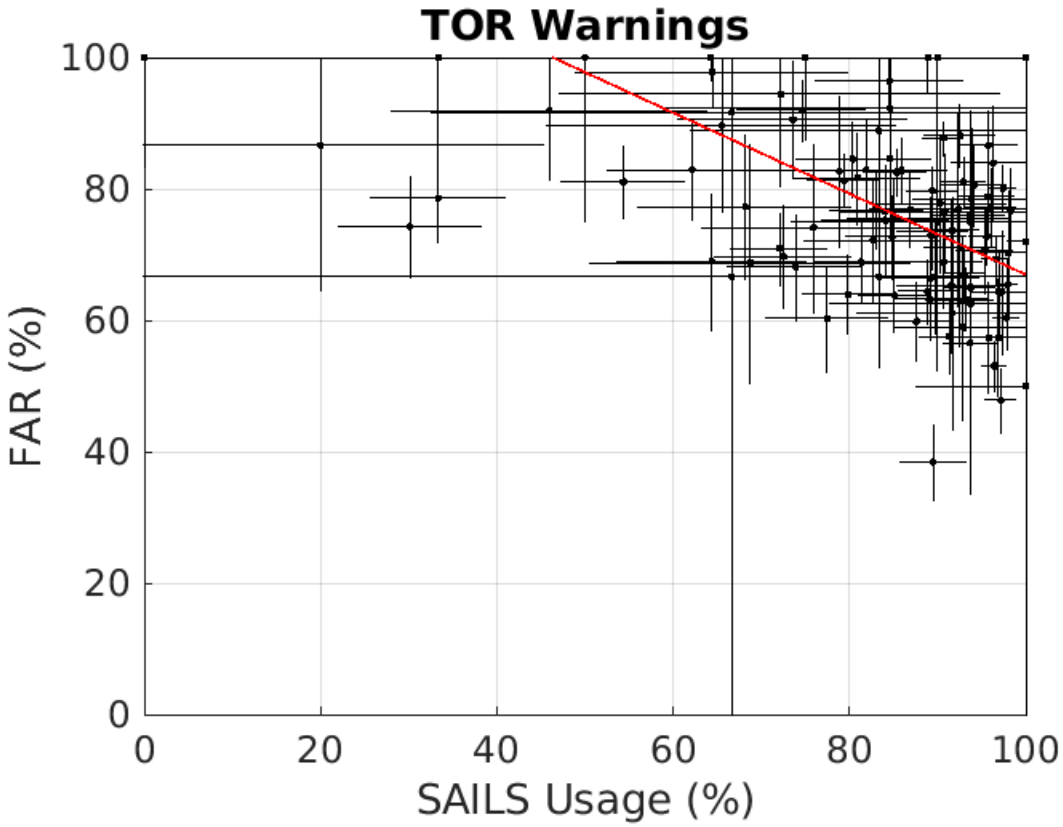

Figure 34. Scatter plot of FAR vs. SAILS usage rate by WFO for TOR warnings. Horizontal and vertical bars denote 95% confidence intervals. The red line is a linear least-squares fit to the data.

Finally, Figure 35 shows MLT vs. SAILS usage rate by WFO for TOR warnings. The linear fit parameter estimates were: *y* intercept = 0.393 ± 3.9 and slope = 0.133 ± 0.044, with a chi-squared residual of 102.

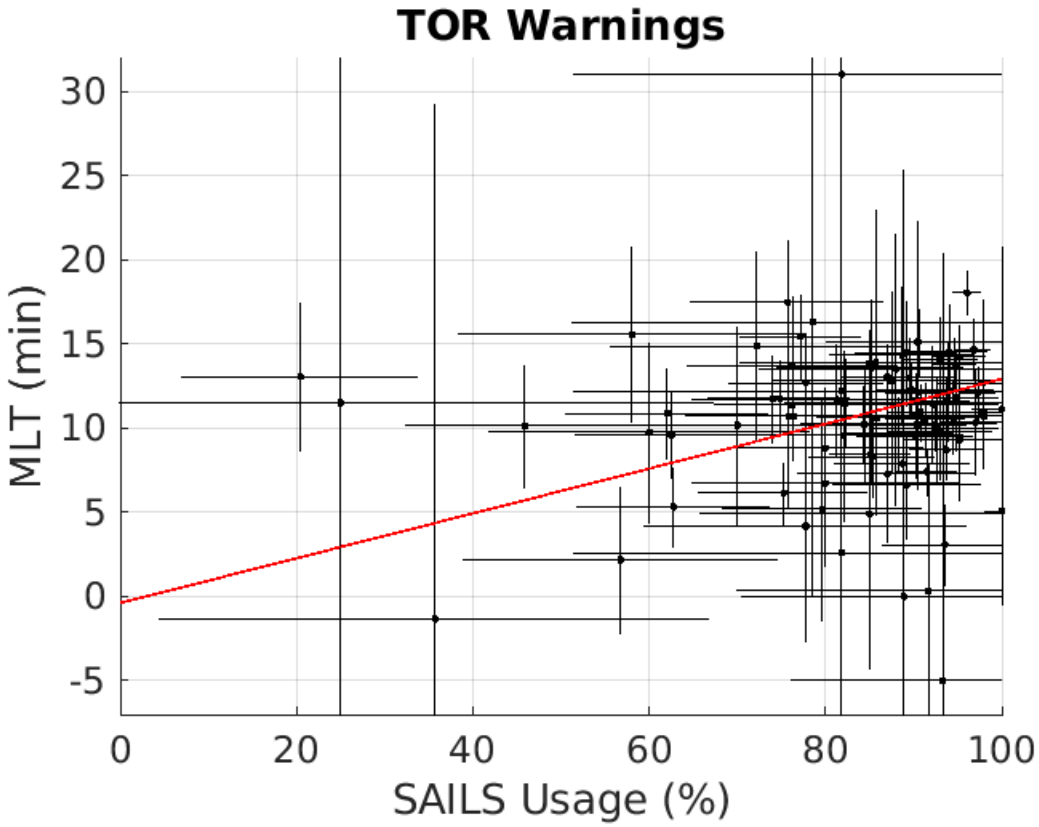

Figure 35. Scatter plot of MLT vs. SAILS usage rate by WFO for TOR warnings. Horizontal and vertical bars denote 95% confidence intervals. The red line is a linear least-squares fit to the data.

The results displayed in Figures 27–35 help support one of the main conclusions to be drawn from the Section 2 results—that SAILS usage is associated with improved SVR, FF, and TOR warning performance. Despite the wide variance in WFO-dependent SAILS usage and warning performance, the aggregate trends are all consistent in this regard. Note, however, that the estimated slope values from Figures 27–35 should not be used to quantitatively predict performance based on SAILS usage due to the poor quality of the fits.

We can also examine the statistical distribution of SAILS and MRLE usage by the WFOs using histograms. Figure 36 shows these histograms for SAILS usage rate for SVR, FF, and TOR warning decisions. The top left histogram is for any SAILS mode, whereas the other histograms are for SAILSx1, x2, and x3. There is an extremely wide range of usage, from around 20% to nearly 100% for any SAILS mode. There is a significant number of WFOs that apparently almost never uses SAILSx3. It would be of great interest to conduct a survey of the WFOs to find out why there is such a large variance in SAILS

usage rate. There may be important factors that we have not touched upon in this report that influence a radar operator's scan mode selections.

Figure 37 shows histograms of MRLE usage by WFOs. The top-left histogram is for any MRLE mode, whereas the other histograms are for MRLE+2, +3, and +4. A significant number of WFOs hardly ever use MRLE, and a relatively small number of WFOs seem to account for most of the MRLE usage.

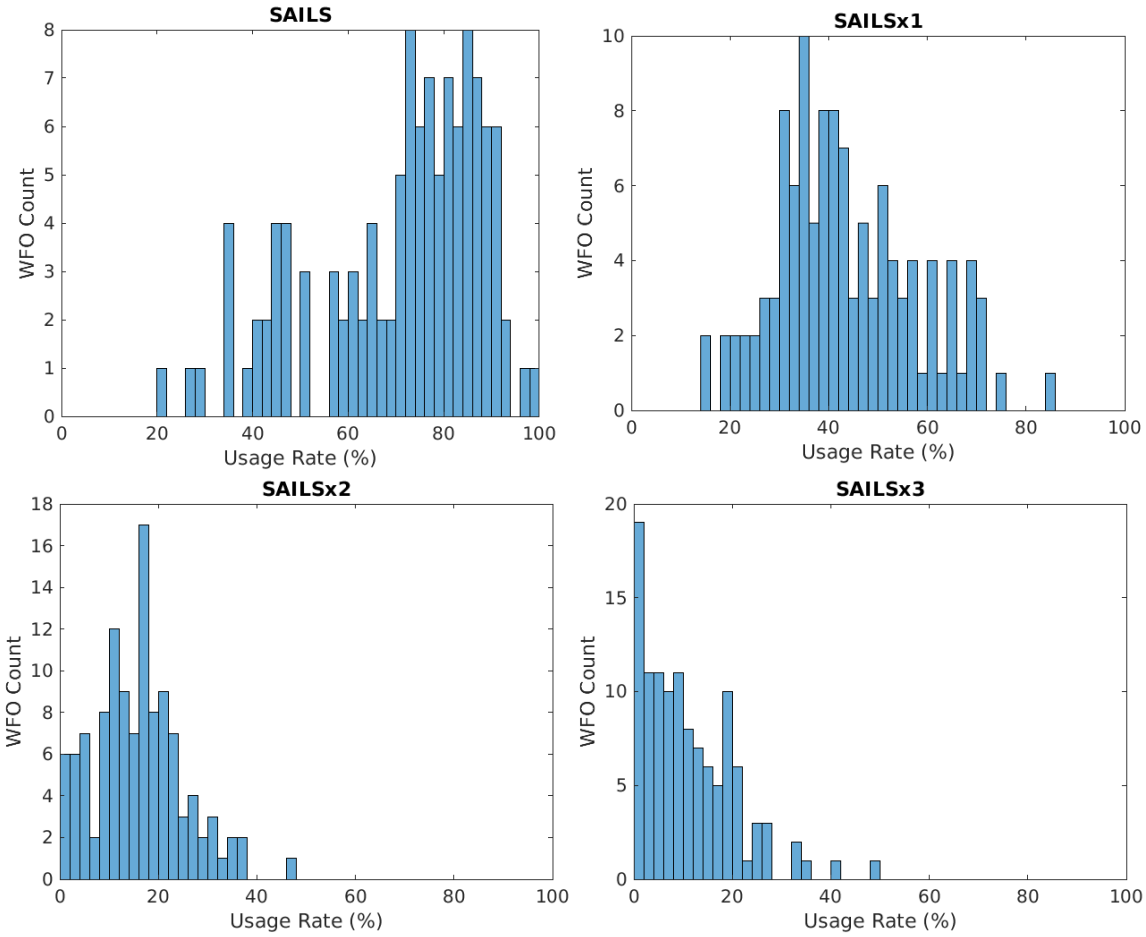

Figure 36. Histograms of SAILS usage rate by WFOs for SVR, FF, and TOR warning decisions (2014–2022).

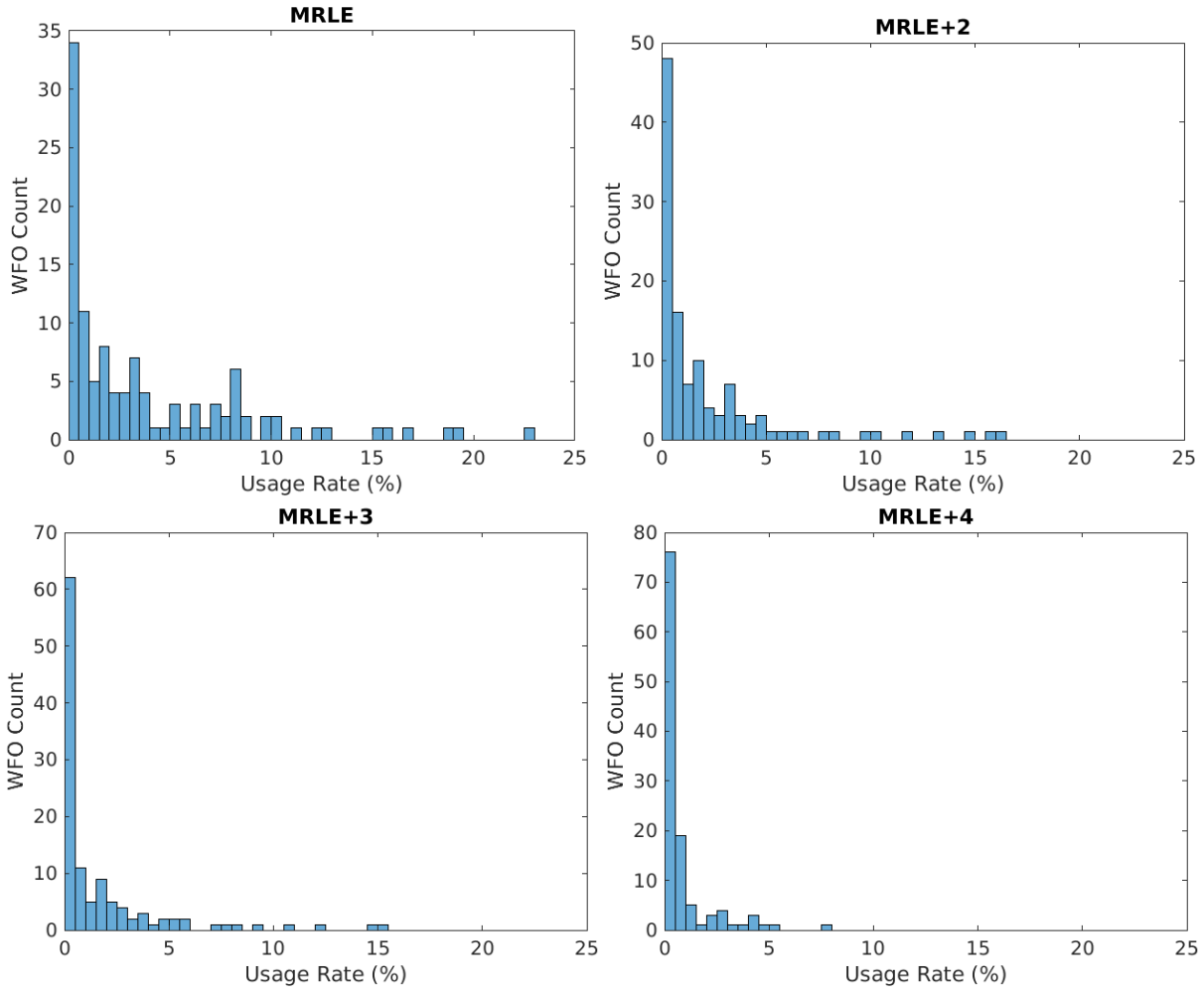

Figure 37. Histograms of MRLE usage rate by WFOs for SVR, FF, and TOR warning decisions (2018–2022).

We also tried looking at the WFO SAILS and MRLE usage by year, but were not able to discern any notable patterns. In general, there was no steady increase or decrease over time; rather, the changes from year-to-year were mostly noisy and unpredictable.

5. SUMMARY DISCUSSION

Aside from potential workload saturation issues, meteorologists want to have their weather radar data updated as frequently as possible. However, because radars have unavoidable trade-offs between update rate, data quality, and spatial coverage, it is impossible to provide arbitrarily rapid updates of operationally acceptable data products. The SAILS and MRLE VCP options were developed to give the radar operator flexibility to obtain more frequent updates of certain elevation angle scans, but at the expense of slowing down the volume update rate. The SAILS option was inspired by the TDWR hazard scan, which intersperses base scans at ~1-minute intervals within a ~2.5-minute volume scan, at the cost of having sparse elevation angle coverage. This scan strategy was optimized for the TDWR's primary mission of low-altitude wind-shear detection, and it has been shown that, on average, it detects microbursts earlier than the WSR-88D, most likely due to the more frequent base scan updates (Cho and Bennett 2023). The TDWR also switches automatically between the monitor and hazard scan modes, based on the presence of weather; thus, it could be argued that it is in optimal scanning mode at all times.

In contrast to the TDWR, the WSR-88D has multiple tri-agency missions that must be considered in real-time by a human operator. The deployment of SAILS and MRLE has provided more radar scanning options, which allows the operator to choose the one that seems to best fulfill the observational needs of the moment. One expects that, based on their understanding of storm morphology and development, as well as experience gained from using the SAILS and MRLE options, meteorologists would, on the whole, tend toward the most effective scan modes for any given situation. However, it is very difficult for an operator to judge fairly whether the scanning choice that they made was better than the others, since they have no access to the parallel outcomes that would have resulted from alternative selections. We hope that our statistical analyses, conducted on a large historical dataset, will provide meaningful objective feedback on measurable outcomes of these radar operational decisions.

Overall, it is clear that SAILS and MRLE have had a positive impact on warning performance. By slicing and dicing the data in different ways, we were able to gain confidence that the statistically meaningful differences in warning performance associated with the different scanning options were not artifacts generated by systematic correlations with other factors. The fact that scans with SAILS and MRLE both turned off were used for only a small fraction of the time while making severe weather warning decisions implies that forecasters have, on the whole, accepted the helpfulness of SAILS and MRLE. And yet, the discrepancies between the most popular scan options and the statistically most effective ones (Table 2) raise the question of whether SAILS and MRLE should be utilized more often under certain circumstances. The very wide range of SAILS and MRLE usage rates by WFOs accentuate this question. We recommend that the NWS conduct a nationwide survey of WFOs to understand how radar operators make decisions on which VCP options to use under what circumstances, and synthesize the results with those of this study to provide enhanced guidance on WSR-88D usage in the future.

The relative importance of base vs. volume scan update rate for severe weather warning performance is tough to evaluate, given the underlying anti-correlation between the two with SAILS and MRLE. However, there was evidence that increasing base scan update rate is more valuable for TOR warnings, especially for the hard-to-warn convective modes of QLCS and disorganized, even at the cost of slowing down the volume updates. This raises the question of whether a new SAILSx4 option might be of additional benefit for these situations.

On the other hand, with SVR warnings, the slowdown in volume update rate with increasing N for SAILSxN seemed to saturate the benefits derived from the correspondingly more frequent base scan updates at SAILSx2, especially for hail events. (An exception was trailing warning MLT for thunderstorm wind events where SAILSx3 outperformed the other options.) Also, with SVR, statistically meaningful correlations were observed between volume scan update rate and warning performance, as well as between base scan update rate and warning performance. Furthermore, MRLE+4 was associated with better SVR warning performance than SAILS, which reinforces the notion that higher-elevation-angle observations were useful and needed; this makes sense, given that hail develops aloft, and there may be precursor signatures aloft for downbursts.

Results for FF warnings were also somewhat mixed regarding the relative importance of base vs. volume scan update rates. For POD and FAR, the slowdown in volume update rate with increasing N for SAILSxN seemed to limit the benefits at SAILSx2. For trailing warning MLT, however, SAILSx3 significantly outperformed the other options. MRLE+4 was the overall winner, perhaps suggesting that short-range predictions of intense rainfall based on frequent observations of surface to mid-level storm evolution can be more important for FF warnings than current QPE based on the fastest updates on the scan closest to the surface.

Admittedly, there may not be one optimal scanning mode for any given instance because forecasters may need to monitor the situation for multiple threat types. Furthermore, the different threats may be in different sectors, whereas the WSR-88D can only carry out one scanning pattern at a time. In principle, PARs could be designed to execute different scan strategies adaptively tailored to different meteorological targets in different sectors, which comes closer to the ideal of optimizing surveillance parameters for each phenomenon. However, even a PAR would be limited by trade-offs between scan update rates, spatial coverage, and data quality, and the trade-off space would, in large part, be dictated by system cost. Therefore, it is of interest to understand better what the range of scan update parameters needs to be in future radar requirements. Experiments with the new generation of polarimetric PARs, such as the National Severe Storm Laboratory's Advanced Technology Demonstrator (ATD; Torres and Wasielewski 2022), where forecasters are tasked to make warning decisions based on a range of sub-sampled data from recorded high-update-rate-everywhere data (*a la* the Phased Array Radar Innovative Sensing Experiment (PARISE; Wilson et al. 2017)) could help refine such requirements.

APPENDIX A. NUMERICAL VALUES UNDERLYING PLOTS

TABLE A-1
Base and Volume Scan Update Periods (s) vs. SAILS Status for VCP 212 for 2012 to 2023 (Figure 1 in Main Text)

Scan Type	Percentile	SAILS off (*M* = 10,291,753)	SAILSx1 (*M* = 8,361,191)	SAILSx2 (*M* = 1,475,107)	SAILSx3 (*M* = 809,097)
Base	25	205	120	95	81
	50	229	127	101	86
	75	269	147	113	95
Volume	25	205	240	284	322
	50	229	254	304	343
	75	269	294	339	379

TABLE A-2
Percentage of Cases During One Hour Prior to When a Warning Decision is Made That a Scanning Mode (VCP Number, SAILS On/Off, and SAILSxN) is Not Changed, Changed Once, or Changed Two or More Times; the Value *M* is the Total Number of Samples for Each Warning Type (Figure 2 in Main Text)

Warning Type	Number of Changes	VCP Number	SAILS On/Off	SAILSxN
SVR (*M* = 138,609)	0	97.45	95.31	92.09
	1	2.54	4.66	7.61
	2+	0.06	0.03	0.30
FF (*M* = 29,443)	0	98.65	98.12	96.77
	1	1.32	1.87	3.15
	2+	0.03	0.01	0.08
TOR (*M* = 17,794)	0	97.60	94.84	87.07
	1	2.37	5.13	12.20
	2+	0.03	0.03	0.73

TABLE A-3
VCP Usage Percentage by Severe Weather Warning Type (Figure 3 in Main Text)

Warning Type	*M*	VCP 12	VCP 212	VCP 215	Others
SVR	138,609	11.32	82.06	4.84	1.78
FF	29,443	11.99	72.37	11.05	4.59
TOR	17,794	8.31	87.73	2.60	1.36

TABLE A-4
Warning Statistics by Category; Percentage of Warnings are (Top) Upper 95% Confidence Limit, (Middle) Mean, and (Bottom) Lower 95% Confidence Limit (Figure 4 in Main Text)

Warning Type		Percentage of Warnings	Mean Warning Area (km^2)	Mean Warning Valid Time (min)
SVR (*M* = 138,609)	Solo	23.74 23.52 23.30	1117 ± 11	36.98 ± 0.13
	Lead	17.51 17.31 17.12	1397 ± 16	42.58 ± 0.15
	Trailing	59.42 59.17 58.91	2104 ± 14	43.94 ± 0.09
FF (*M* = 29,443)	Solo	40.83 40.27 39.71	971 ± 22	181.1 ± 2.0
	Lead	18.45 18.01 17.57	1653 ± 51	206.5 ± 2.3
	Trailing	42.29 41.72 41.16	2447 ± 48	217.6 ± 1.7
TOR (*M* = 17,794)	Solo	32.18 31.65 31.12	656 ± 11	28.60 ± 0.27
	Lead	19.75 19.30 18.85	731 ± 15	32.38 ± 0.33
	Trailing	49.63 49.10 48.49	830 ± 12	33.93 ± 0.23

TABLE A-5

SAILS Usage Percentage by Severe Weather Warning Type; (Top) Upper 95% Confidence Limit, (Middle) Mean, and (Bottom) Lower 95% Confidence Limit (Figure 5 in Main Text)

Warning Type		*M*	SAILS off	SAILSx1	SAILSx2	SAILSx3
SVR	All	138,609	27.09 26.85 26.62	45.70 45.44 45.18	16.70 16.50 16.31	11.37 11.21 11.04
	Solo	32,602	35.71 35.19 34.68	47.01 46.46 45.92	11.91 11.55 11.21	7.07 6.79 6.52
	Lead	23,998	30.92 30.33 29.75	46.72 46.09 45.46	14.87 14.42 13.98	9.53 9.16 8.80
	Trailing	82,009	22.81 22.52 22.23	45.18 44.84 44.50	19.35 19.08 18.81	13.80 13.56 13.33
FF	All	29,443	34.25 33.71 33.17	47.43 46.86 46.29	10.78 10.42 10.08	9.35 9.01 8.69
	Solo	11,856	40.48 39.59 38.72	47.75 46.85 45.96	8.71 8.21 7.73	5.77 5.35 4.96
	Lead	5302	34.80 33.52 32.26	48.59 47.25 45.91	11.59 10.73 9.93	13.03 12.43 11.86
	Trailing	12,285	28.91 28.11 27.32	47.57 46.69 45.81	13.03 12.43 11.86	13.37 12.77 12.19
TOR	All	17,794	9.25 8.83 8.42	35.95 35.25 34.55	24.08 23.45 22.83	33.16 32.47 31.79
	Solo	5631	12.50 11.63 10.82	40.30 39.02 37.75	25.00 23.87 22.77	26.64 25.48 24.36
	Lead	3434	10.91 9.87 8.92	37.03 35.41 33.83	25.69 24.23 22.82	32.05 30.49 28.97
	Trailing	8729	7.15 6.61 6.11	33.74 32.75 31.78	23.77 22.88 22.01	38.78 37.76 36.75

TABLE A-6
SAILS Usage Percentage by Year for SVR, FF, and TOR Warning Decisions
(Figure 6 in Main Text)

Year	*M*	SAILSx1	SAILSx2	SAILSx3
2014	10,420	65.71	0	0
2015	24,135	75.33	0	0
2016	23,478	47.74	13.87	18.09
2017	24,014	33.63	24.74	20.19
2018	21,595	38.17	19.92	14.92
2019	25,765	36.36	21.39	17.19
2020	19,976	33.99	18.24	13.78
2021	20,109	33.90	18.61	10.61
2022	21,425	35.11	17.35	10.88

TABLE A-7

SVR Warning Performance vs. SAILS Usage Status for All Warnings; POD and FAR Values are (Top) Upper 95% Confidence Limit, (Middle) Mean, and (Bottom) Lower 95% Confidence Limit (Figures 7, 8, 22, and 23 in Main Text)

Event Type	SAILS Status	*M* for POD	POD (%)	*M* for MLT	MLT (min)	*M* for FAR	FAR (%)
All	Off	39,408	75.26 74.69 74.26	29,433	20.28 ± 0.17	31,672	49.82 49.27 48.72
	On	137,854	78.36 78.14 77.92	107,719	21.67 ± 0.09	97,759	46.65 46.34 46.02
	x1	80,197	77.07 76.77 76.48	61,571	21.00 ± 0.11	59,353	47.52 47.12 46.72
	x2	34,891	80.63 80.22 79.79	27,988	22.41 ± 0.17	22,874	45.48 44.84 44.19
	x3	22,766	80.28 79.77 79.24	18,160	22.80 ± 0.22	15,532	46.34 45.56 44.78
Hail	Off	14,665	79.19 78.53 77.86	11,517	20.14 ± 0.27	—	—
	On	46,517	80.00 79.64 79.27	37,046	20.56 ± 0.15	—	—
	x1	28,860	79.47 79.01 78.53	22,801	20.18 ± 0.19	—	—
	x2	10,622	81.41 80.67 79.91	8569	21.17 ± 0.31	—	—
	x3	7035	82.59 80.68 79.74	5676	21.17 ± 0.38	—	—
Wind	Off	24,743	72.96 72.41 71.85	17,916	20.37 ± 0.21	—	—
	On	91,337	77.65 77.38 77.10	70,673	22.25 ± 0.11	—	—

	x1	51,337	75.89 75.52 75.15	38,770	21.48 ± 0.14	—	—
	x2	24,269	80.51 80.02 79.51	19,419	22.96 ± 0.21	—	—
	x3	15,731	79.98 79.36 78.72	12,484	23.54 ± 0.26	—	—

TABLE A-8

SVR Warning Performance vs. SAILS Usage Status for Solo Warnings; FAR Values are (Top) Upper 95% Confidence Limit, (Middle) Mean, and (Bottom) Lower 95% Confidence Limit (Figures 7 and 8 in Main Text)

Event Type	SAILS Status	*M* for MLT	MLT (min)	*M* for FAR	FAR (%)
All	Off	5098	13.03 ± 0.32	9251	63.10 62.11 61.12
	On	11,136	13.50 ± 0.22	19,862	63.73 63.06 62.39
	x1	7877	13.36 ± 0.26	13,882	63.39 62.59 61.78
	x2	2174	14.10 ± 0.50	3767	64.84 63.31 61.76
	x3	1085	13.35 ± 0.71	2213	67.52 65.58 63.56
Hail	Off	1996	12.57 ± 0.51	—	—
	On	4545	12.60 ± 0.33	—	—
	x1	3196	12.62 ± 0.39	—	—
	x2	916	12.98 ± 0.75	—	—
	x3	433	11.67 ± 0.99	—	—
Wind	Off	3102	13.32 ± 0.42	—	—
	On	6591	14.12 ± 0.29	—	—
	x1	4681	13.86 ± 0.34	—	—
	x2	1258	14.92 ± 0.66	—	—
	x3	652	14.47 ± 0.98	—	—

TABLE A-9

SVR Warning Performance vs. SAILS Usage Status for Lead Warnings; FAR Values are (Top) Upper 95% Confidence Limit, (Middle) Mean, and (Bottom) Lower 95% Confidence Limit (Figures 7 and 8 in Main Text)

Event Type	SAILS Status	*M* for MLT	MLT (min)	*M* for FAR	FAR (%)
All	Off	6811	19.32 ± 0.34	6153	44.15 42.91 41.67
	On	19,123	19.42 ± 0.20	16,045	42.85 42.08 41.32
	x1	12,357	19.35 ± 0.25	10,386	42.89 41.94 41.00
	x2	4274	19.57 ± 0.42	3460	43.30 41.65 40.01
	x3	2492	19.51 ± 0.58	2199	45.51 43.43 41.37
Hail	Off	3136	20.08 ± 0.52	—	—
	On	8629	19.83 ± 0.30	—	—
	x1	5635	19.77 ± 0.37	—	—
	x2	1863	20.10 ± 0.64	—	—
	x3	1131	19.65 ± 0.83	—	—
Wind	Off	3675	18.68 ± 0.45	—	—
	On	10,494	19.09 ± 0.27	—	—
	x1	6722	19.00 ± 0.33	—	—
	x2	2411	19.16 ± 0.56	—	—
	x3	1361	19.40 ± 0.80	—	—

TABLE A-10

SVR Warning Performance vs. SAILS Usage Status for Trailing Warnings; FAR Values are (Top) Upper 95% Confidence Limit, (Middle) Mean, and (Bottom) Lower 95% Confidence Limit (Figures 7 and 8 in Main Text)

Event Type	SAILS Status	*M* for MLT	MLT (min)	*M* for FAR	FAR (%)
All	Off	17,521	22.77 ± 0.22	16,268	45.15 44.38 43.62
	On	77,450	23.40 ± 0.10	61,852	42.46 42.07 41.68
	x1	41,332	22.95 ± 0.14	35,085	43.05 42.53 41.02
	x2	21,540	23.81 ± 0.20	15,647	41.87 41.09 40.33
	x3	14,578	24.07 ± 0.24	11,120	42.92 42.00 41.08
Hail	Off	6385	22.54 ± 0.37	—	—
	On	23,866	22.35 ± 0.18	—	—
	x1	13,965	22.08 ± 0.24	—	—
	x2	5790	22.81 ± 0.37	—	—
	x3	4111	22.69 ± 0.44	—	—
Wind	Off	11,136	22.90 ± 0.28	—	—
	On	53,584	23.87 ± 0.12	—	—
	x1	27,367	23.40 ± 0.17	—	—
	x2	15,750	24.18 ± 0.23	—	—
	x3	10,467	24.65 ± 0.29	—	—

TABLE A-11

FF Warning Performance vs. SAILS Usage Status for All Warnings; POD and FAR Values are (Top) Upper 95% Confidence Limit, (Middle) Mean, and (Bottom) Lower 95% Confidence Limit (Figures 9 and 24 in Main Text)

SAILS Status	*M* for POD	POD (%)	*M* for MLT	MLT (min)	*M* for FAR	FAR (%)
Off	6155	84.53 83.62 82.68	5147	63.18 ± 1.90	6939	54.12 52.95 51.77
On	19,048	86.47 85.99 85.49	16,379	71.59 ± 1.23	17,898	46.00 45.27 44.55
x1	12,142	86.80 86.20 85.57	10,466	68.70 ± 1.50	12,175	47.56 46.68 45.79
x2	3717	86.15 85.04 83.86	3161	68.69 ± 2.61	3069	45.33 43.56 41.82
x3	3189	87.45 86.30 85.06	2752	85.89 ± 3.46	2654	42.69 40.81 38.95

TABLE A-12

FF Warning Performance vs. SAILS Usage Status for Solo Warnings; FAR Values are (Top) Upper 95% Confidence Limit, (Middle) Mean, and (Bottom) Lower 95% Confidence Limit (Figure 9 in Main Text)

SAILS Status	*M* for MLT	MLT (min)	*M* for FAR	FAR (%)
Off	1792	40.51 ± 2.34	3281	63.73 62.08 60.41
On	4097	43.03 ± 1.69	6333	58.03 56.81 55.95
x1	2914	41.50 ± 1.97	4726	59.23 57.83 56.42
x2	745	49.55 ± 4.09	973	55.95 52.83 49.68
x3	438	42.06 ± 5.56	634	59.19 55.36 51.47

TABLE A-13

FF Warning Performance vs. SAILS Usage Status for Lead Warnings; FAR Values are (Top) Upper 95% Confidence Limit, (Middle) Mean, and (Bottom) Lower 95% Confidence Limit (Figure 9 in Main Text)

SAILS Status	*M* for MLT	MLT (min)	*M* for FAR	FAR (%)
Off	1356	70.14 ± 3.54	1245	47.11 44.34 41.60
On	4015	70.89 ± 2.23	3258	41.19 39.50 37.84
x1	2711	69.81 ± 2.71	2238	41.32 39.28 37.27
x2	719	73.43 ± 5.22	569	45.39 41.30 37.33
x3	585	72.77 ± 6.03	451	42.93 38.36 33.99

TABLE A-14

FF Warning Performance vs. SAILS Usage Status for Trailing Warnings; FAR Values are (Top) Upper 95% Confidence Limit, (Middle) Mean, and (Bottom) Lower 95% Confidence Limit (Figure 9 in Main Text)

SAILS Status	*M* for MLT	MLT (min)	*M* for FAR	FAR (%)
Off	1999	78.80 ± 3.52	2413	46.96 44.96 42.99
On	8267	86.08 ± 1.95	8307	39.79 38.74 37.70
x1	4841	84.45 ± 2.51	5211	41.08 39.74 38.42
x2	1697	75.09 ± 3.88	1527	40.97 38.51 36.10
x3	1729	101.44 ± 4.74	1569	38.03 35.63 33.30

TABLE A-15

TOR Warning Performance vs. SAILS Usage Status for All Warnings; POD and FAR Values are (Top) Upper 95% Confidence Limit, (Middle) Mean, and (Bottom) Lower 95% Confidence Limit (Figures 10, 11, and 25 in Main Text)

EF#	SAILS Status	*M* for POD	POD (%)	*M* for MLT	MLT (min)	*M* for FAR	FAR (%)
All	Off	650	48.46 44.62 40.84	290	11.00 ± 1.40	1250	80.98 78.80 76.45
	On	8709	68.77 67.79 66.80	5904	12.24 ± 0.32	15,840	71.17 70.47 69.75
	x1	3198	61.88 60.19 58.49	1925	11.66 ± 0.55	5889	73.67 72.54 71.39
	x2	2159	70.52 68.60 66.61	1481	11.33 ± 0.63	4173	73.42 72.08 70.70
	x3	3352	75.97 74.52 73.02	2498	13.23 ± 0.49	5778	68.38 67.19 65.96
0–1	Off	590	45.71 41.69 37.78	246	10.90 ± 1.48	—	—
	On	7681	66.46 65.41 64.34	5024	11.94 ± 0.34	—	—
	x1	2888	59.79 58.00 56.19	1675	11.47 ± 0.59	—	—
	x2	1908	68.39 67.30 64.15	1265	10.87 ± 0.68	—	—
	x3	2885	73.84 72.24 70.57	2084	12.97 ± 0.54	—	—
2	Off	49	80.48 69.39 55.47	34	13.50 ± 5.01	—	—
	On	825	85.77 83.15 80.45	686	13.70 ± 0.97	—	—

	x1	240	81.19 76.25 70.48	183	13.01± 1.97	—	—
	x2	215	89.65 85.58 80.26	184	13.89 ± 1.93	—	—
	x3	370	89.36 86.22 82.33	319	13.98 ± 1.37	—	—
3–5	Off	11	98.38 90.91 62.26	10	4.90 ± 6.49	—	—
	On	203	97.65 95.57 91.79	194	14.91 ± 1.70	—	—
	x1	70	98.53 95.71 88.14	67	12.76 ± 2.83	—	—
	x2	36	95.59 88.89 74.69	32	14.91 ± 4.24	—	—
	x3	97	99.43 97.94 92.79	95	16.42 ± 2.50	—	—

TABLE A-16

TOR Warning Performance vs. SAILS Usage Status for Solo Warnings; FAR Values are (Top) Upper 95% Confidence Limit, (Middle) Mean, and (Bottom) Lower 95% Confidence Limit (Figures 10 and 11 in Main Text)

EF#	SAILS Status	*M* for MLT	MLT (min)	*M* for FAR	FAR (%)
All	Off	82	4.49 ± 1.97	516	86.66 83.72 80.29
	On	1096	4.71 ± 0.53	4800	82.37 81.29 80.16
	x1	422	4.72 ± 0.87	2021	83.98 82.39 80.66
	x2	306	4.37 ± 1.01	1344	82.68 80.65 78.46
	x3	368	4.96 ± 0.88	1435	82.32 80.35 78.21
0–1	Off	74	4.08 ± 1.87	—	—
	On	1034	4.79 ± 0.55	—	—
	x1	400	4.75 ± 0.90	—	—
	x2	294	4.49 ± 1.05	—	—
	x3	340	5.10 ± 0.92	—	—
2	Off	7	9.57 ± 14.73	—	—
	On	59	3.59 ± 2.07	—	—
	x1	21	4.67 ± 3.97	—	—
	x2	12	1.33 ± 3.10	—	—
	x3	26	3.77 ± 3.43	—	—
3–5	Off	1	-1.00	—	—
	On	3	-3.33 ± 10.34	—	—
	x1	1	-4.00	—	—
	x2	0	—	—	—
	x3	2	-3.00 ± 50.82	—	—

TABLE A-17

TOR Warning Performance vs. SAILS Usage Status for Lead Warnings; FAR Values are (Top) Upper 95% Confidence Limit, (Middle) Mean, and (Bottom) Lower 95% Confidence Limit (Figures 10 and 11 in Main Text)

EF#	SAILS Status	*M* for MLT	MLT (min)	*M* for FAR	FAR (%)
All	Off	109	10.39 ± 2.29	270	78.60 73.70 68.15
	On	1715	10.10 ± 0.56	3023	65.24 63.55 61.81
	x1	592	10.28 ± 0.97	1144	66.97 64.25 61.43
	x2	453	8.88 ± 1.06	832	68.42 65.26 61.97
	x3	670	10.76 ± 0.89	1047	64.32 61.42 58.43
0–1	Off	93	10.83 ± 2.46	—	—
	On	1465	10.10 ± 0.60	—	—
	x1	512	10.22 ± 1.01	—	—
	x2	393	9.01 ± 1.13	—	—
	x3	559	10.74 ± 0.98	—	—
2	Off	11	9.55 ± 9.08	—	—
	On	204	9.92 ± 1.77	—	—
	x1	62	11.21 ± 3.73	—	—
	x2	52	8.44 ± 3.48	—	—
	x3	90	9.88 ± 2.45	—	—
3–5	Off	5	4.00 ± 14.24	—	—
	On	47	10.89 ± 3.73	—	—
	x1	18	8.83 ± 7.48	—	—
	x2	8	5.13 ± 8.00	—	—
	x3	21	14.86 ± 4.84	—	—

TABLE A-18

TOR Warning Performance vs. SAILS Usage Status for Trailing Warnings; FAR Values are (Top) Upper 95% Confidence Limit, (Middle) Mean, and (Bottom) Lower 95% Confidence Limit (Figures 10 and 11 in Main Text)

EF#	SAILS Status	*M* for MLT	MLT (min)	*M* for FAR	FAR (%)
All	Off	99	17.07 ± 2.30	464	79.94 76.29 72.22
	On	3090	16.11 ± 0.44	8017	67.62 66.60 65.56
	x1	911	15.78 ± 0.79	2724	70.44 68.72 66.96
	x2	722	15.82 ± 0.91	1997	71.14 69.15 67.09
	x3	1457	16.47 ± 0.65	3296	64.92 63.29 61.63
0–1	Off	79	17.38 ± 2.49	—	—
	On	2523	15.95 ± 0.49	—	—
	x1	763	15.84 ± 0.87	—	—
	x2	578	15.37 ± 1.02	—	—
	x3	1182	16.30 ± 0.73	—	—
2	Off	16	17.94 ± 7.35	—	—
	On	423	16.93 ± 1.17	—	—
	x1	100	15.88 ± 2.52	—	—
	x2	120	17.50 ± 2.28	—	—
	x3	203	17.11 ± 1.65	—	—
3–5	Off	4	7.50 ± 11.21	—	—
	On	144	16.60 ± 1.86	—	—
	x1	48	14.58 ± 2.79	—	—
	x2	24	18.17 ± 4.51	—	—
	x3	72	17.42 ± 2.92	—	—

TABLE A-19
SAILS Usage Rate (%) vs. Storm Type for TOR Warning Decisions (2014–2020; Figure 12 in Main Text)

Storm Type	*M*	SAILS Off	SAILSx1	SAILSx2	SAILSx3
Right-Moving Supercell	3440	14.27	42.12	17.94	25.67
Right-Moving Supercell Line	661	9.83	37.22	20.88	32.07
Right-Moving Supercell Cluster	1691	13.60	42.87	17.50	26.02
Right-Moving Supercell Discrete	1083	18.10	44.04	16.81	21.05
Quasi-Linear Convective System	1537	8.13	34.16	23.36	34.35
Disorganized	4465	7.23	40.18	21.41	31.13
Line (any type)	4529	8.52	39.99	21.13	30.36
Discrete	1248	19.55	44.07	16.51	19.87
Tropical Cyclone	172	2.91	23.26	12.21	61.63

TABLE A-20

TOR Warning POD (%) and Corresponding *M* vs. Storm Type and SAILS Mode; POD Values are (Top) Upper 95% Confidence Limit, (Middle) Mean, and (Bottom) Lower 95% Confidence Limit (Figure 13 in Main Text)

Storm Type		SAILS Off	SAILS On	SAILSx1	SAILSx2	SAILSx3
Right-Moving Supercell	*M*	491	2949	1449	617	883
	POD	74.03 69.63 64.85	80.54 78.93 77.23	77.12 74.67 72.05	81.14 77.66 73.76	88.80 86.49 83.79
Right-Moving Supercell Line	*M*	65	596	246	138	212
	POD	86.00 76.47 63.24	82.23 78.76 74.81	82.28 76.92 70.52	84.94 78.10 69.27	86.52 81.33 74.71
Right-Moving Supercell Cluster	*M*	230	1461	725	296	440
	POD	77.22 71.02 63.93	81.41 79.17 76.73	78.17 74.73 70.95	80.75 75.65 69.71	90.97 88.04 84.33
Right-Moving Supercell Discrete	*M*	196	887	477	182	228
	POD	72.81 65.81 58.04	81.64 78.79 75.64	77.80 73.61 68.96	85.81 80.26 73.22	92.29 88.40 82.91
Quasi-Linear Convective System	*M*	125	1412	525	359	528
	POD	49.08 38.64 29.14	62.00 58.89 55.72	50.51 45.25 40.09	64.79 58.75 52.43	76.85 72.44 67.55
Disorganized	*M*	325	4140	1794	956	1390
	POD	49.48 43.36 37.43	73.39 71.84 70.23	67.48 64.98 62.39	74.52 71.33 67.91	83.12 80.87 78.39
Line (any type)	*M*	386	4143	1811	957	1375
	POD	61.35 55.78 50.07	74.66 73.13 71.54	69.88 67.43 64.89	74.58 71.39 67.96	83.92 81.69 79.23
Discrete	*M*	244	1004	550	206	248
	POD	61.86 54.97 47.89	74.81 71.79 68.56	70.68 66.35 61.73	78.13 71.93 64.77	87.88 83.33 77.52

TABLE A-21
TOR Warning MLT (min) and Corresponding *M* vs. Storm Type and SAILS Mode (Figure 14 in Main Text)

Storm Type		SAILS Off	SAILS On	SAILSx1	SAILSx2	SAILSx3
Right-Moving Supercell	*M*	266	1843	843	379	621
	MLT	16.18 ± 1.51	14.69 ± 0.50	14.50 ± 0.73	13.38 ± 1.09	15.74 ± 0.88
Right-Moving Supercell: Line	*M*	39	367	150	82	135
	MLT	23.00 ± 4.90	13.31 ± 1.11	12.22 ± 1.64	14.33 ± 2.68	13.89 ± 1.82
Right-Moving Supercell: Cluster	*M*	125	912	414	174	324
	MLT	15.26 ± 2.07	14.81 ± 0.72	14.92 ± 1.11	12.85 ± 1.54	15.71 ± 1.20
Right-Moving Supercell: Discrete	*M*	102	561	279	122	160
	MLT	14.71 ± 2.29	15.46 ± 0.90	15.10 ± 1.20	13.56 ± 1.92	17.53 ± 1.83
Quasi-Linear Convective System	*M*	34	553	157	141	255
	MLT	9.47 ± 2.82	12.91 ± 0.86	12.31 ± 1.49	11.84 ± 1.70	13.88 ± 1.32
Disorganized	*M*	111	2242	874	510	858
	MLT	13.57 ± 2.02	14.27 ± 0.45	14.11 ± 0.71	13.00 ± 0.93	15.18 ± 0.74
Line (any type)	*M*	164	2270	909	509	852
	MLT	14.90 ± 1.93	14.26 ± 0.45	14.10 ± 0.69	13.04 ± 0.93	15.18 ± 0.74
Discrete	*M*	105	570	282	123	165
	MLT	14.41 ± 2.25	15.43 ± 0.89	15.04 ± 1.19	13.48 ± 1.91	17.55 ± 1.78

TABLE A-22
Base and Volume Scan Update Periods (s) vs. MRLE Status for VCP 212 for 2012–2022 (Figure 15 in Main Text)

Scan Type	Percentile	MRLE off (*M* = 10,291,753)	MRLE+2 (*M* = 108,045)	MRLE+3 (*M* = 39,675)	MRLE+4 (*M* = 17,212)
Base	25	205	120	95	81
	50	229	127	101	86
	75	269	147	113	95
Volume	25	205	240	284	322
	50	229	254	304	343
	75	269	294	339	379

TABLE A-23

MRLE Usage Percentage by Severe Weather Warning Type; (Top) Upper 95% Confidence Limit, (Middle) Mean, and (Bottom) Lower 95% Confidence Limit (Figure 16 in Main Text)

Warning Type		*M*	MRLE+2	MRLE+3	MRLE+4
SVR	All	142,511	1.28 1.22 1.17	1.11 1.05 1.00	0.50 0.46 0.43
	Solo	33,213	1.04 0.93 0.83	0.71 0.62 0.54	0.36 0.29 0.24
	Lead	24,588	1.36 1.21 1.08	0.98 0.85 0.75	0.41 0.33 0.27
	Trailing	84,710	1.42 1.34 1.27	1.36 1.28 1.20	0.62 0.57 0.52
FF	All	29,993	1.09 0.97 0.87	0.75 0.65 0.57	0.27 0.21 0.16
	Solo	12,062	1.16 0.97 0.81	0.68 0.53 0.42	0.31 0.21 0.14
	Lead	5405	1.32 1.02 0.78	0.86 0.61 0.44	0.46 0.28 0.17
	Trailing	12,526	1.14 0.96 0.80	0.95 0.78 0.64	0.28 0.18 0.12
TOR	All	2190	1.29 1.12 0.98	1.51 1.33 1.17	1.05 0.91 0.78
	Solo	855	1.67 1.34 1.07	1.49 1.18 0.94	1.19 0.91 0.70
	Lead	454	1.50 1.10 0.80	1.88 1.44 1.09	1.04 0.70 0.48
	Trailing	881	1.22 1.00 0.81	1.65 1.38 1.16	1.21 0.99 0.80

TABLE A-24
MRLE Usage Percentage by Year for SVR, FF, and TOR Warning Decisions; (Figure 17 in Main Text)

Year	*M*	MRLE+2	MRLE+3	MRLE+4
2018	21,595	0.81	0.21	0.33
2019	25,765	0.44	0.64	0.34
2020	19,976	2.49	2.49	1.03
2021	20,109	3.99	3.08	1.08
2022	21,425	3.05	2.86	1.44

TABLE A-25

SVR Warning Performance vs. MRLE Usage Status for All Warnings; POD and FAR Values are (Top) Upper 95% Confidence Limit, (Middle) Mean, and (Bottom) Lower 95% Confidence Limit (Figures 18 and 19 in Main Text)

Event Type	MRLE Status	*M* for POD	POD (%)	*M* for MLT	MLT (min)	*M* for FAR	FAR (%)
All	Off	39,408	75.26 74.69 74.26	29,433	20.28 ± 0.17	31,672	49.82 49.27 48.72
	On	5875	81.92 80.94 79.91	4755	22.62 ± 0.42	3796	44.63 43.05 41.48
	+2	2673	78.18 76.62 74.98	2048	22.72 ± 0.65	1709	48.01 45.64 43.29
	+3	2093	85.00 83.47 81.82	1747	22.43 ± 0.70	1438	44.50 41.93 39.41
	+4	1109	88.45 86.56 84.43	960	22.79 ± 0.90	649	42.48 38.67 35.01
Hail	Off	14,665	79.19 78.53 77.86	11,517	20.14 ± 0.27	—	—
	On	1752	86.96 85.39 83.66	1496	21.98 ± 0.75	—	—
	+2	726	83.55 80.85 77.83	587	20.85 ± 1.17	—	—
	+3	713	90.76 88.64 86.10	632	22.72 ± 1.19	—	—
	+4	313	91.58 88.50 84.49	277	22.69 ± 1.71	—	—
Wind	Off	24,743	72.96 72.41 71.85	17,916	20.37 ± 0.21	—	—
	On	4123	80.26 79.04 77.78	3259	22.92 ± 0.51	—	—

	+2	1947	76.91 75.04 73.07	1461	23.47 ± 0.78	—	—
	+3	1380	82.79 80.80 78.63	1115	22.26 ± 0.88	—	—
	+4	796	88.06 85.80 83.21	683	22.83 ± 1.05	—	—

TABLE A-26

SVR Warning Performance vs. MRLE Usage Status for Solo Warnings; FAR Values are (Top) Upper 95% Confidence Limit, (Middle) Mean, and (Bottom) Lower 95% Confidence Limit (Figures 18 and 19 in Main Text)

Event Type	MRLE Status	*M* for MLT	MLT (min)	*M* for FAR	FAR (%)
All	Off	5098	13.03 ± 0.32	9251	63.10 62.11 61.12
	On	301	11.94 ± 134	565	66.20 62.30 58.23
	+2	140	11.65 ± 1.97	296	70.72 65.54 59.96
	+3	100	10.90 ± 2.24	179	66.68 59.78 52.46
	+4	61	14.30 ± 3.24	90	66.42 56.67 46.36
Hail	Off	1996	12.57 ± 0.51	—	—
	On	139	9.47 ± 1.64	—	—
	+2	60	8.43 ± 2.39	—	—
	+3	53	10.13 ± 2.86	—	—
	+4	26	10.50 ± 3.97	—	—
Wind	Off	3102	13.32 ± 0.42	—	—
	On	162	14.06 ± 2.02	—	—
	+2	80	14.06 ± 2.88	—	—
	+3	47	11.77 ± 3.61	—	—
	+4	35	17.11 ± 4.75	—	—

TABLE A-27

SVR Warning Performance vs. MRLE Usage Status for Lead Warnings; FAR Values are (Top) Upper 95% Confidence Limit, (Middle) Mean, and (Bottom) Lower 95% Confidence Limit (Figures 18 and 19 in Main Text)

Event Type	MRLE Status	*M* for MLT	MLT (min)	*M* for FAR	FAR (%)
All	Off	6811	19.32 ± 0.34	6153	44.15 42.91 41.67
	On	793	21.08 ± 1.04	565	41.05 36.99 33.11
	+2	416	19.63 ± 1.35	291	39.99 34.36 29.14
	+3	261	22.58 ± 1.92	194	48.79 41.75 35.04
	+4	116	22.92 ± 2.84	80	45.92 35.00 25.45
Hail	Off	3136	20.08 ± 0.52	—	—
	On	343	21.57 ± 1.57	—	—
	+2	159	19.68 ± 2.17	—	—
	+3	133	22.60 ± 2.69	—	—
	+4	51	24.75 ± 4.20	—	—
Wind	Off	3675	18.68 ± 0.45	—	—
	On	450	20.71 ± 1.38	—	—
	+2	257	19.59 ± 1.74	—	—
	+3	128	22.55 ± 2.77	—	—
	+4	65	21.49 ± 3.91	—	—

TABLE A-28

SVR Warning Performance vs. MRLE Usage Status for Trailing Warnings; FAR Values are (Top) Upper 95% Confidence Limit, (Middle) Mean, and (Bottom) Lower 95% Confidence Limit (Figures 18 and 19 in Paper)

Event Type	MRLE Status	*M* for MLT	MLT (min)	*M* for FAR	FAR (%)
All	Off	17,521	22.77 ± 0.22	16,268	45.15 44.38 43.62
	On	3661	23.84 ± 0.48	2666	42.12 40.25 38.40
	+2	1492	24.62 ± 0.76	1122	46.23 43.32 40.44
	+3	1386	23.23 ± 0.78	1065	41.93 38.97 36.08
	+4	783	23.43 ± 0.97	479	40.30 35.91 31.74
Hail	Off	6385	22.54 ± 0.37	—	—
	On	1014	23.83 ± 0.89	—	—
	+2	368	23.37 ± 1.46	—	—
	+3	446	24.25 ± 1.39	—	—
	+4	200	23.75 ± 1.98	—	—
Wind	Off	11,136	22.90 ± 0.28	—	—
	On	2647	23.84 ± 0.56	—	—
	+2	1124	25.02 ± 0.89	—	—
	+3	940	22.74 ± 0.94	—	—
	+4	583	23.32 ± 1.12	—	—

TABLE A-29

FF Warning Performance vs. MRLE Usage Status for All Warnings; POD and FAR Values are (Top) Upper 95% Confidence Limit, (Middle) Mean, and (Bottom) Lower 95% Confidence Limit (Figure 20 in Main Text)

MRLE Status	*M* for POD	POD (%)	*M* for MLT	MLT (min)	*M* for FAR	FAR (%)
Off	6155	84.53 83.62 82.68	5147	63.18 ± 1.90	6939	54.12 52.95 51.77
On	474	91.54 89.03 85.90	422	75.45 ± 7.74	436	45.73 41.06 36.54
+2	275	92.25 89.09 84.85	245	72.22 ± 9.57	276	51.55 45.65 39.88
+3	110	90.84 85.45 77.67	94	89.80 ± 18.48	105	49.56 40.00 31.14
+4	89	96.87 93.26 86.06	83	68.76 ± 18.00	55	32.36 20.00 11.55

TABLE A-30

FF Warning Performance vs. MRLE Usage Status for Solo Warnings; FAR Values are (Top) Upper 95% Confidence Limit, (Middle) Mean, and (Bottom) Lower 95% Confidence Limit (Figure 20 in Main Text)

MRLE Status	*M* for MLT	MLT (min)	*M* for FAR	FAR (%)
Off	1792	40.51 ± 2.34	3281	63.73 62.08 60.41
On	113	43.06 ± 11.84	170	64.83 57.65 50.13
+2	61	51.51 ± 17.49	113	69.55 61.06 51.85
+3	23	33.04 ± 22.77	36	75.22 61.11 44.86
+4	29	33.24 ± 22.95	21	54.63 33.33 17.19

TABLE A-31

FF Warning Performance vs. MRLE Usage Status for Lead Warnings; FAR Values Are (Top) Upper 95% Confidence Limit, (Middle) Mean, and (Bottom) Lower 95% Confidence Limit (Figure 20 in Main Text)

MRLE Status	*M* for MLT	MLT (min)	*M* for FAR	FAR (%)
Off	1356	70.14 ± 3.54	1245	47.11 44.34 41.60
On	114	71.23 ± 12.20	83	49.31 38.55 28.81
+2	70	69.10 ± 13.96	51	56.73 43.14 30.50
+3	24	95.54 ± 29.94	19	63.72 42.11 23.14
+4	20	49.50 ± 35.98	13	42.23 15.38 4.33

TABLE A-32

FF Warning Performance vs. MRLE Usage Status for Trailing Warnings; FAR Values are (Top) Upper 95% Confidence Limit, (Middle) Mean, and (Bottom) Lower 95% Confidence Limit (Figure 20 in Main Text)

MRLE Status	*M* for MLT	MLT (min)	*M* for FAR	FAR (%)
Off	1999	78.80 ± 3.52	2413	46.96 44.96 42.99
On	195	96.69 ± 12.84	183	33.62 26.78 20.89
+2	114	85.21 ± 16.09	112	40.34 31.25 23.41
+3	47	114.64 ± 29.90	50	37.41 24.00 14.30
+4	34	110.38 ± 29.75	21	28.91 9.52 2.65

TABLE A-33

TOR Warning Performance vs. MRLE Usage Status for All Warnings; POD and FAR Values are (Top) Upper 95% Confidence Limit, (Middle) Mean, and (Bottom) Lower 95% Confidence Limit (Figure 21 in Main Text)

MRLE Status	*M* for POD	POD (%)	*M* for MLT	MLT (min)	*M* for FAR	FAR (%)
Off	650	48.46 44.62 40.84	290	11.00 ± 1.40	1250	80.98 78.80 76.45
On	368	70.94 66.30 61.33	244	8.91 ± 1.31	602	70.42 66.78 62.92
+2	121	72.43 64.46 55.61	78	7.99 ± 2.40	205	73.82 67.80 61.13
+3	154	69.60 62.34 54.47	96	9.70 ± 2.25	230	71.90 66.09 59.75
+4	93	82.92 75.27 65.62	70	8.87 ± 2.18	167	73.19 66.47 59.01

TABLE A-34

TOR Warning Performance vs. MRLE Usage Status for Solo Warnings; POD and FAR Values are (Top) Upper 95% Confidence Limit, (Middle) Mean, and (Bottom) Lower 95% Confidence Limit (Figure 21 in Main Text)

MRLE Status	*M* for MLT	MLT (min)	*M* for FAR	FAR (%)
Off	82	4.49 ± 1.97	516	86.66 83.72 80.29
On	37	1.27 ± 2.44	194	86.73 81.96 75.94
+2	11	-1.27 ± 4.15	76	91.72 85.53 75.92
+3	13	1.15 ± 5.28	65	90.28 83.08 72.18
+4	13	3.54 ± 3.88	53	85.07 75.47 62.43

TABLE A-35
TOR Warning Performance vs. MRLE Usage Status for Lead Warnings; POD and FAR Values are (Top) Upper 95% Confidence Limit, (Middle) Mean, and (Bottom) Lower 95% Confidence Limit (Figure 21 in Main Text)

MRLE Status	*M* for MLT	MLT (min)	*M* for FAR	FAR (%)
Off	109	10.39 ± 2.29	270	78.60 73.70 68.15
On	66	6.71 ± 2.60	111	63.02 54.05 44.80
+2	26	7.81 ± 4.21	39	66.13 51.28 36.20
+3	22	6.18 ± 5.28	47	77.83 65.96 51.67
+4	18	5.78 ± 4.74	25	55.48 36.00 20.25

TABLE A-36

TOR Warning Performance vs. MRLE Usage Status for Trailing Warnings; POD and FAR Values are (Top) Upper 95% Confidence Limit, (Middle) Mean, and (Bottom) Lower 95% Confidence Limit (Figure 21 in Main Text)

MRLE Status	*M* for MLT	MLT (min)	*M* for FAR	FAR (%)
Off	99	17.07 ± 2.30	464	79.94 76.29 72.22
On	141	11.95 ± 1.62	297	66.97 61.62 55.97
+2	41	10.59 ± 3.31	90	69.51 60.00 49.67
+3	61	12.79 ± 2.56	118	65.36 56.78 47.77
+4	39	12.08 ± 2.77	89	78.24 69.66 59.46

This page intentionally left blank.

GLOSSARY

ASP	Archive III Status Product
ATD	Advanced Technology Demonstrator
AVSET	automated volume scan evaluation and termination
CONUS	contiguous United States
EF	enhanced Fujita
FAR	false alarm ratio
FF	flash flood
FVO	fraction of vertical volume observed
LM	left-moving
MCS	mesoscale convective system
MESH	maximum estimated size of hail
MESO	multiple elevation scan option
MLT	mean lead time
MRLE	mid-volume rescan of low-level elevations
NCEI	National Center for Environmental Information
NOAA	National Oceanic and Atmospheric Administration
NWS	National Weather Service
PAR	phased-array radar
POD	probability of detection
POSH	probability of severe hail
QLCS	quasi-linear convective system
QPE	quantitative precipitation estimation
RM	right-moving
SAILS	supplemental adaptive intra-volume low-level scan
SPC	Storm Prediction Center
SVR	severe thunderstorm

TOR	tornado
VCP	volume coverage pattern
VIF	variance inflation factor
VPR	vertical profile of reflectivity
WFO	weather forecast office
WSR-88D	Weather Surveillance Radar 1988-Doppler

REFERENCES

[1.] Anderson-Frey, A. K., and H. Brooks, 2021: Compared to what? Establishing environmental baselines for tornado warning skill. *Bull. Amer. Meteor. Soc.*, **102**, E738–E747, https://doi.org/10.1175/BAMS-D-19-0310.1.

[2.] Andra, Jr., D. L., E. M. Quoetone, and W. F. Bunting, 2002: Warning decision making: The relative roles of conceptual models, technology, strategy, and forecaster expertise on 3 May 1999. *Wea. Forecasting*, **17**, 559–566, https://doi.org/10.1175/1520-0434(2002)017%3C0559:WDMTRR%3E2.0.CO;2.

[3.] Berkson, J., 1944: Application of the logistic function to bio-assay. *J. Amer. Stat. Assoc.*, **39**, 357–365, https://doi.org/10.1080/01621459.1944.10500699.

[4.] Bluestein, H. B., M. M. French, R. L. Tanamachi, S. Frasier, K. Hardwick, F. Junyent, and A. L. Pazmany, 2007: Close-range observations of tornadoes in supercells made with a dual-polarization, X-band, mobile Doppler radar. *Mon. Wea. Rev.*, **135**, 1522–1543, https://doi.org/10.1175/MWR3349.1.

[5.] Bowden, K. A., and P. L. Heinselman, 2016: A qualitative analysis of NWS forecasters' use of phased-array radar data during severe hail and wind events. *Wea. Forecasting*, **31**, 43–55, https://doi.org/10.1175/WAF-D-15-0089.1.

[6.] Brooks, H. E., and J. Correia, Jr., 2018: Long-term performance metrics for National Weather Service tornado warnings. *Wea. Forecasting*, **33**, 1501–1511, https://doi.org/10.1175/WAF-D-18-0120.1.

[7.] Brotzge, J., and S. Erickson, 2010: Tornadoes without NWS warning. *Wea. Forecasting*, **25**, 159–172, https://doi.org/10.1175/2009WAF2222270.1.

[8.] Brotzge, J., S. Nelson, R. Thompson, and B. Smith, 2013: Tornado probability of detection and lead time as a function of convective mode and environmental parameters. *Wea. Forecasting*, **28**, 1261–1276, https://doi.org/10.1175/WAF-D-12-00119.1.

[9.] Brown, R. A., J. M. Janish, and V. T. Wood, 2000: Impact of WSR-88D scanning strategies on severe storm algorithms. *Wea. Forecasting*, **15**, 90–102, https://doi.org/10.1175/15200434(2000)015%3C0090:IOWSSO%3E2.0.CO;2.

[10.] Burgess, D. W., and L. R. Lemon, 1990: Severe thunderstorm detection by radar. In *Radar in Meteorology*, Amer. Meteor. Soc., Boston, MA, 619–647, https://link.springer.com/content/pdf/10.1007%2F978-1-935704-15-7.pdf.

[11.] Cho, J. Y. N., and B. J. Bennett, 2023: WSR-88D microburst detection performance evaluation. Project Rep. ATC-455, MIT Lincoln Laboratory, Lexington, MA.

[12.] Cho, J. Y. N., and J. M. Kurdzo, 2019a: Monetized weather radar network benefits for tornado cost reduction. Project Rep. NOAA-35, MIT Lincoln Laboratory, 88 pp., https://www.ll.mit.edu/sites/default/files/publication/doc/monetized-weather-radar-network-benefits-cho-noaa-35.pdf.

[13.] Cho, J. Y. N., and J. M. Kurdzo, 2019b: Weather radar network benefit model for tornadoes. *J. Appl. Meteor. Climatol.*, **58**, 971–987, https://doi.org/10.1175/JAMC-D-18-0205.1.

[14.] Cho, J. Y. N., and J. M. Kurdzo, 2020a: Weather radar network benefit model for flash flood casualty reduction. *J. Appl. Meteor. Climatol.*, **59**, 589–604, https://doi.org/10.1175/JAMC-D-19-0176.1.

[15.] Cho, J. Y. N., and J. M. Kurdzo, 2020b: Weather radar network benefit model for nontornadic thunderstorm wind casualty reduction. *Wea. Climate Soc.*, **12**, 789–804, https://doi.org/10.1175/WCAS-D-20-0063.1.

[16.] Cho, J. Y. N., J. M. Kurdzo, B. J. Bennett, M. E. Weber, J. W. Dellicarpini, A. Loconto, and H. Frank, 2022: Impact of WSR-88D intra-volume low-level scans on severe weather warning performance. *Wea. Forecasting*, **37**, 1169–1189, https://doi.org/10.1175/WAF-D-21-0152.1.

[17.] Chrisman, J. N., 2013: Dynamic scanning. *NEXRAD Now*, **22**, NOAA/NWS/Radar Operations Center, Norman, OK, 1–3, https://www.roc.noaa.gov/WSR88D/PublicDocs/NNOW/NNow22c.pdf.

[18.] Chrisman, J. N., 2014: The continuing evolution of dynamic scanning. *NEXRAD Now*, **23**, NOAA/NWS/Radar Operations Center, Norman, OK, 8–13, http://www.roc.noaa.gov/WSR88D/PublicDocs/NNOW/NNow23a.pdf.

[19.] Chrisman, J. N., 2016: Mid-volume rescan of low-level elevations (MRLE): A new approach to enhance sampling of quasi-linear convective systems (QLCSs). New Radar Technologies web page, NOAA/NWS/Radar Operations Center, Norman, OK, 21 pp., https://www.roc.noaa.gov/WSR88D/PublicDocs/NewTechnology/DQ_QLCS_MRLE_June_2016.pdf.

[20.] Crum, T. D., and R. L. Alberty, 1993: The WSR-88D and the WSR-88D operational support facility. *Bull. Amer. Meteor. Soc.*, **74**, 1669–1688, https://doi.org/10.1175/1520-0477(1993)074<1669:TWATWO>2.0.CO;2.

[21.] Donavon, R. A., and K. A. Jungbluth, 2007: Evaluation of a technique for radar identification of large hail across the Upper Midwest and Central Plains of the United States. *Wea. Forecasting*, **22**, 244–254, https://doi.org/10.1175/WAF1008.1.

[22.] Doviak, R. J., and D. S. Zrnic, 1993: *Doppler Radar and Weather Observations*. Academic Press, 562 pp.

[23.] Fulton, R. A., J. P. Breidenbach, D.-J. Seo, D. A. Miller, and T. O'Bannon, 1998: The WSR-88D rainfall algorithm. *Wea. Forecasting*, **13**, 377–395, https://doi.org/10.1175/1520-0434(1998)013%3C0377:TWRA%3E2.0.CO;2.

[24.] Heinselman, P., D. LaDue, D. M. Kingfield, and R. Hoffman, 2015: Tornado warning decisions using phased-array radar data. *Wea. Forecasting*, **30**, 57–78, https://doi.org/10.1175/WAF-D-14-00042.1.

[25.] Kirstetter, P.-E., H. Andrieu, G. Delrieu, and B. Boudevillain, 2010: Identification of vertical profiles of reflectivity for correction of volumetric radar data using rainfall classification. *J. Appl. Meteor. Climatol*., **49**, 2167–2180, https://doi.org/10.1175/2010JAMC2369.1.

[26.] Kosiba, K., J. Wurman, Y. Richardson, P. Markowski, P. Robinson, and J. Marquis, 2013: Genesis of the Goshen County, Wyoming, tornado on 5 June 2009 during VORTEX2. *Mon. Wea. Rev.*, **141**, 1157–1181, https://doi.org/10.1175/MWR-D-12-00056.1.

[27.] Kurdzo, J. M., F. Nai, D. J. Bodine, T. A. Bonin, R. D. Palmer, B. L. Cheong, J. Lujan, A. Mahre, and A. D. Byrd, 2017: Observations of severe local storms and tornadoes with the atmospheric imaging radar. *Bull. Amer. Meteor. Soc.*, **98**, 915–935, https://doi.org/10.1175/BAMS-D-15-00266.1.

[28.] Kurdzo, J. M., J. Y. N. Cho, and B. J. Bennett, 2021: Impact of WSR-88D SAILS usage on quantitative precipitation estimation accuracy. In *37th Conf. on Environmental Information Processing Technologies*, Virtual meeting, Amer. Meteor. Soc., 10.2, https://ams.confex.com/ams/101ANNUAL/meetingapp.cgi/Paper/378382.

[29.] Markowski, P., and Y. Richardson, 2010: *Mesoscale Meteorology in Midlatitudes*. John Wiley & Sons, Ltd., 407 pp., https://doi.org/10.1002/9780470682104.

[30.] Meléndez, D., K. Abshire, and J. Sokich, 2018: NEXRAD weather radar coverage and National Weather Service warning performance. In *AGU 2018 Fall Meeting*, Washington, DC, Amer. Geophys. Union, A11K-2394, https://doi.org/10.1002/essoar.10500135.1.

[31.] NOAA, 2020: Weather radar follow-on plan: Research and risk reduction to inform acquisition decisions. Report to Congress, Office of Oceanic and Atmospheric Research, National Oceanic and Atmospheric Administration, 21 pp., https://www.nssl.noaa.gov/publications/mpar_reports/RadarFollowOnPlan_ReporttoCongress_2020June_Final.pdf.

[32.] NWS, 2009: Verification procedures. NWSI 10-1610, Operations and Services, National Weather Service, 83 pp, http://www.nws.noaa.gov/directives/010/archive/pd01016001d.pdf.

[33.] Pobocikova, I., 2010: Better confidence intervals for a binomial proportion. *Comm.—Sci. Lett. Univ. Zilina*, **12**, 31–37, http://komunikacie.uniza.sk/index.php/communications/article/download/897/861/.

[34.] Polger, P. D., B. S. Goldsmith, R. C. Przywarty, and J. S. Bocchieri, 1994: National Weather Service warning performance based on the WSR-88D. *Bull. Amer. Meteor. Soc.*, **75**, 203–214, https://doi.org/10.1175/1520-0477(1994)075%3C0203:NWSWPB%3E2.0.CO;2.

[35.] Press, W. H., S. A. Teukolsky, W. T. Vetterling, and B. P. Flannery, 1992: *Numerical Recipes in C: The Art of Scientific Computing, 2nd Ed*. Cambridge Univ. Press, New York, NY, 994 pp.

[36.] Rees, D. G., 2001: *Essential Statistics*, 4th Ed. Chapman and Hall/CRC, 384 pp.

[37.] Roberts, R. D., and J. W. Wilson, 1989: A proposed microburst nowcasting procedure using single-Doppler radar. *J. Appl. Meteor.*, **28**, 285–303, https://doi.org/10.1175/1520-0450(1989)028%3C0285:APMNPU%3E2.0.CO;2.

[38.] Sachidananda, M., and D. S. Zrnic, 1999: Systematic phase codes for resolving range overlaid signals in a Doppler weather radar. *J. Atmos. Oceanic Technol.*, **16**, 1351–1363, https://doi.org/10.1175/1520-0426(1999)016%3C1351:SPCFRR%3E2.0.CO;2.

[39.] Schaumann, J. S., and R. W. Przbylinski, 2012: Operational application of 0-3 km bulk shear vectors in assessing QLCS mesovortex and tornado potential. In *26th Conf. on Severe Local Storms*, Amer. Meteor. Soc., New Orleans, LA, P142, https://ams.confex.com/ams/26SLS/webprogram/Manuscript/Paper212008/SchaumannSLS2012_P142.pdf.

[40.] Schmocker, G. K., R. W. Przybylinksi, and Y.-J. Lin, 1996: Forecasting the initial onset of damaging winds associated with a mesoscale convective system (MCS) using the mid-altitude radial convergence (MARC) signature. In *15th Conf. on Wea. Analysis and Forecasting*, Amer. Meteor. Soc., Norfolk, VA, 306–311.

[41.] Sessa, M. F., and R. J. Trapp, 2020: Observed relationship between tornado intensity and pretornadic mesocyclone characteristics. *Wea. Forecasting*, **35**, 1243–1261, https://doi.org/10.1175/WAF-D-19-0099.1.

[42.] Simmons, K. M., and D. Sutter, 2005: WSR-88D radar, tornado warnings, and tornado casualties. *Wea. Forecasting*, **20**, 301–310, https://doi.org/10.1175/WAF857.1.

[43.] Simon, S., 2009: *A Modern Approach to Regression with R*. Springer, 392 pp., https://doi.org/10.1007/978-0-387-09608-7.

[44.] Smith, S. B., 2011: The impact of NWS Weather Forecast Office culture on tornado warning performance. NOAA Office of Science and Technology seminar, Meteorological Development Laboratory, Silver Spring, MD, 61 pp., https://www.nws.noaa.gov/mdl/seminar/Presentations/November_30_2011.pdf.

[45.] Straka, J. M., and J. R. Anderson, 1993: Numerical simulations of microburst-producing storms: Some results from storms observed during COHMEX. *J. Atmos. Sci.*, **50**, 1329–1348, https://doi.org/10.1175/1520-0469(1993)050%3C1329:NSOMPS%3E2.0.CO;2.

[46.] Stumpf, G. J., and A. E. Gerard, 2021: National Weather Service severe weather warnings as Threats-in-Motion. *Wea. Forecasting*, **36**, 627–643, https://doi.org/10.1175/WAF-D-20-0159.1.

[47.] Torres, S., and D. Wasielewski, 2022: The Advanced Technology Demonstrator at the National Severe Storms Laboratory: Challenges and successes. In *2022 IEEE Radar Conf.*, New York, NY, IEEE, 1–6, https://doi.org/10.1109/RadarConf2248738.2022.9764231.

[48.] Weber, M. E., and co-authors, 2021: Towards the next generation operational meteorological radar. *Bull. Amer. Meteor. Soc.*, **102**, E1357–E1383, https://doi.org/10.1175/BAMS-D-20-0067.1.

[49.] Wen, Y., T. J. Schuur, H. Vergara, and C. Kuster, 2021: Effect of precipitation sampling error on flash flood monitoring and prediction: Anticipating rapid-update weather radars. *J. Hydrometeor.*, **22**, 1913–1929, https://doi.org/10.1175/JHM-D-19-0286.1.

[50.] Wilson, E. B., 1927: Probable inference, the law of succession, and statistical inference. *J. Amer. Stat. Assoc.*, **22**, 209–212, https://doi.org/10.1080/01621459.1927.10502953.

[51.] Wilson, K. A., P. L. Heinselman, C. M. Custer, D. M. Kingfield, and Z. Kang, 2017: Forecaster performance and workload: Does radar update time matter? *Wea. Forecasting*, **32**, 253–274, https://doi.org/10.1175/WAF-D-16-0157.1.

[52.] Witt, A., M. D. Eilts, G. J. Stumpf, J. T. Johnson, E. D. W. Mitchell, and K. W. Thomas, 1998: An enhanced hail detection algorithm for the WSR-88D. *Wea. Forecasting*, **13**, 286–303, https://doi.org/10.1175/1520-0434(1998)013%3C0286:AEHDAF%3E2.0.CO;2.

[53.] Wurman, J., Y. Richardson, C. Alexander, S. Weygandt, and P. F. Zhang, 2007: Dual-Doppler analysis of winds and vorticity budget terms near a tornado. *Mon. Wea. Rev.*, **135**, 2392–2405, https://doi.org/10.1175/MWR3404.1.

REPORT DOCUMENTATION PAGE

Form Approved
OMB No. 0704-0188

1. REPORT DATE *(DD-MM-YYYY)*	**2. REPORT TYPE**	**3. DATES COVERED** *(From - To)*
	Project Report	

4. TITLE AND SUBTITLE
Impacts of WSR-88D SAILS and MRLE VCP Options on Severe Weather Warning

5a. CONTRACT NUMBER

5b. GRANT NUMBER

5c. PROGRAM ELEMENT NUMBER

6. AUTHOR(S)
John Cho, Jim Kurdzo, Betty Bennett, and Alexandra Anderson-Frey

5d. PROJECT NUMBER
10215

5e. TASK NUMBER

5f. WORK UNIT NUMBER

7. PERFORMING ORGANIZATION NAME(S) AND ADDRESS(ES)

MIT Lincoln Laboratory
244 Wood Street
Lexington, MA 02421-6426

8. PERFORMING ORGANIZATION REPORT NUMBER
NOAA-36

9. SPONSORING / MONITORING AGENCY NAME(S) AND ADDRESS(ES)
NOAA/National Oceanic and Atmospheric Administration
1401 Constitution Avenue NW, Room 5128
Washington, DC 20230

10. SPONSOR/MONITOR'S ACRONYM(S)
NOAA

11. SPONSOR/MONITOR'S REPORT NUMBER(S)

12. DISTRIBUTION / AVAILABILITY STATEMENT
DISTRIBUTION STATEMENT A. Approved for public release. Distribution is unlimited.

13. SUPPLEMENTARY NOTES

13. ABSTRACT
The impacts of supplemental adaptive intra-volume low-level scan (SAILS) and mid-volume rescan of low-level elevations (MRLE) usage on the Weather Surveillance Radar 1988-Doppler (WSR-88D) with respect to severe weather warning performance were evaluated. This is an update and expansion of an earlier study by Cho et al. (2022). Statistical methods applied to historical data from 2014–2022 yielded the following major results.
Severe thunderstorm (SVR) warning performance metrics are shown in the figure below, where the vertical bars represent 95% confidence intervals and the numbers at the bottom correspond to the sample sizes. The results are divided according to the scanning option that is estimated to have been used at the time the decision to issue (or not issue) a warning was made. The first point to note is that probability of detection (POD), false alarm ratio (FAR), and mean lead time (MLT) improvements were associated with the usage of supplemental adaptive intra-volume low-level scan (SAILS or MRLE) in a statistically meaningful manner. As for the different sub-modes of SAILS, the multiple elevation scan option (MESO), i.e., SAILSx2 and SAILSx3, appeared to give more benefit than SAILSx1. However, the fact that the fastest base-scan update rates provided by SAILSx3 hardly yielded more benefit than SAILSx2 may indicate that the slowdown in volume scan update rates counteracted the more frequent base scans when going from SAILSx2 to SAILSx3. For POD and FAR, MRLE+4 significantly outperformed MESO-SAILS, which may also indicate that more frequent updates of elevations angle scans higher than the lowest tilt are needed by forecasters to make accurate SVR warning decisions.

15. SUBJECT TERMS

16. SECURITY CLASSIFICATION OF:			**17. LIMITATION OF ABSTRACT**	**18. NUMBER OF PAGES**	**19a. NAME OF RESPONSIBLE PERSON**
a. REPORT	**b. ABSTRACT**	**c. THIS PAGE**	None	126	**19b. TELEPHONE NUMBER** *(include area code)*
UNCLASSIFIED	UNCLASSIFIED	UNCLASSIFIED			